MINISTRY OF NATIONAL EDUCATION

THE ANNALS OF "DUNAREA DE JOS" UNIVERSITY OF GALATI

Fascicle IX
METALLURGY AND MATERIALS SCIENCE

YEAR XXXVII (XLII)
March 2019, no. 1

ISSN 2668-4748; e-ISSN 2668-4756

2019
GALATI UNIVERSITY PRESS

EDITORIAL BOARD

THE ANNALS OF "DUNAREA DE JOS" UNIVERSITY OF GALATI
FASCICLE IX. METALLURGY AND MATERIALS SCIENCE
Nº. 1 - 2019, ISSN 2668-4748; e-ISSN 2668-4756
Volume DOI: https://doi.org/10.35219/mms.2019.1

Table of Contents

THE ANNALS OF "DUNAREA DE JOS" UNIVERSITY OF GALATI
FASCICLE IX. METALLURGY AND MATERIALS SCIENCE
Nº. 1 - 2019, ISSN 2668-4748; e-ISSN 2668-4756
Volume DOI: https://doi.org/10.35219/mms.2019.1

THE ANNALS OF "DUNAREA DE JOS" UNIVERSITY OF GALATI
FASCICLE IX. METALLURGY AND MATERIALS SCIENCE
N°. 1 - 2019, ISSN 2668-4748; e-ISSN 2668-4756
Article DOI: https://doi.org/10.35219/mms.2019.1.01

ABOUT THE INFLUENCE OF THE MACHINED DEFECT SHAPE AND POSITION ON THE STRESS DISTRIBUTION FOR PIPELINES WITH VOLUMETRIC DEFECTS

Ionuţ LAMBRESCU
Universitatea Petrol-Gaze din Ploieşti, Bd. Bucureşti 39, Ploieşti, Romania
e-mail: ilambrescu@upg-ploiesti.ro

ABSTRACT

The aim of the paper is to analyse how the shape and position of the machined volumetric surface defects (VSD) may influence the stresses and displacements distributions for pipelines with VSD. The machined defect is usually rectangular, with edges oriented parallel/perpendicular to the pipe's axis.

We attempt to analyse in this paper what happens when the machined defect is no longer rectangular, but circular or elliptical and with different positions relative to the pipe's axis. We also consider different fillet radius of the machined VSD.

KEYWORDS: Volumetric surface defect, VSD

1. Introduction

In the case of pipelines with volumetric surface defects, a number of methods were developed and included in standards and normatives such as ASME B31G; ASME B31.8; API Standard 579, BS 7910.

Basically, we speak about the following approach:

- Initial anomality evaluation. The result of this stage is the conclusion that the anomality is acceptable and no further actions are necessary, or if it is considered a defect, a repairing process has to follow.
- If the anomality is considered a defect, then the affected area is machined and after that, the defect area will withstand a repairing process. This process includes the use of a filler that will fill the VSD and of a wrap applied around the pipe in the VSD area [1-6].

In the literature for the machined VSD only a rectangular shape is considered. This is why we appreciated that attention should be given also to other shapes for the machined VSDs.

At that stage we took into consideration three shapes: circular, elliptical and rectangular. We also took into consideration, for the elliptical and rectangular machined VSDs, the orientation of the machined defect.

In order to compare the results, we considered machined defects with equal areas.

For all of the considered cases, the analysis was performed on a pipe with the following properties:

- Outside Diameter De = 508 mm.
- Wall Thickness t = 10 mm.
- Maximum Allowable Pressure MOP = 20 bar.
- Specify Minimum Yield Strength SMYS = 290 N/mm^2.
- Maximum Depth of VSD dp = 7.5 mm.

2. Circular machined VSD

The first machined VSD considered is a circular one, as can be seen in Figure 1. We mention that the defect is positioned at the middle of the considered pipe segment and that a fillet radius is also considered as a parameter of the evaluation. The fillet radius will vary between 7.5 mm (the defect depth) and 20 mm, with a 2.5 mm step. Due to the circular shape of the machined VSD, there is not the case to speak about the orientation of the machined VSD. A scenario analysis produced the results presented in Fig. 2.

Figure 3 presents the Von Mises stress distribution for a quarter of the pipe (due to symmetry reasons) for the "optimal" case (with the smallest Von Mises stress). As can be seen, the maximal value is recorded on the interior face of the pipe.

The analysis of the last row in Table 1 allows us to state that the fillet radius, at least for the interval considered, does not influence significantly the stress or displacement distributions.

THE ANNALS OF "DUNAREA DE JOS" UNIVERSITY OF GALATI
FASCICLE IX. METALLURGY AND MATERIALS SCIENCE
Nº. 1 - 2019, ISSN 2668-4748; e-ISSN 2668-4756
Article DOI: https://doi.org/10.35219/mms.2019.1.01

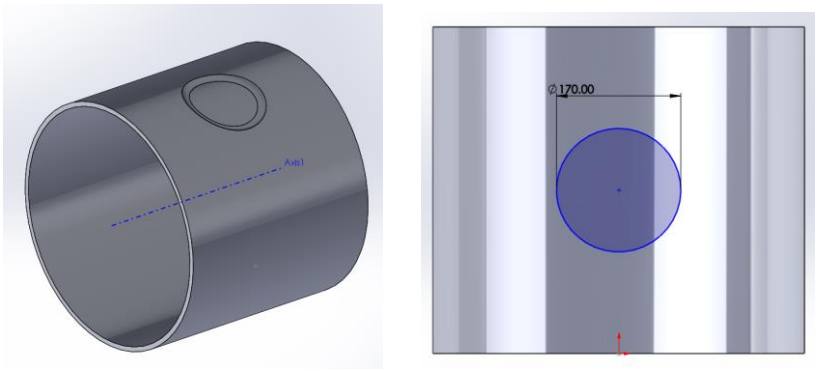

a. 3D view b. Top view

Fig. 1. *Circular machined VSD*

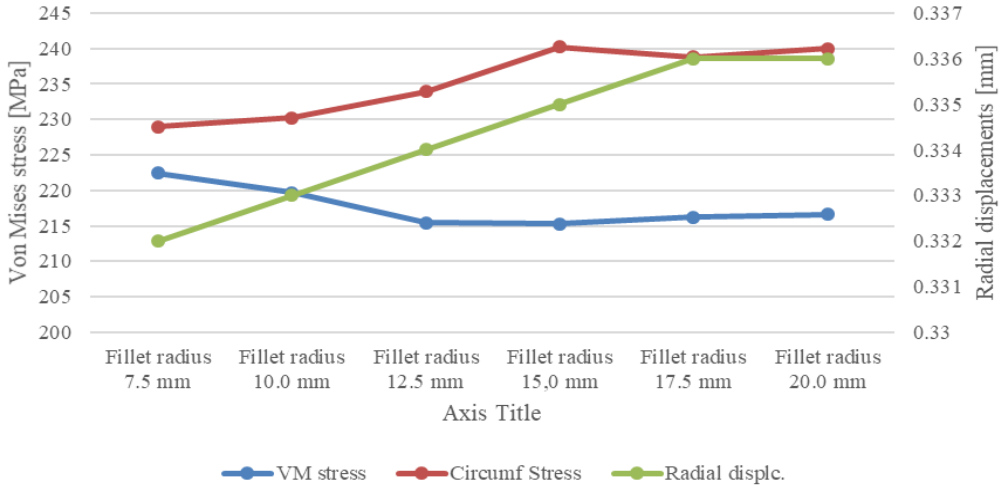

Fig. 2. *Stress and displacement tendencies for the 6 scenarios*

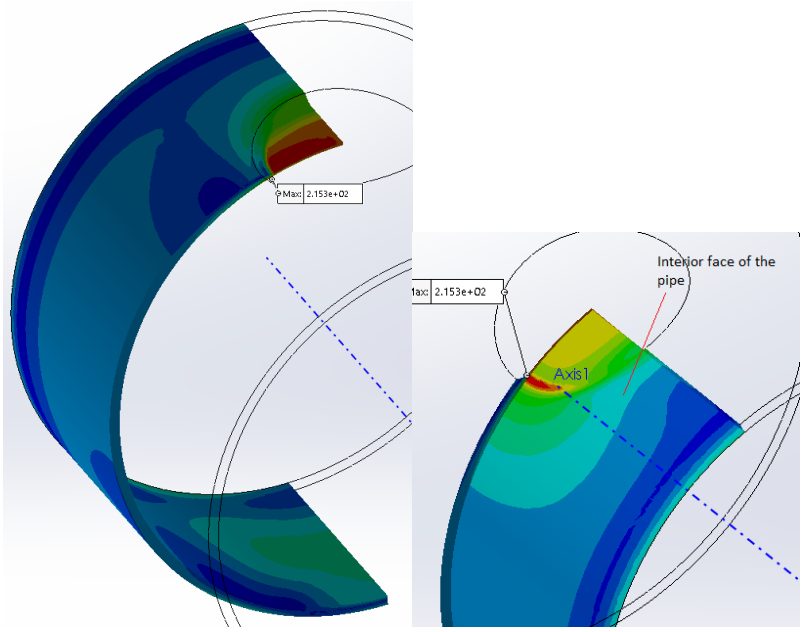

a. Section view b. Detail view

Fig. 3. *Stress distribution for the optimal scenario (Von Mises [MPa])*

THE ANNALS OF "DUNAREA DE JOS" UNIVERSITY OF GALATI
FASCICLE IX. METALLURGY AND MATERIALS SCIENCE
Nº. 1 - 2019, ISSN 2668-4748; e-ISSN 2668-4756
Article DOI: https://doi.org/10.35219/mms.2019.1.01

2. Elliptical machined VSD

For the case where the machined VSD has an elliptical shape, apart from the fillet radius, a new parameter has been considered. It is the position/orientation of the machined VSD. We express that using an angle, as can be seen in Figure 4. We also mention that the area of the ellipse is equal to that of the circle used for the circular machined VSD, and that the ratio between the axis of the ellipse is 2.

This time the scenario analysis turned into an optimization analysis, with tow parameters: the fillet radius (varying between 10 and 20 mm with a 2 mm step) and the angle that positioned the VSD (varying between 0 and 90 degrees with 10 degrees step). This approach led to 60 scenarios.

The results indicate that the minimum Von Mises stress is recorded for the ellipse positioned with the big axis perpendicular to the pipe's axis.

As for the way the fillet radius influences the results, we may say that its importance is bigger for small values of the angle. As expected, we record smaller Von Mises stress for bigger fillet radius values (see Figure 6). The most important parameter in terms of how it influences the Von Mises stress is the position angle of the machined VSD.

Figure 5 presents the Von Mises stress distribution for a quarter of the pipe (due to symmetry reasons) for the case where the Von Mises stress records the minimal value among scenarios (fillet radius 20 mm and orientation angle 90 degrees). As can be seen, this maximal value is on the exterior face of the pipe.

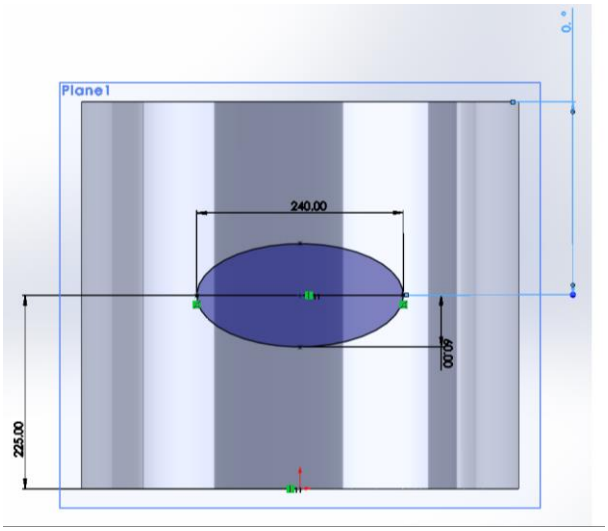

Fig. 4. *Elliptical machined VSD*

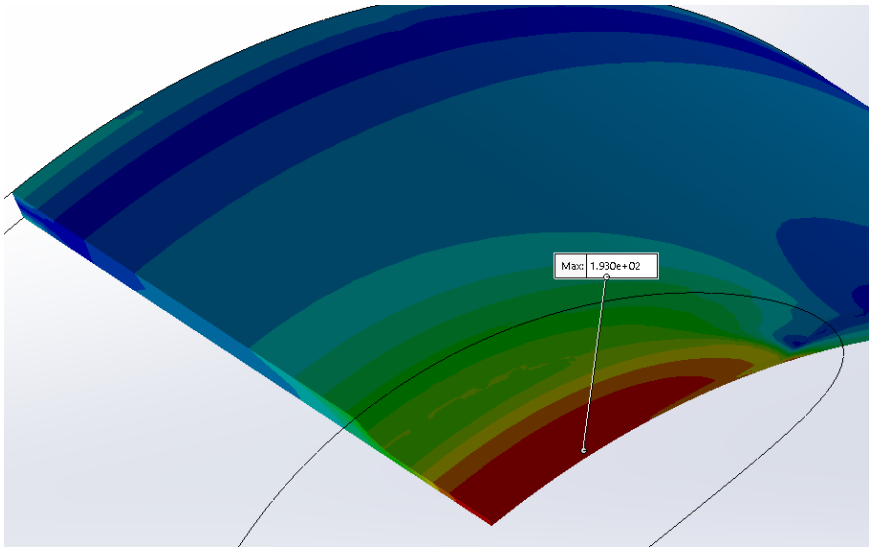

Fig. 5. *Von Mises stress distribution [MPa]*

THE ANNALS OF "DUNAREA DE JOS" UNIVERSITY OF GALATI
FASCICLE IX. METALLURGY AND MATERIALS SCIENCE
N°. 1 - 2019, ISSN 2668-4748; e-ISSN 2668-4756
Article DOI: https://doi.org/10.35219/mms.2019.1.01

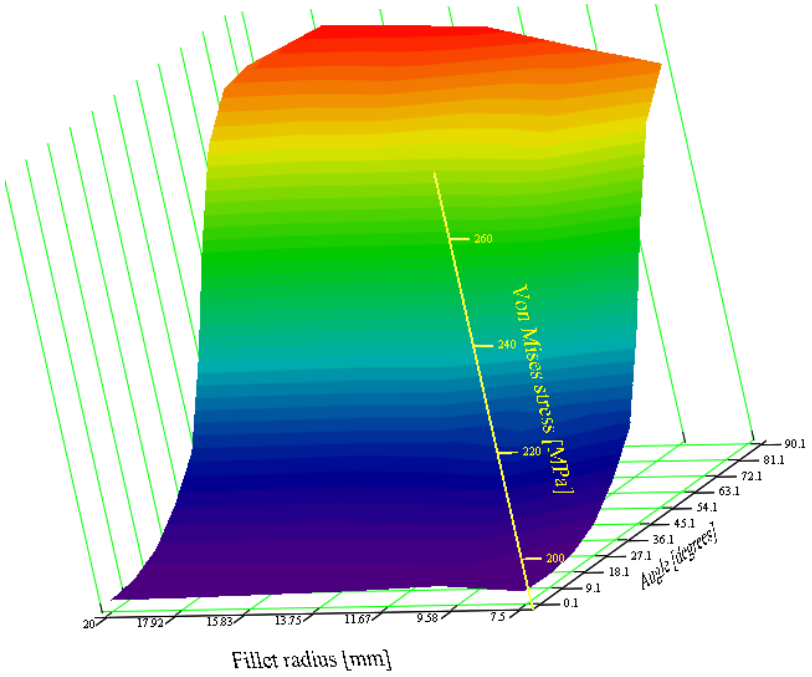

Fig. 6. *Influence of Fillet radius and position angle on Von Mises stress*

For the elliptical machined VSD, we can conclude that the most favourable scenario corresponds to the orientation of the major axis perpendicular to the pipe's axis and the fillet radius of 20 mm. This position ensures the minimum length of the machined VSD along the pipe's axis.

The most detrimental situation is recorded for the VSD oriented with the major axis parallel to the pipe axis and the fillet radius of 12 mm. We have to mention that for the case when the VSD is oriented along the pipe's axis, the value of the fillet radius has not a significant influence (relative difference of 1.39%).

In the meantime, we stress that the relative difference between the most detrimental and the most favourable scenario, for the Von Mises stress, is 40.85%, which indicates a very strong influence of the VSD orientation on the stress distribution.

3. Rectangular machined VSD

We considered a rectangular VSD with the same area as the previous two types (circular and elliptical), with a ratio between the rectangle dimensions of 2. We run 60 scenarios, corresponding to the variation of the fillet radius between 10 and 20 mm, with a step of 2 mm, and of the orientation of the VSD with an angle between 0 and 90 degrees, with a 10 degrees step (see Figure 7).

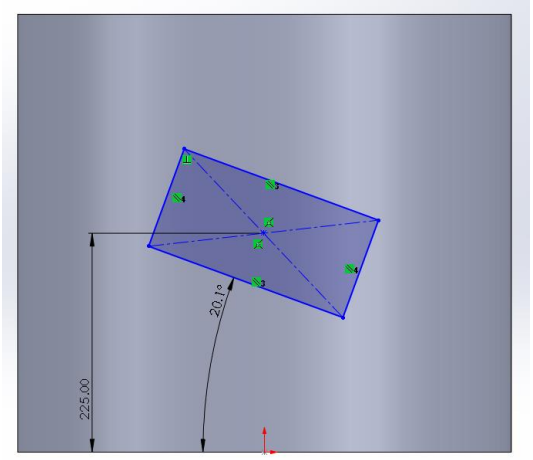

Fig. 7. *Machined VSD position*

THE ANNALS OF "DUNAREA DE JOS" UNIVERSITY OF GALATI
FASCICLE IX. METALLURGY AND MATERIALS SCIENCE
N°. 1 - 2019, ISSN 2668-4748; e-ISSN 2668-4756
Article DOI: https://doi.org/10.35219/mms.2019.1.01

The first round of the 60 scenarios produced a most favourable situation (the smallest Von Mises stress) for the case when the fillet radius is 14 mm and the orientation of the VSD is 20 degrees. The most detrimental situation is recorded when the VSD is aligned with the pipe's axis and the fillet radius is 16 mm.

The relative difference between those two extreme scenarios is 47.13%.

Figure 8 presents the Von Mises stress distribution for the most favourable scenario in a section along the VSD axis, while Figure 9 presents the Von Mises stress distribution for the most detrimental situation.

Figure 10 presents the variation of the Von Mises stress for the 60 scenarios. One can see a region with smaller values for the Von Mises stress around the value of 20 degrees for the VSD position.

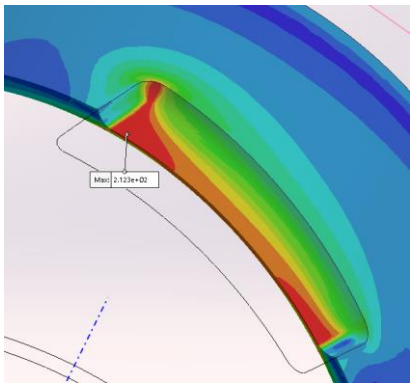

Fig. 8. *Von Mises stress distribution for the most favourable scenario [MPa]*

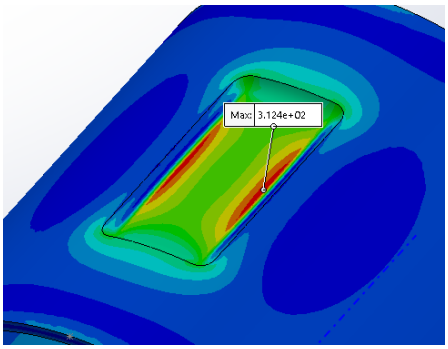

Fig. 9. *Von Mises stress distribution for the most detrimental scenario [MPa]*

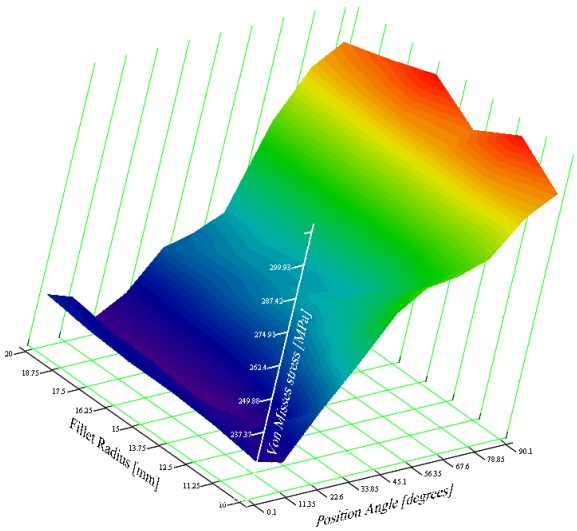

Fig. 10. *Von Mises stress distribution for the 60 scenarios*

THE ANNALS OF "DUNAREA DE JOS" UNIVERSITY OF GALATI
FASCICLE IX. METALLURGY AND MATERIALS SCIENCE
N°. 1 - 2019, ISSN 2668-4748; e-ISSN 2668-4756
Article DOI: https://doi.org/10.35219/mms.2019.1.01

For the rectangular VSD, we also considered other scenarios, that would analyse the cases when, maintaining the area of the VSD, the rectangle dimensions would vary (in fact the ratio between the rectangle edges – we considered, apart from ratio 2, another three values, 1.5, 2.5 and 3). This approach leads to the values for the rectangle edges presented in Table 1.

In our scenarios we maintain the same parameters we used previously, that is the fillet radius and the position angle of the machined VSD.

The content of Tables 2 and 3 is presented in a graphical form in Figures 11 and 12.

Table 1. *Machined VSD edges*

Edges ratio	**1.5**	**2**	**2.5**	**3**
Long edge	184.5	213	238.2	261
Short edge	123	106.5	95.3	87

Table 2. *Results of the scenario analysis. Most favorable cases*

Edges ratio	**1.5**	**2**	**2.5**	**3**
Angle [deg]	30	20	10	10
Fillet radius [mm]	20	14	12	16
Von Mises stress [MPa]	225.34	212.35	209.0	199.83
Circumferential stress [MPa]	244.04	237.37	235.39	226.88
Radial displacement [mm]	0.352	0.309	0.283	0.262

Table 3. *Results of the scenario analysis. Most detrimental cases*

Edges ratio	**1.5**	**2**	**2.5**	**3**
Angle [deg]	90	90	90	80
Fillet radius [mm]	12	16	12	10
Von Mises stress [MPa]	307.86	312.44	322.53	317.24
Circumferential stress [MPa]	342.42	348.74	360.64	355.06
Radial displacement [mm]	0.349	0.383	0.400	0.411

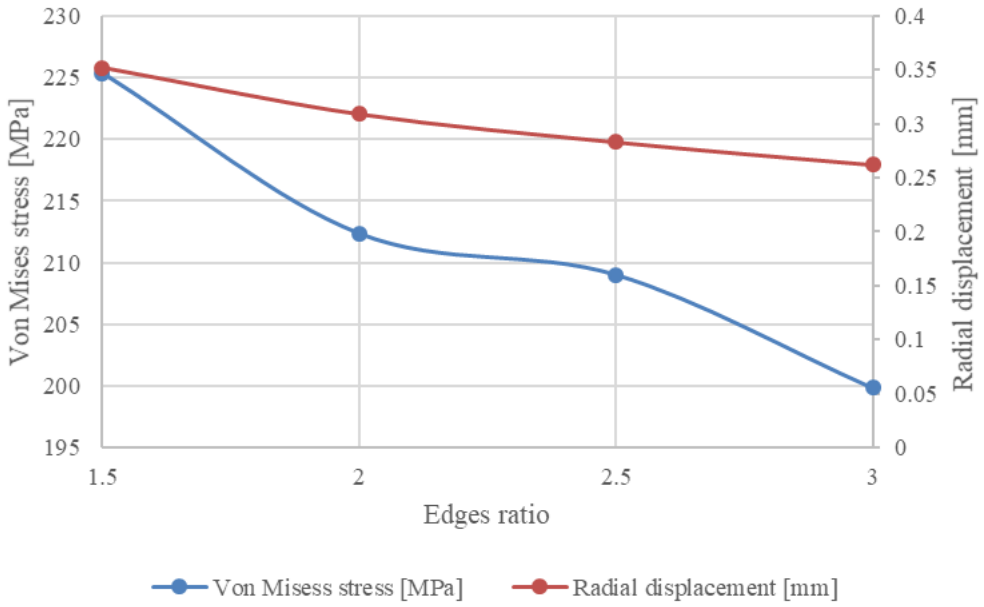

Fig. 11. *Von Mises stress and radial displacement for the most favourable cases*

THE ANNALS OF "DUNAREA DE JOS" UNIVERSITY OF GALATI
FASCICLE IX. METALLURGY AND MATERIALS SCIENCE
N°. 1 - 2019, ISSN 2668-4748; e-ISSN 2668-4756
Article DOI: https://doi.org/10.35219/mms.2019.1.01

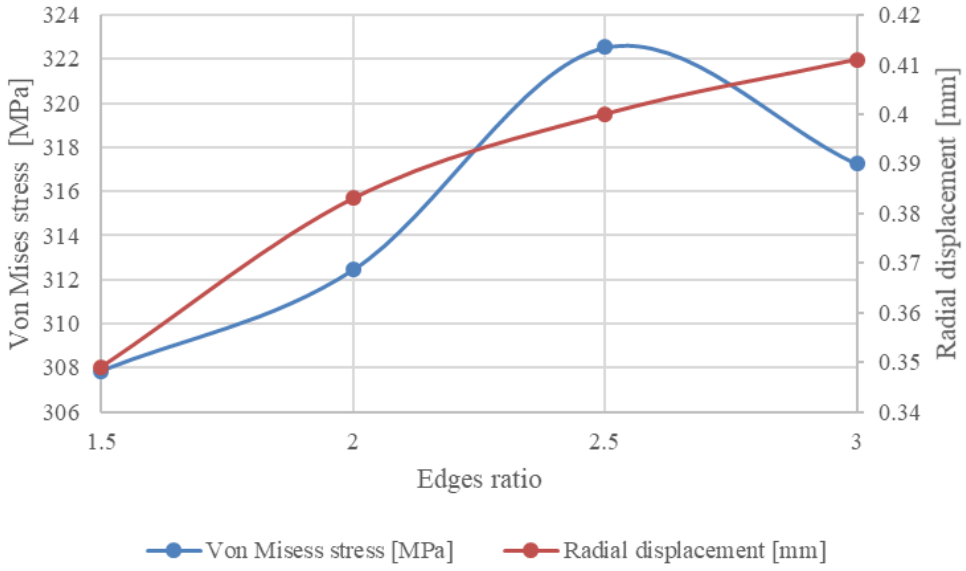

Fig. 12. *Von Mises stress and radial displacement for the most detrimental cases*

4. Conclusions

The interpretation of all the data obtained after the scenario analysis, allows us to formulate the following observations:

- The shape and position, along with the fillet radius of the machined VSD, are important for the stress distribution;
- The shape of the machined distribution influences not only the values of stress or displacement, but also the place in the VSD region where the maximal values are recorded (for example, in the case of the circular VSD, the maximal value is registered on the interior side of the pipe, while in other cases, on the exterior face);
- In the case of the elliptical machined VSD, the values of the fillet radius have a small influence on the stress distribution. In this case, only the orientation of the VSD is relevant, with the most favourable case when the major axis of the ellipse is perpendicular to the pipe's axis and the most detrimental case when the major axis is oriented parallel to the pipe's axis;
- In the case of rectangular machined VSDs, the most frequent situation appearing in real life, the combined influence of the fillet radius, VSD orientation or edges' ratios can produce favourable or detrimental cases;
- For the rectangular machined VSDs, the differences between the most favourable and detrimental cases are important, reaching nearly 50%;
- Taking into account all the above conclusions, we can assess that before machining a VSD as a preparation for the reparation, an analysis of the best choice in terms of fillet radius, and shape and position of the machined VSD is necessary and can produce solution close to optimum.

The present stage of the analysis was limited to put into light the influence of the shape and position of the machined VSDs on the stress and displacement distributions. This fact has not been taken into consideration so far.

The next stage will deal with a more complex analysis. Starting from a real VSD, will try to find the best shape and position of the machined VSD. This will involve a geometric optimization, followed by a scenario analysis in order to find the best shape and position for the machined VSD.

References

[1]. ***, *B31G - Manual for Determining the Remaining Strength of Corroded Pipelines.*
[2]. Zecheru Ghe., Yukhymets P., Drăghici Ghe., Dumitrescu A., REV. CHIM. (Bucharest), 66, no. 5, 2015.
[3]. Duell J. M., Wilson J. M., Kessler M. R., *Analysis of a carbon composite overwrap pipeline repair system*, Journal of Pressure Vessels and Piping, Elsevier, 2008.
[4]. Amr A. Abd-Elhady, Hossam El-Din M. Sallam, Muhammad A. Mubaraki, *Failure Analysis of Composite Repaired Pipelines with an Inclined Crack under Static Internal Pressure*, 2nd International Conference on Structural Integrity, ICSI 2017, Funchal, Madeira, Portugal, 4-7 September 2017.
[5]. Chebakov M., Nedin R., Lyapin A., *Finite-Element Modeling of a Repaired Pipeline Containing Two Volumetric Surface Defects*, Non-destructive Testing and Repair of Pipelines.
[6]. Yukhymets P. Gopkalo A., Zecheru Ghe., Mihovski M., *Residual Life of Pipeline with Volumetric Surface Defect in the Weld Zone*, International Journal of Offshore and Polar Engineering, vol. 26, Issue 03, 2016.

THE ANNALS OF "DUNAREA DE JOS" UNIVERSITY OF GALATI
FASCICLE IX. METALLURGY AND MATERIALS SCIENCE
N°. 1 - 2019, ISSN 2668-4748; e-ISSN 2668-4756
Article DOI: https://doi.org/10.35219/mms.2019.1.02

CHROMITE. PROCESSING AND APPLICATIONS

Marius VASILESCU, Mircea DOBRESCU
Politehnica University of Bucharest, Romania
e-mail: vmarius_sim_pub@yahoo.com

ABSTRACT

In the paper are shown the history, processing and applications of chromite.

Chromite is an oxide of iron and chromium with the chemical composition $FeO.Cr_2O_3$ and belonging to the spinel group.

Theoretically it contains 46.5%Cr and 25.8%Fe and their oxides.

The technology of obtaining chromite is based on the principle of gravity separation and agglomeration.

Among the applications we mentioned: - Ferrochrome; - Stainless steel; - Nickel chromium alloys; - Nonferrous alloys; - Foundry.

KEYWORDS: chromite, processing, applications

1. Introduction

Chromite is the only commercially exploited ore of chromium, and is also referred to as "chrome ore" [1, 2].

In nature, the ferrous iron is generally replaced partially by magnesium, and the chromium by ferric iron or aluminium, with consequent variations in the Cr/Fe ratio. Thus, its composition is represented by the generalized formula $(Fe, Mg)O.(Cr, Al, Fe)_2O_3$ [3]. It occurs in ultrabasic igneous rocks generally associated with peridotite, pyroxenite, serpentinite and dunite. Its commercial deposits are broadly of two types – podiform and stratiform. The former is generally high-alumina and the latter iron-rich.

Chromite was first mined in Norway in 1820 as a refractory material. In 1903, its mining commenced in Beluchistan, Pakistan, then in Mysore and Singbhum districts, India, in 1907 and 1909 respectively. But the most famous and the largest resources of Orissa state were discovered only in 1943. During the 44 year-period, from 1903 to 1946, the cumulative total production in the states of then India (i.e., including present Pakistan) was 1.4 million tonnes, out of which about 0.74 million tonnes were in the states belonging to present India.

The production reached the peak figure of about 62000 tonnes in 1937, and thereafter, during the five-year period 1942-1946, averaged only 24000 tonnes per year. In India, since independence in 1947, the production profile of chromite was as follows (Table 1).

Table 1. *Chromite production in India*

Years	Chromite production [t]
1950	17000
1960	107000
1970	274000
1980	321000
1990	959000
April, 2000 – March, 2001	1970000

During the year 2000, the world production stood at 14.6 million tonnes, and India ranked third after South Africa and Kazakhstan.

In India, although a chromite beneficiation plant was in operation in the 1970s, the widespread commercial practice of beneficiation of low-grade chromite is relatively recent, dating back to the 1990s. But it has made a drastic difference to the resource availability of chromite. Chromite concentrate is not an end product, but it is a tradable

THE ANNALS OF "DUNAREA DE JOS" UNIVERSITY OF GALATI
FASCICLE IX. METALLURGY AND MATERIALS SCIENCE
N°. 1 - 2019, ISSN 2668-4748; e-ISSN 2668-4756
Article DOI: https://doi.org/10.35219/mms.2019.1.02

product in the domestic as well as international market.

2. Technology

Typically, the technology is based on the principle of gravity separation. The friable and the fine-sized ores are crushed and ground to (-) 150-micron size, and the beneficiation process consists of desliming in hydrocyclones, followed by spiralling and tabling [4]. These processes serve to increase the Cr_2O_3 content and reduce the SiO_2 content, but no appreciable improvement in Cr/Fe ratio takes place. Magnetic separator may also be introduced in the circuit for treatment of ferruginous ores to improve Cr/Fe ratio. The low-grade lumpy ores containing lots of clay that are not directly usable, are crushed and washed.

The product of beneficiation, i.e. the concentrate, is fine grained, but in conventional metallurgical processes it cannot be directly used [5, 6]. For that purpose, concentrates and also high-grade natural fines are agglomerated into briquettes, sinters, pellets and sintered pellets. Briquettes are made by pressing the fines or without bonding material. This is the simplest and cheapest method of agglomeration, but in many cases, briquettes do not retain their shape under the smelting conditions [7, 8].

Sintering is carried out by partial fusion of the corners of the grains, and fluxes (e.g. limestone) are generally added at this stage itself [9]. Pelletizing involves mixing the fines with bentonite (bonding material), fluxing material and coke, and then subjecting the mixture to rotational motion in drum or disc. Sintered pellet is essentially a combination product of pellet and sinter, and is considered superior to the other agglomeration products. For manufacturing this product, green pellets are burnt to a temperature ranging from 1350-1450 °C in a sintering furnace.

3. Applications

3.1. Ferrochrome

Taking advantage of the natural association of chromium and iron, ferrochrome – not metallic chromium is added to steel for making stainless steels and other alloys of chromium and steel. This is added to steel as an alloying metal for improving various properties such as resistance to heat, corrosion and abrasion, as well as strength, hardness etc., and the physical and mechanical properties of chromium are taken advantage of [10].

The alloy steel products include low to high carbon steels including stainless steels and tool steels for ordinary level performances. Ferrochrome is classified into six types:

(a) High carbon ferrochrome;
(b) Charge chrome;
(c) Silicochrome;
(d) Medium carbon ferrochrome;
(e) Low carbon ferrochrome;
(f) Exothermic ferrochromium.

Except silicochrome, all the other four types differ from each other mainly by carbon content. These types are discussed as follows.

3.1.1. High carbon ferrochrome

The carbon content in the high carbon ferrochrome is in the range of 4-8%, while the chromium and silica contents may vary from 60-70% and 1-2% respectively, although 64-66% Cr and 5.0-6.5% C are relatively more typical. The conventional manufacturing process involves smelting in an electric arc furnace (EAF). Chromite (in the form of natural lumps or agglomerated products) along with coke and some slag-forming materials like limestone, dolomite etc. are charged into the furnace. Some silica and alumina-bearing materials such as quartz, bauxite etc. are also added for balancing the composition and volume of the slag depending on need. Improvements in the process mainly by way of preheating the charge have been carried out with a view to reducing power consumption and cost and to improving metal recovery.

The process is highly power-intensive, the consumption of power being in the range of 4200-5000 kwh per tonne of the product. There is one more technology, namely the plasma arc smelting technology. Plasma arc furnaces are in operation in Sweden and South Africa. In this process, the heat is produced by plasma torches. Its advantage lies in its ability to use ore fines and noncoking coal, but its main disadvantage is the high requirement of electricity.

3.1.2. Charge chrome

Charge chrome is a very high carbon low grade ferrochrome. It is actually "charge grade chromium", as it is in this form that chromium is charged into the furnace for stainless steel manufacturing since the development of highly effective decarburization technologies, namely vacuum oxygen decarburization (VOD) and argon oxygen decarburization (AOD). Its carbon-content, as in the case of high carbon ferrochrome, varies up to 8% - generally 6-8%, but the chromium content is below 60% and may be as low as 50%; silica is also high, 3-6%. Decarburization is critically important in stainless

THE ANNALS OF "DUNAREA DE JOS" UNIVERSITY OF GALATI
FASCICLE IX. METALLURGY AND MATERIALS SCIENCE
N°. 1 - 2019, ISSN 2668-4748; e-ISSN 2668-4756
Article DOI: https://doi.org/10.35219/mms.2019.1.02

steel manufacturing, because carbon combines with chromium to form chromium carbide thus robbing the stainless steel of a portion of the chromium added.

The VOD and AOD technologies achieve decarburization very effectively, and so, low-chromium charge chrome combined with a high degree of decarburization can yield the same grade of stainless steel as high-chromium ferrochrome with a low degree of decarburization. That is how charge chrome has become a cheaper and popular option after the advent of the new decarburization technologies. The process employed for its manufacture is the same as in the case of high carbon ferrochrome.

3.1.3. Silicochrome

Ferrochrome silicon or chrome silicide or silicochrome is both an intermediate product used in making low carbon ferrochrome and a final salable product for charging in alloy steel making. Silicochrome is a high-silicon low-iron low-carbon product. In effect, silicon takes the place of a portion of iron. Typically, it contains 35-41%Cr, 35-45%Si and 0.05%C. It can be made by resmelting high carbon ferrochrome with silica and coke or charcoal.

But the most common method of producing it is by smelting in an EAF of charge composed of chromite, silica and coke or charcoal. Since no lime is added, there is no slag, and the silica does not go to form silicate.

In the first method, carbon of the high carbon ferrochrome and the coke is oxidized by the silica and the silicon goes into solid solution with chromium. In the second method, the coke reduces both the chromite and the silica, and the chromium and silicon form the silicochrome [11].

3.1.4. Medium carbon ferrochrome

The range of carbon is 1-4% and that of chromium 65-75%. Simply by blowing oxygen through molten high carbon ferrochrome in a converter and reducing the carbon content, the desired lower range of carbon can be achieved.

3.1.5. Low carbon ferrochrome

This is used in making very high quality stainless and other alloy steels meant for special products like chemical-manufacturing and food processing equipment, surgical instruments, cryogenic vessels, nuclear power stations, spaceship components, etc. Carbon should be below 0.5%, and more commonly varies from 0.015-0.05%; chromium 65-75%; and silicon less than 1%. Low carbon ferrochrome can be manufactured by oxygen refining of high carbon ferrochrome and reducing its carbon content in multiple stages.

But this process is expensive. The common method uses high-silicon low-carbon silicochrome and chromite as the starting materials. The principle essentially consists of smelting the chromite with lime in an open arc furnace producing a chromium-rich chromite/lime slag, and treating this slag with the low carbon high silicon silicochrome. The silicon of the silicochrome goes to react with the lime of the slag to form calcium silicate slag, while the chromium of the silicochrome and that of the slag add up to increase the chromium content of the product i.e., low carbon ferrochrome [12].

3.1.6. Exothermic ferrochrome

Exothermic ferrochrome is used when the chilling effect of adding conventional ferrochrome to the molten steel is undesirable. One such product is composed of ferrochrome, a small quantity of ferrosilicon or silicochrome, and sodium nitrate. It is produced in both low and high carbon grades.

3.2. Stainless steel

Stainless steel has been dealt with in the chapter on hematite. Chromium is the key element in it. It is defined as an alloy steel containing more than 9% chromium – with or without other elements. It is characterized by a high degree of resistance to corrosion or oxidation or rusting. In ordinary steels, the initial oxidation forms a loose permeable scale which holds moisture and allows oxygen to diffuse readily and progressively attacking the metal below [13].

In contrast, in stainless steels, the initial oxidation forms a very thin, transparent and highly adherent skin of chromium oxide which, being impervious to oxygen, prevents progressive oxidation of the body of the stainless steel below.

Amongst the other optional elements, nickel is the most important. For manufacturing stainless steel, a mixture of steel, stainless steel scrap, chromium (in the form of ferrochrome) and nickel (optional) is changed into an electric arc furnace (EAF) and smelted. Carbon (the original carbon present in the steel plus the carbon got through the ferrochrome) is an important factor in stainless steel.

It melts in the EAF, and combines with chromium to form chromium carbide thus robbing the stainless steel of a portion of the chromium added. This problem can be overcome by adding ferrochrome containing very low carbon or by adding

THE ANNALS OF "DUNAREA DE JOS" UNIVERSITY OF GALATI
FASCICLE IX. METALLURGY AND MATERIALS SCIENCE
Nº. 1 - 2019, ISSN 2668-4748; e-ISSN 2668-4756
Article DOI: https://doi.org/10.35219/mms.2019.1.02

ferrochrome containing high carbon with simultaneous decarburization of the molten bath by argon oxygen decarburization (AOD) and vacuum oxygen decarburization (VOD) technologies.

The aim is to minimize the formation of chromium carbide and maximize the availability of chromium for alloying. Examples of stainless steels are presented in Table 2.

Table 2. *Examples of stainless steels*

Chromium content [%]	Other elements [%]	Properties/Uses
12	0.3%C	Hard. Used in table knives
14-18	max. 0.12%C	Nonhardenable
14-18	max. 0.12%C; min. 0.15%Se	Free machinability
16-18	0.95-1.20%C; max. 0.75%Mo	Fully hardenable
23-27	max. 0.20%C	Resistant to scale formation when hot
18	18%Ni; 0.07%C; 3.5%Mo; 0.6%Ti; 2.0%Cu	Suitable for applications requiring strong resistance to chemical attacks by sulphuric and other acids, and sulphates and other salts (e.g. chemical equipment)
24-26	19-22%Ni; max. 0.08%C	Uses requiring resistance to scale and stress at temperatures as high as 1000 °C (e.g. staking equipment, furnace parts)
16-18	6-8%Ni; max. 0.15%C	Ferritic. Hardenable
(+) 20	Low nickel	Mixture of austenite and ferrite (duplex); can be strengthened by addition of nitrogen. Very high-performance stainless steel, strong, with high corrosion resistance and very good weldability. Used in appliances, in nuclear stations, in fabrication of large diameter tubes, in coins.
18-20	8-12%Ni; max. 0.8%C	Austenitic; superior corrosion resistance
18-20	8-12%Ni; max. 0.3%C	It resists the formation of chromium carbide around crystal boundaries.
16-18	10-14%Ni; max. 0.8%C; 2-3%Mo	Superior corrosion resistance
17-19	9-12%Ni; max. 0.08%C; 5-times carbon-content Ti	It resists the formation of chromium carbide around crystal boundaries.
17-19	9-13%Ni; max. 0.08%C; 10-times carbon-content Nb	It resists the formation of chromium carbide around crystal boundaries.
17	4%Ni; 3.5%Cu	Martensitic. Used in aircraft industry
20	34%Ni; 3.5%Cu; 2.5%Mo	Austenitic; highly resistant to the action of sulphuric acid.
21	0.3%Ti	Nickel-moly free stainless steel. Resistant to corrosion, malleable, low cost

3.3. Nickel chromium alloys

These alloys are rich in nickel with chromium and other metals.

Nickel and chromium readily dissolve.

Such alloys are very highly resistant to corrosion, acids alkalis and heat. Some of the grades possess good electrical resistivity, and some others are resistant to creep at high temperatures. There are five grades:

- Inconel containing 76%Ni, 15.8%Cr, 7.2%Fe, 0.2%Si, 0.1%Cu and 0.04%C; it is resistant to corrosion at high temperatures. It finds application in engineering goods for use in severely corrosive environment at high temperatures.
- Incoloy containing 32%Ni, 20.5%Cr, 46%Fe, 0.3%Cu and 0.04%C; it resists oxidation, carburization, corrosion and sulphur attack at high temperatures.
- Nimonic containing 58%Ni, 20%Cr, 17%Co, 2.5%Ti, 1.5%Al and 0.13%(max) C; it is

THE ANNALS OF "DUNAREA DE JOS" UNIVERSITY OF GALATI
FASCICLE IX. METALLURGY AND MATERIALS SCIENCE
N°. 1 - 2019, ISSN 2668-4748; e-ISSN 2668-4756
Article DOI: https://doi.org/10.35219/mms.2019.1.02

creep resistant at temperatures up to 920 °C. It is used in gas turbine blades and discs, hot-working tools.

- Nimocast containing 76%Ni, 19%Cr, 0.3%Mn, 0.3%Cu, 0.4%Ti, 0.3%Al, 1.5%Co and 0.1%C; it resists oxidation at temperatures up to 1100 °C. It is a casting alloy.
- Nichrome with two sub-grades namely, "chronin" containing 80%Ni and 20%Cr or "ferrochronin" containing 60%Ni, 15%Cr and 25%Fe. Both possess high electrical resistivity and resistance to thermal shocks due to repeated heating and cooling. They are used in heating elements of electric furnaces, toasters, stoves, etc. The former is suitable for use at temperatures up to 1150 °C and the latter, up to 800 °C.

3.4. Other alloy steels

These can be made by adding some chromite directly to steel furnaces along with ferrosilicon as reductant or, more commonly, by adding a suitable type of ferrochrome depending on the composition of the alloyed product aimed at. Some important types of products are:

3.5. Chromium metal

Until 1950s, metallic chromium used to be made by the aluminothermy route. It involved smelting of chromic oxide. The grade of the metal was 97% (min) Cr and 1% (max) Fe. In this method, chromite is first oxidized by air in molten alkali to yield sodium chromate ($Na_2Cr_2O_4$), which is converted to Cr_2O_3 (chrome oxide green) by dissolving it in water. The oxide is then precipitated and reduced by carbon. The metal thus obtained is further reduced and refined by aluminium powder. But the method is costly. Alternatively, the final refining can be done by using silicon as reductant. The common method nowadays is by electrolysis.

This involves dissolution of Cr_3O_3 in sulphuric acid to give an electrolyte. In a process developed by the US Bureau of Mines, the electrolyte was made from high carbon ferrochrome. The purity of electrolytic chromium is 99% (min) Cr. There are three types of chromium metal produced:

- High carbon, containing 87% (min) Cr and 9-11%C;
- Low carbon, containing 97% (min) Cr and 0.1% (max) C;
- Electrolytic, containing 99.5%Cr and 0.2%C.

3.6. Nonferrous alloys

Since there is no iron in such alloys, ferrochrome cannot be used as additive. Instead, chromium metal is used. Stellite, chromin are example of such alloys.

3.7. Foundry

The use of chromite sand as moulding medium was first practised in the 1950s in South Africa, for producing manganese and steel castings. It is used when a refractory medium is required as in the case of casting of metals with high melting point, where siliceous sand is not suitable.

The high fusion temperature, resistance to thermal shocks and chilling effect of chromium are the main criteria. Besides, the brittleness and uneven fracture make it easy to crush into angular grains.

The high fusion temperature and resistance to thermal shocks prevent the casting from damaging the moulding surface. The chilling effect facilitates the quick solidification of the casting. Preparation of chromite for this use involves crushing, washing and screening, and freeing it from impurities such as silica, talc, serpentine and asbestos by heavy media separation.

3.8. Chrome-plating

Chrome-plated surfaces have a bright bluish white finish with a high reflecting power. Such surfaces also possess a fair degree of electrical resistance. The corrosion resistance, high reflecting power and relatively low electrical conductivity of chromium are the chief criteria.

But Chromium plating is not just for imparting a durable and decorative finish to articles of common use [14], it is also done to resize machine parts by thickening their surfaces, to improve wear resistance of tools, and to line pump rods, engine cylinders and machine gun barrels. Chrome-plating is achieved by precipitation of chromium in an anodizing bath containing chromic acid through electrolysis.

3.9. Metallization

Chromium is used to metallize surfaces to make them corrosion-resistant [15]. Metallization is the process in which very small globules of a liquid metal are blown by a spray gun and sprayed on other metal surfaces to improve corrosion or wear resistance. The surface to be sprayed is first roughened by rough-machining or rough-grinding. The molten globules of metal, on being sprayed, immediately solidify and interlock by flattening.

THE ANNALS OF "DUNAREA DE JOS" UNIVERSITY OF GALATI
FASCICLE IX. METALLURGY AND MATERIALS SCIENCE
N°. 1 - 2019, ISSN 2668-4748; e-ISSN 2668-4756
Article DOI: https://doi.org/10.35219/mms.2019.1.02

3.10. Chemicals

The important chemicals are sodium dichromate, lead chromate, chromates of zinc and barium, chromic oxide, chromic acid, basic chromium sulphate, potassium dichromate, hydrated sodium chromate, potash-chrome alum and chromium dioxide.

Sodium dichromate ($Na_2Cr_2O_7$) is the mother chemical from which most of the other chemicals are derived. It is produced directly from chromite. Ground chromite is first roasted with soda ash and lime in the presence of oxygen to separate the impurities iron, alumina and silica of the ore, and to yield a mixture containing sodium chromate, which is extracted by quenching in water and leaching.

It is treated with sulphuric acid to finally produce a commercial grade of sodium dichromate. Both the intermediate product sodium chromate and the final product sodium dichromate are important industrial chemicals used for leather-tanning and for organic chemical oxidation, for bleaching of oils, fats and waxes, and as additive in drilling mud to prolong the life of drill strings.

Lead chromate ($PbCrO_4$) in pure form supplies the chrome reds. By mixing it with other substances the painters make various yellow pigments. When mixed with Prussian blue, it yields green pigments. It is a natural occurring mineral also – "crocoite" or "red lead", and the Siberian red lead is prized as a red pigment for oil. But the synthetic chemical, being more easily available and cheaper, is more popular.

Chromates of zinc and barium ($ZnCrO_4$ and $BaCrO_4$) are extensively used for colouring linoleum, rubber and ceramics.

One of chromic oxide (Cr_2O_3) products called "chrome green" contains 97-99% of this chemical, and is a green pigment used in paints particularly for outside applications required to withstand severe weather conditions. Other uses include manufacture of linoleum, ceramic glazes, coloured glass, stainless electrode, polishing material and chromium metal [15].

Chromium acid ($CrO_2(OH)_2$) solutions are used in chrome-plating, in anodizing of aluminium and in protection of magnesium-based alloys. It is also used as oxidizing agent and as laboratory reagent.

Basic chromium sulphate ($CrOHSO_4.Na_2SO_4$) is used in leather tanning to obtain what are called "wet blue chrome skins". Chrome-tanned leather has high wear resistance. This chemical is also used in the manufacture of "mineral khaki".

Potassium dichromate ($K_2Cr_2O_7$) is mainly used in the manufacture of safety matches and explosives. Other uses include printing ink, synthetic perfumery, adhesives, engraving and lithography, photography and film processing.

Hydrated sodium chromate ($Na_2CrO_4.4H_2O$) is used as an anticorrosive salt in cooling water and chilled brine systems, and as a component in inhibitor formulations.

Potash-chrome alum ($K_2SO_4.Cr_2(SO_4)_3.2H_2O$) is used for fixing bath in photography, as a mordant in textile industry, and for leather tanning.

Chromium dioxide (CrO_2) finds use in high quality magnetic audio and video recording tapes.

4. Conclusions

In a time of sophisticated and expensive technologies, even if chromite needs simple technology and is a simple oxide of iron, the importance of this oxide is increasing, watching the production profile and applications.

The technology of manufacturing is also very simple and with low cost.

The advantages offered by chromite (in different forms) properties are:

- Machinability;
- Resistance;
- Corrosion resistance to the attack of sulphuric acid.

References

[1]. Zhang W., Zhang P., Liu F., *Simultaneous oxidation of Cr(III) and extraction of Cr(IV) from chromite ore processing residue by silicate-assisted hydrothermal treatment*, Chemical Engineering Journal, vol. 371, p. 565-574, 2019.

[2]. Mishra U., Chandroth A., Basantaray A. K., *Assesing chromite ore processing residue (COPR) waste dump site using electrical resistivity tomography (ERT): a case study from Umaran, Kanpur, India*, Environmental Monitoring and Assessment, vol. 191, issue 8, 2019.

[3]. Gervilla F., Asta M. P., Fanlo I., *Diffusion pathways of Fe^{2+} and Fe^{3+} during the formation of ferrian chromite: a mu XANES study*, Contributions to Mineralogy and Petrology, vol. 174, issue 8, 2019.

[4]. Song Y., Li J., Peng M., *Identification of Cr(VI) speciation in ferrous sulfate-reduced chromite ore processing residue (rCOPR) and impacts of environmental factors erosion on Cr(VI) leaching*, Journal of Hazardous Materials, vol. 373, p. 389-396, 2019.

[5]. ***, *ASM Handbook, vol. 9, Metallography and Microstructures*, ASM International, Materials Park, OH, 2004.

[6]. Su B., Hu Y., Teng F., *Light Mg isotopes in mantle-derived lavas caused by chromite crystallization, instead of carbonatite metasomatism*, Earth and Planetary Science Letters, vol. 522, p. 79-86, 2019.

[7]. Steyn A., Kemper C., Schuer T., Zietsman J., Weisweiler E., *Understanding the energy consumption of melt-ing chromite-lime mixtures*, Proceedings of EMC, p. 1, 2019.

[8]. Muhammad F., Xia M., Li S., *The reduction of chromite ore processing residues by green tea synthesized nano zerovalent iron and its solidification/stabilization in composite geopolymer*, Journal of Cleaner Production, vol. 234, p. 381-391, 2019.

[9]. Camalan M., Hosten C., *Assessment of grinding additives for promoting chromite liberation*, Minerals Engineering, vol. 136, p. 18-35, 2019.

[10]. ***, *ASM Handbook, vol. 1, Properties and Selection: Iron, Steels, and High-Performance Alloys*, ASM International, Materials Park, OH, 1990.

[11]. Pakzad E., Ranjbar Z., Ghahari M., *Synthesized of octahedral cupper chromite spinel for spectrally selective absorber (SSA) coatings*, vol. 132, p. 21-28, 2019.
[12]. Li C., Barasa G. O., Zerihun G., *Structure and magnetic switching effect in iron-doped europium chromite ceramics*, Journal of Alloys and Compounds, vol. 787, p. 463-468, 2019.
[13]. ***, *ASM Handbook, vol. 2, Properties and Selection: Nonferrous Alloys and Special-Purpose Materials*, ASM International, Materials Park, OH, 1991.
[14]. Farrelly L., *Basic Architecture - Construction and Materiality*, AVA Publishing SA, 2009.
[15]. Chatterjee K. K., *Uses of Metals and Metallic Minerals*, New Age International (P) Ltd. Publishers, 2007.
[16]. Duggal S. K., *Building Materials 3rd Edition*, New Age International (P) Ltd. Publishers, 2008.

THE ANNALS OF "DUNAREA DE JOS" UNIVERSITY OF GALATI
FASCICLE IX. METALLURGY AND MATERIALS SCIENCE
N°. 1 - 2019, ISSN 2668-4748; e-ISSN 2668-4756
Article DOI: https://doi.org/10.35219/mms.2019.1.03

HEMATITE. PROCESSING AND APPLICATIONS

Mircea DOBRESCU, Marius VASILESCU
Politehnica University of Bucharest, Romania
e-mail: vmarius_sim_pub@yahoo.com

ABSTRACT

In the paper are shown the history, processing and applications of hematite.

Hematite is an oxide of iron having the composition Fe_2O_3. Pure hematite, also called "red ore" contains 70% Fe.

Manufacturing processes for steel are made in furnaces (open hearth, Bessemer processes, oxygen furnace, electric arc furnaces).

Hematite is used both as an ore of iron and as an industrial mineral in order to produce intermediate products such as: - Sinter; - Pellets; - Pig iron; - Malleable cast iron; - High duty cast iron; - Wrought iron; - Directly reduced iron; - Iron carbide; - Steel.

KEYWORDS: hematite, processing, applications

1. Introduction

Hematite is an oxide of iron having the composition Fe_2O_3. Pure hematite, also called "red ore" (in fact, the name hematite comes from the word "hemo" meaning blood), contains 70% Fe [1]. Almost pure hematite occurs on the edge of Cockatoo island in Western Australia. But generally, it contains various other constituents, namely SiO_2, Al_2O_3, P, S, TiO_2, Zn, Cu, As, Sn, Cr and Ni [2]. Out of these, the first four are common in Indian hematite.

In nature, its structure varies from compact specular and columnar to foliated (micaceous hematite). When mixed with clay or sand, it is called argillaceous hematite or clay iron stone. The coarse-grained variety with brilliant metallurgical luster is known as "specular iron ore", [3]. Hematite is the most widely distributed and mined iron ore. Mining is generally by open cast method.

The only exceptions are a few underground mines in USA and the Hiparsa mine in Argentina, which was mined by underground method until 1993, and plans were afoot in 2004 to revive it. Kryvy Rich of Ukraine and Carajas of Brazil are regarded as the two largest deposits of the world. As in 2004, the estimated reserves in the former were 24 billion tonnes and, in the latter, 18 billion tonnes (66% Fe).

In India, hematite occurs mainly as banded formations (e.g., banded hematite quartzite or BHQ) belonging to the Precambrian age, and is fairly widely distributed in the states of Jharkhand, Orissa, Chhattisgarh, Kamataka, Goa and Maharashtra. Iron ore bodies occur as pockets at the top of these formations enriched in iron due to weathering and leaching out of silica [4]. The hematite iron ore of India is generally high-alumina and high-silica at places containing up to 6% Al_2O_3 and up to 8% SiO_2.

The other main impurity is phosphorus (up to 0.1%). The ore occurs in both "lumps" and "fines" forms. In some places of eastern India, very high grade ultra-fine blue dust occurs in significant quantities.

In the evolution of civilization, the year 1800 BC is an important milestone. Right since the paleolithic age through the Neolithic age, copper age and thereafter bronze age till 1800 BC, the entire period is referred to as "old world". The oldest evidence of manufacture and use of iron dates back to the year 1800 BC, and this is regarded as the beginning of "iron age" and what is referred to as the "new world".

Invention of iron set off a chain of technological revolutions which has been continuing ever since. But the use of hematite is believed to be known to man long before the invention of iron metal. In rock paintings discovered by archaeologists in Mirzapur district of Uttar Pradesh, India and believed to be 8000 years old, various colours have been observed. It has been concluded that among different colours, different shades of red were obtained from hematite. In the beginning of iron age, it is believed that some pure iron materials were accidentally found and such iron was used during the times of Pharaohs in Egypt.

Most probably the iron was sourced to some meteorites, which used to be referred to as "star metal" or "stones from heaven" or "gift of the gods".

THE ANNALS OF "DUNAREA DE JOS" UNIVERSITY OF GALATI
FASCICLE IX. METALLURGY AND MATERIALS SCIENCE
N°. 1 - 2019, ISSN 2668-4748; e-ISSN 2668-4756
Article DOI: https://doi.org/10.35219/mms.2019.1.03

Manufacturing of iron is believed to begin in around 1200 BC. Steel making technology more or less coincided with the beginning of Christian era. In the 14th century, large scale operations started with the invention of blast furnace in Great Britain.

Initially, for a couple of hundred years, wood charcoal was used as fuel; but later on, in 1710, coal revolutionized the iron-making technology. Large scale manufacturing of steel became possible only after 1856, when Bessemer invented his conversion process.

In USA, although the use of iron ore was known in 1608, organized iron industry began in 1844 after the Lake Superior deposits were discovered. In India, iron-made weapons were mentioned in mythology, but the first recorded history regarding the use of iron-made weapons dates back to the time of Alexander's invasion (326 BC). Iron casting technology was not known in those days, and canons and guns were mostly made by forging wrought iron.

The iron pillar in New Delhi (310 AD) was an excellent example of forged wrought iron. The technology for melting and shaping of "wootz", a kind of ultra-high carbon steel containing 1.5% C also known as "Damascus steel" or "Ukku" or "Bulat" or "Ondanique", which used to be exported to Damascus from India for making "Damascus swords", was known in India as early as 300 BC. The indigenous iron and steel industries, though small scale and unorganized, were widely spread throughout India during the ancient and Medieval periods. During 1778-1795, some sporadic operations were carried out by M/S Farquhar & Motte in Birbhum district of Bengal. Their operations were based on local methods, most probably using charcoal, and were eventually abandoned.

The European methods of smelting iron ore were successfully adopted for the first time in 1830, when the India Steel Iron and Chrome Company was established by J. M. Heath and a pig iron plant based on ore from Salem district of Tamil Nadu, was set up in Porto Novo in South Arcot district of Tamil Nadu. These works were taken over in 1883 by Porto Novo Steel & Iron Co. and the East Indian Iron Co, which expanded the industry by starting additional pig iron plants in UK. But because of bad financial management, the company finally closed down in 1867. During the period 1839-1875, unsuccessful attempts for manufacturing iron using charcoal, were made in Bengal, in Nainital district of present Uttaranchal state and in Indore, Madhya Pradesh.

By 1875, both coal mining and coke manufacturing had commenced in Bengal, and using coke based on coal from Raniganj coal field, pig iron manufacturing was started in Kulti and Hirapur in Bengal by a private company, which was taken over by the government in 1884 and again resold in 1889 to Bengal Iron &Steel Co. Ltd. (renamed as BengalIron Co. Ltd. in 1919). In that plant, steel was manufactured during a brief period 1903-1905, in an open-heart furnace.

In 1911, Tata Iron &Steel Co. established its plant in Jamshedpur in present Jharkhand. This was followed by the furnaces of Indian Iron & Steel Co. at Burnpur in present West Bengal in 1992, which took over the Kulti plant of Bengal Iron Co. Ltd. in 1936. Based on pig iron produced in the Hirapur works, Burn & Co. started manufacturing steel products at Kolkata in 1937. Meanwhile, in 1933, Mysore Government started a charcoal-based iron plant at Bhadravati in 1993.

Table 1. *Hematite production in India*

Years	Hematite production [t]
1900	70000
1940	3.00 million
1950	3.14 million
1960	16.61 million
1970	31.37 million
1980	41.94 million
1990	54.58 million
April, 2000 – March, 2001	80.59 million
April, 2001 – March, 2002	96.96 million
April, 2004 – March, 2005	142.71 million

These plants kept on introducing newer and newer technologies and built the foundation of the Indian iron and steel industry before its independence in 1947. After independence, in 1953, the Government of India set up Hindustan Steel Ltd., and three steel plants came up at Rourkela in Orissa, at Bhilai in present Chhattisgarh and at Durgapur in West Bengal. This company was later renamed as Steel Authority of India Ltd. (SAIL), and a few more plants manufacturing steel and special steels at

THE ANNALS OF "DUNAREA DE JOS" UNIVERSITY OF GALATI
FASCICLE IX. METALLURGY AND MATERIALS SCIENCE
N°. 1 - 2019, ISSN 2668-4748; e-ISSN 2668-4756
Article DOI: https://doi.org/10.35219/mms.2019.1.03

Bokaro in present Jharkhand, at Slem in Tamil Nadu and at Chandrapur in Maharashtra were added to it.

By the early 21st century, there were 11 primary iron and steel plants and a number of secondary steel plants. The production of pig iron, which was a meagre 12700 tonnes during the 5-year period 1875-1879, rose to 1.67 million tonnes of pig iron plus 1.46 million tonnes of steel ingots in 1950, and then to 4.07 million tonnes of pig iron plus 31.63 million tonnes of steel in 2001-02 compared to world steel production of 965 million tonnes during 2003.

History of iron ore (hematite) mining in India is as old as the history of iron and steel production. The recorded history of production of hematite is presented in Table 1.

Contrary to steel, the iron ore production of India compares better to the world production which stood at 1098 million tonnes during 2003.

2. Criteria of use

Hematite is used both as an ore of iron and as an industrial mineral. Its typical characteristics that make it suitable for different uses are as follows:

- The chemical composition is ferric oxide (Fe_2O_3) with the highest degree of oxidation possible. The most important element in it is iron, the theoretical content of which is 70% Fe. But in nature, chemically pure hematite is difficult to mine economically due to its physical properties, and some residual impurities (e.g., Al_2O_3, SiO_2) get into the mineral. Because of the highest degree of oxidation, this compound of iron is saturated with oxygen and it is, therefore, easier to reduce (in case of under-saturation, the affinity between iron and oxygen is somewhat strong and it becomes relatively difficult to separate the two elements).
- Physically, pure hematite is a medium hard mineral, its hardness being in the range of 5.5-6.5 in the Mohs scale [5]. But in nature, the economically significant hematites occur near the surface as a result of erosion of silicates. Hence these hematites are softer and also porous, i.e., not very dense or compact even when they are in lumpy form. Besides, they occur also as friable ore prone to breaking into fines during mining and handling.
- It is resistant to corrosion [5].
- It has a high refractive index ranging in values from 2.94-3.22 when in the form of very thin laminae as in the case of micaceous hematite [6]. Refractive index is a measure of the change in direction that oblique light rays undergo when travelling from air to another medium (in this case the hematite laminae) and is expressed with reference to air (refractive index practically 1). Refractive index has some relation to luster.
- Although colour of hematite is dark grey to black, it is blood red when in powder form.
- The micaceous hematite has a mica-like platy structure. It crumbles easily to powder.

3. Applications

Hematite is mostly used to produce some intermediate products, and in a lesser degree, some directly usable products. These, as well as the relatively less popular ones are sinter, pellets, pig iron, cast iron, malleable cast iron, high duty cast iron, wrought iron, directly reduced iron, iron carbide and steel.

3.1. Sinter

One of the methods to convert iron ore fines is sintering [7]. By application of just enough heat to fuse the corners of the ore particles, they are made to join together to form a lumpy mass.

This product is called "sinter". Sinters are not very compact, having 11-18% porosity, because some comers of a particle melt, and not the entire particle. But, at the same time, they are tough enough to withstand the stress within a blast furnace. These are good substitutes of natural lumps, and can be blended with the latter in the blast furnace charge.

For optimizing productivity of blast furnaces, the fluxing material i.e. limestone powder (90% 3 mm size) is intimately mixed at the sintering stage itself. The limestone adds strength to the sinter if it is distributed uniformly in the matrix. This super-fluxing of sinters eliminates the need for raw limestone charge [8]. Coke breeze (85% 3 mm size), dolomite mill scales and flue dust fines along with limestone, can also be mixed to make the sinter a completely self-sufficient feed. Sinters are made on rectangular flat tops of cylinders tapering downward to grate bottoms.

3.2. Pellets

Very fine particles (size of microns) cannot be sintered as they will fuse altogether. So, they are formed into spherical objects called "pellets", and the process is called palletisation. To the iron ore fines, 0.5-3.0% bentonite is added as binder [9].

Coke breeze and some flux (limestone) may also be added. The mixture is placed in cones, drums or discs, out of which discs are relatively more flexible with regard to types of ore and they can be controlled better. A disc pelletizer is a rotating inclined flat plate table. The particles gradually coalesce – first into very small pellets, which go on taking more and more

THE ANNALS OF "DUNAREA DE JOS" UNIVERSITY OF GALATI
FASCICLE IX. METALLURGY AND MATERIALS SCIENCE
N°. 1 - 2019, ISSN 2668-4748; e-ISSN 2668-4756
Article DOI: https://doi.org/10.35219/mms.2019.1.03

particles and keep enlarging in size till they attain specified sizes. Water is sprayed as required.

These are called green pellets, and the operation is called "balling". The control is affected by changing the angle (20-80°) and the r.p.m. (+8) of the disc. The green pellets are then heat treated at a temperature of above 1200 °C – generally around 1315 °C – in grate kilns, followed by air cooling with a view to obtaining necessary strength.

The quality of pellets usable in the blast furnace is mainly determined by their characteristics of size, crushing and abrasion resistance, reducibility and the free growth and porosity index. The values of the parameters are determined through industrial scale experiments by setting the prerequisite that when using pellets in the blast furnaces, their diameters should be in range 9.5-25.0 mm and within this range the size fraction 10-15 mm should represent a minimum of 85%. Values of 6% for crushing and 5% for abrasion (drum values i.e., percentage of pellets not able to withstand the stress in a standard rotating drum) are considered acceptable [10].

A reducibility index of 0.7-0.8% per minute for basic pellets is considered good. A maximum of 14% free growth index (increase in volume expressed as a percentage of initial volume under test conditions i.e., 1050 °C for 30 minutes in a CO blow). Porosity should be between 20% and 30%. Unlike sinter, even if limestone is added to raw mix for pellets, supplementary limestone addition in blast furnace is necessary [11].

A minimum of 25% of pellets in the blast furnace charge has been found to have a salutary effect on productivity.

3.3. Pig iron

Pig iron is both an intermediate product for steel manufacturing and a material for direct use in casting (cast iron) or fabricating (wrought iron) parts of machines, structures, etc. In old references, pig iron for these different types of uses used to be mentioned as "foundry" and "basic" grades of pig iron.

Nowadays, this classification is no longer used. A special type of low-phosphorus pig iron is used for making "spun pipes". Pig iron is produced in tall blast furnaces into which, conventionally, a charge of lumpy iron ore (either natural lumps or fines converted to this form), limestone, coke and manganese oxide is dripped from the top, and subjected to blasts of air through the sides at the lower zone; and to which some initial heat is applied.

So far as natural lumps are concerned, they are seldom mined in the required grades, and it has now become an established practice to subject them to some preparation or beneficiation. The conventional methods consist of plain water washing and scrubbing, tromelling, wet screening, classification, and jigging or cycloning. But these methods achieve only limited success inasmuch as the ultra-fine grains of Al_2O_3 are not eliminated, and also considerable iron values are lost in the slimes.

A specialized method consists in the selective dispersion (flocculation) of aluminous gangue from a dilute slurry system using organic/inorganic additives (e.q., sodium humate, starch, polyacrylamide, phenol- and lignite-based polymer additives etc. [12].

The reactions within a blast furnace are very complex. But the essential principle can be explained thus. The carbon of the coke reacts with the oxygen of the air to produce heat and carbon monoxide (CO). The heat melts the charge, and the CO, being unsaturated oxide, combines with the oxygen of the hematite reducing the latter to metallic iron, and generating carbon dioxide (CO_2), [12, 13].

The impurities such as SiO_2 and Al_2O_3 present in the hematite react with the limestone producing lime-alumina silicates (with heavy metal oxides) called "slag" and a mixture of CO, CO_2 and NO_2 that escape as top gas. The molten slag, being lighter than and immiscible in the molten iron metal, floats on the surface of the latter.

The upper layer of the molten slag is tapped out through an outlet at the upper level of the blast furnace, processed depending on its future use and stacked separately where it cools and solidifies. The molten iron of the blast furnace is transferred into the pig bed (sand moulds for ingots) or mobile ladles.

In fact, the name "pig iron" originated in the early days of iron ore reduction when the total output of the blast furnace was sand-cast into masses of iron resembling the shape of a reclining pig. The oldest method of pig-casting in sand beds has now been replaced by pig-casting machines. Pig iron contains 3-4%C in general (may be up to 6%) besides little quantities of manganese, phosphorus, sulphur and silicon. High carbon content makes it hard and brittle.

Depending on the form in which the carbon occurs within pig iron, it can be either grey pig iron or white pig iron. In grey pig iron, carbon is precipitated in the fractures as graphite flakes; in the white pig iron, it is dissolved as iron carbide. White pig iron is harder and more brittle in comparison to grey pig iron.

Both types of pig iron are the basic raw materials for making downstream products such as cast iron, wrought iron, spheroidal graphite iron and steel. The differences amongst these products lie mainly in the carbon content.

3.4. Cast iron

Pig iron ingot or cast-iron scrap is remelted in cupola furnaces, carbon and other elements are added

THE ANNALS OF "DUNAREA DE JOS" UNIVERSITY OF GALATI
FASCICLE IX. METALLURGY AND MATERIALS SCIENCE
N°. 1 - 2019, ISSN 2668-4748; e-ISSN 2668-4756
Article DOI: https://doi.org/10.35219/mms.2019.1.03

according to the required specification, and cast in foundry moulds in the desired shapes and sizes as per the end products.

The cast iron made from white pig iron is called "white cast iron"; and that from grey pig iron, "grey cast iron". White cast iron is used where the components require a hard wear-resistant surface. It is called "chilled cast iron" and is produced by sudden cooling of the melt to form a hard zone.

The carbon is in form of iron carbide and its content varies from 3-4%. The other elements are silicon (0.5%), sulphur (0.1%), phosphorus (0.1%) and manganese (0.8%). It is used to make crusher jaws of rock-cutting machines, metal and paper rollers, ball milling plants, etc.

Grey cast iron also contains 3-4% C, but as graphite; other elements are silicon (2-3%), sulphur (0.08%), phosphorus (0.15%), manganese (0.8%). It is less brittle and more machinable than white cast iron, and is used for making machine bases, engine blocks, brackets, pulleys, gears, etc.

3.5. Malleable cast iron

Malleable cast iron is produced by giving the white cast iron a modifying heat treatment involving slow heating for long duration (annealing). It is fairly ductile with 4-14% elongation (hence it is also called "ductile iron"), capable of withstanding suddenly applied stress, corrosion resistant, strong, tough and machinable.

Carbon content in the form of iron carbide varies from 2.5-3.0%, silicon 0.5-1.1%, sulphur 0.10-0.15%, Phosphorus up to 0.1% and manganese 0.4%. It is used to make transmission line hardware, water fittings, tools, conveyor links, etc.

3.6. High duty cast iron

High duty cast irons are stronger than grey cast iron in which much of the carbon is originally in the form of coarse flakes. These contain metals such as nickel, chromium, copper and also some other substances such as calcium silicide, cerium or magnesium may also be added. Its carbon content may vary from 2.5-3.5%, silicon from 1.5-2.5%, sulphur 0.02-0.1%, phosphorus from 0.02-2.0% and its manganese content is around 0.8 %.

If calcium silicate is added to the liquid metal, graphite is transformed into fine flakes, and the cast iron is known as "mechanite cast iron". It is used to make products like gears, fly wheels etc., where strength is needed. If cerium and/or magnesium is added to the liquid metal, then the graphite is transformed to fine spheroidal form, and the cast iron is called "spheroidal graphitic cast iron or SG cast iron". The metal may be annealed before use, in which case the elongation increases by up to 20%, and the product is called "ductile iron". It is used for making crank shafts, metal working rolls and for other works where high strength is needed.

3.7. Wrought iron

Wrought iron is defined by the American Society for Testing Materials (ASTM) as "a ferrous material, aggregated from a solidifying mass of pasty. Crystalline particles of highly refined metallic iron, with which, without subsequent fusion, is incorporated a minutely and uniformly distributed quantity of slag".

The main distinguishing characteristics are:

- Carbon is practically absent, i.e. it is an almost pure form of pig iron;
- It must contain some slag (1-3%) ferrous silicate), which is the result of oxidizing reactions of refining, and which is uniformly distributed as minute threads imparting a fibrous structure (cf. crystalline structure of steel). Because of the absence of carbon, it is highly malleable and it can be shaped into useful articles by reheating and forging. Wrought iron was the product in use since the prehistoric age till the advent of the age of steel in 1856.

The furnace used was small and the heat applied was low – up to 1500 °C or so, i.e., less than the melting point of iron (1800 °C). The technology was somewhat improved by H. Court in 1784.

But even then, it was limited by the small size of the furnace (called "puddling furnace") and low temperature that could heat the mixture of ore and flux to a semisolid mass, and it required constant manual stirring for the oxidizing reactions to take place.

As, unlike in steel-making, the metal and the slag were not in molten state, they could not be separated and thus the slag got thoroughly impregnated in the metal. By squeezing and rolling the semisolid mixture, the content of slag could, at best, be reduced, but not totally removed. This is how characteristic fibrous structure was formed in wrought iron.

After the advent of steel, the highly labour-intensive nature of the technology of making wrought iron and its low productivity resulted in fast obsolescence of this primitive product, but, even then, it continued to find some use where corrosion and shock-resistance were important criteria.

3.8. Directly reduced iron

Directly reduced iron (solid reduction), when in lump form, is called "sponge iron"; when in briquette

THE ANNALS OF "DUNAREA DE JOS" UNIVERSITY OF GALATI
FASCICLE IX. METALLURGY AND MATERIALS SCIENCE
N°. 1 - 2019, ISSN 2668-4748; e-ISSN 2668-4756
Article DOI: https://doi.org/10.35219/mms.2019.1.03

form, called "hot briquetted iron or HBI"; and when in liquid form, it is called simply "hot metal" [13]. All these products are feedstock for steel-making in electric arc furnaces.

These are produced by non-blast furnace methods, and the reduction of iron ore takes place either in solid state or in liquid phase. The technology was first tried on pilot scale in the 1920s, and the trials were intensified after 1939. At least, 32 processes have been investigated since 1939. The relatively more important and currently relevant processes can be grouped under the following generic names:

- Direct Reduction (DR);
- Smelting Reduction (SM);
- Plasmasmelt.

3.9. Iron carbide (Fe_3C)

Fe_3C is a reduced iron oxide with 5-6% chemically fixed carbon. It is a direct feed for steel-making and it provides added energy through the in-built carbon content. It is produced in a fluidized bed reactor through a gas-solids reaction. Preheated iron oxide fines (0.1-1.0 mm size) are supported in an upward stream of gas composed of CO, CO_2, H_2, CH_4 and water vapour at a temperature of 550-600 °C which is lower than the one required by sponge iron [13].

Hydrogen reduces iron oxide to iron which reacts with carbonaceous gases to produce Fe_3C. The viability of the technology depends on a steady and assured supply of natural gas. Its commercial viability has not been established in India.

3.10. Steel

Iron and steel scrap, sponge iron, hot metallic iron and pig iron – all are processed to obtain the end product steel (also called "plain carbon steel"). Steel is essentially a refined alloy of iron and carbon with carbon content lower than in pig iron – generally varying from 0.01-1.7%, but it may go up to 2% [14].

Total absence of carbon would make it very soft and unusable for most of the purposes. Steel-making is, therefore, nothing but the removal, by combustion, of the carbon contained in the iron.

As a result, the structure of the metal becomes more resilient, more flexible, stronger and better workable than iron. Besides carbon, sulphur and phosphorus are also removed by oxidation, a little manganese and silicon are added to improve the mechanical properties of steel (if too much of these are added, then the steel would be called "alloy steel").

For removing the impurities, coke and flux are charged along with the pig iron. Some iron ore is also added to the charge for providing oxygen for reaction with the fuel for heat generation and better operational control by which the impurities (including those in the fuel) are removed in the form of slag.

4. Conclusions

Hematite, an iron oxide, can be found in large deposits; it provides important estimated reserves, most in mined iron.

The two possibilities of using hematite are as iron ore and industrial mineral.

Hematite is useful in different forms and applications.

Now, the production of hematite is increasing due to its properties:

- Resistant to corrosion;
- Refractarity;
- Medium hardness;
- High degree of oxidation, so it is difficult to separate in the constitutive elements.

References

[1]. Ralls K. M., Courtney T. H., Wulff J., *Introduction to Materials Science and Engineering*, John Wiley & Sons, New York, 1976.
[2]. Smith W. F., Hashemi J., *Principles of Materials Sience and Engineering*, 4th edition, McGraw-Hill Book Company, New York, 2006.
[3]. ***, *ASM Handbook, vol. 9, Metallography and Microstructures*, ASM International, Materials Park, OH, 2004.
[4]. Glicksman M., *Diffusion in Solids*, Wiley-Interscience, New York, 2000.
[5]. Dowling N. E., *Mechanical Behavior of Materials*, 2nd edition, Prentice Hall PTR, Paramus, NJ, 1998.
[6]. McClintock F. A., Argon A. S., *Mechanical Behavior of Materials*, Addison-Wesley Publishing Co., Reading, MA, 1966, Reprinted by CBLS Publishers, Marietta, OH, 1993.
[7]. Jankovic A., *Iron Ore-Mineralogy*, Processing and Environmental Sustainability, p. 251-282, 2015.
[8]. Tolod K. R., Hernandez S., Quadrelli E. A., Russo N., *Studies in Surface Science and Catalysis*, vol. 178, p. 65-84, 2019.
[9]. Pawar R. C., Lee C. S., *Heterogeneous Nanocomposite-Photocatalysis for Water Purification*, p. 43-96, 2015.
[10]. Wagh A. S., *Chemically Bonded Phosphate Ceramics (Second Edition)*, Twenty-First Century Materials with Diverse Applications, p. 157-164, 2016.
[11]. Koy J., Ladebeck J., Hill J. R., *Studies in Surface Science and Catalysis*, vol. 119, p. 479-484, 1998.
[12]. Chen L., Xiong D., *Progress in Filtration and Separation*, p. 287-324, 2015.
[13]. Clout J. M. F., Manuel J. R., *Iron Ore-Mineralogy*, Processing and Environmental Sustainability, p. 45-84, 2015.
[14]. Dai H. X. *et al.*, *Process Mineralogy of an Oolitic Hematite Ore and its Implications for Mineral Processing*, Advanced Materials Research, vol. 567, p. 131-134, 2012.

THE ANNALS OF "DUNAREA DE JOS" UNIVERSITY OF GALATI
FASCICLE IX. METALLURGY AND MATERIALS SCIENCE
N°. 1 - 2019, ISSN 2668-4748; e-ISSN 2668-4756
Article DOI: https://doi.org/10.35219/mms.2019.1.04

PERFORMANCE ANALYSIS OF ELECTRIC VEHICLES AVAILABLE IN THE CURRENT AUTOMOTIVE MARKET

Florin MARIASIU[1*], Adela BORZAN[1], Marius S. MOTOGNA[2], Ioan SZABO[1]

[1]Technical University of Cluj-Napoca, Cluj-Napoca, Romania
[2]Porsche Engineering Romania, Cluj-Napoca, Romania
e-mail: florin.mariasiu@auto.utcluj.ro

ABSTRACT

In the current car market, electric vehicles have begun to be accepted more and more by consumers, which has led the conventional vehicles' manufacturers (and not only) to produce and sale a wider range of such vehicles. However, there is still a huge potential for development in this respect, with every car class still being available to accept new electric vehicle models. In this context, the present paper presents a research on identifying the main technical and performance characteristics of electric vehicles available in the current automotive market and establishing degrees of correlation between them. The strongest statistical correlation has been identified as finding that of the battery's energy capacity and the possible autonomy/range can be achieved for a full battery's charge.

KEYWORDS: electric vehicle, parameters, performance, autonomy, statistical correlation

1. Introduction

Lately, electric vehicles (EV) have gained popularity among consumers, and the motives behind them are many and diversified at the same time. The most important reason is related to their contribution to reducing greenhouse gas (GHG) emissions. In 2009, the transport sector has emitted 25% of the total GHG generated by the energy-related economic sectors. Electric vehicles (EV), in conditions of a sufficient penetration in the automotive market and the transport sector, are expected to further reduce the level of pollutant emissions, especially in large urban agglomerations [1].

This is not the only reason for bringing back to life the old and once dead (!) concept of using electricity as a source of energy for a vehicle's propulsion group, this time this concept of the electric vehicle being produced and developed now as a viable and commercial product available to all those interested. As a vehicle, an electric propelled/powered vehicle is silent, easy to maneuver, has no fuel costs and maintenance (maintenance) associated with conventional vehicles equipped with internal combustion engines. As a means of urban transport, in the conditions of large urban agglomerations with a high degree of pollution due to transport, it is (proves to be) a very useful means of transport.

Not surprisingly, at present, the growth rate of the number of electric and hybrid vehicles in the car market is much higher than the growth of the market for conventional cars equipped with an internal combustion engine (thermal engine), and in some regions around the globe (car) electric and hybrid vehicles end up with vehicles equipped with internal combustion engines (ICE), in terms of the number of units sold annually.

With its demographic characteristics, technological development and environmental challenges, China has become the largest market for electric vehicles, with 56% of the total world sales in 2018 (compared to a market share of just 6.3 % in 2013 and 35.4% in 2017 [2]). In this context, China has the largest number of electric vehicle and components manufacturers, which together sold 1200000 vehicles based on electric propulsion in 2018 (compared to 663,000 units in 2007). This huge market also attracted most car manufacturers around the world - Ford, Volkswagen, Volvo and General Motors - which have their own versions of electric vehicles on the Chinese market and are ready to introduce more / diversified models in the coming years [3].

THE ANNALS OF "DUNAREA DE JOS" UNIVERSITY OF GALATI
FASCICLE IX. METALLURGY AND MATERIALS SCIENCE
Nº. 1 - 2019, ISSN 2668-4748; e-ISSN 2668-4756
Article DOI: https://doi.org/10.35219/mms.2019.1.04

From a global perspective, compared to 2017, in 2018, the sales of electric vehicles grew by 79% in the US; Europe recorded an increase of 34%, while Japan fell by 6% (!). From companies' perspective, BYD's products dominated the world market with a 13.2% share, followed by Tesla in the second place (9.9%); the other major contributors being the Volkswagen Group, the BMW Group and Nissan. However, Tesla S remained the best-selling electric vehicle in the world in 2016, with 50,935 units sold, followed by Nissan Leaf EV with 49,818 units [4]. The top ten best-selling electric vehicles world-wide is shown in Figure 1.

The US market was predictably dominated by the Tesla S model in 2016 (28,821 units sold) and the Chevrolet Volt EREV model sold in 24,739 units, making it the second place. The third place was made by another model Tesla, Model X, with 18,192 SUVs also sold in 2016 [5]. Renault Zoe was Europe's most sold electric vehicle in 2016, with 21,338 units sold, followed by Nissan Leaf with 18,614 units. In the PHEV segment, Mitsubishi Outlander PHEV was the market leader in Europe in 2016, with 21,333 units sold and Volkswagen Passat GTE held its second position with 13,330 units [6]. The purpose of this article is to identify the possible existence of correlation relationships between several constructive and functional parameters characteristic of existing electric vehicles in the current automotive market, in order to provide a primary image of setting the parameters for designing and developing a new electric vehicle model.

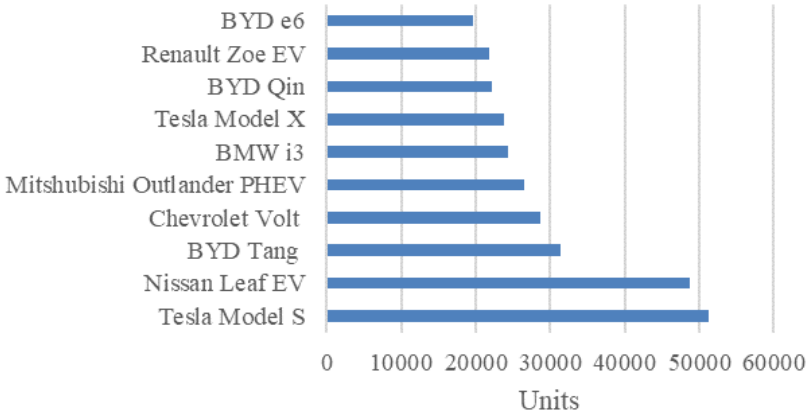

Fig. 1. *Top 10 best-selling electric and hybrid vehicles worldwide in 2016* [4]

2. Method and methodology

The development and production of electric vehicles has been achieved through two major approaches by electric vehicle manufacturers in the current automotive market:

• Using a platform (chassis' structure and body) already existent in the manufacturer's production portfolio, the major change is the replacement of an internal combustion engine-based powertrain group with an electric propulsion group.

• Designing a new platform concept dedicated to the optimal placement in terms of weight distribution of the electric propulsion group and battery as a source of energy for it.

Table 1. *Technical characteristics of EV premium class*

EV type Premium class	Power [kW]	Autonomy [km]	Battery energetic capacity [kWh]	Acceleration [0-100 km/h] sec	Maximum speed [km/h]
Jaguar I-PACE electric	300	386	90	4.8	200
Tesla Model 3	211	354	75	5.4	210
Tesla Model S	285	416	75	5.2	190
Tesla Model X	193	380	75	6.0	210
Tesla Roadster	514	1000	200	1.9	400
Porsche Taycan	440	500	90	3.5	250
Audi E-Tron electric	300	328	95	5.5	200

THE ANNALS OF "DUNAREA DE JOS" UNIVERSITY OF GALATI
FASCICLE IX. METALLURGY AND MATERIALS SCIENCE
N°. 1 - 2019, ISSN 2668-4748; e-ISSN 2668-4756
Article DOI: https://doi.org/10.35219/mms.2019.1.04

In both above-mentioned approaches, it has been attempted to reduce the overall weight of the vehicle, because weight is an important parameter in achieving a maximum distance in km that can be covered with a single (full) charge of the battery (EV's autonomy).

For the global performance and technical characteristic analysis of electric vehicles present in the current car market, the main models available for sale in Europe (23), from a number of 14 manufacturers and divided into 3 characteristic classes were considered.

The main parameters considered for the proposed analysis were the vehicle type, the power of the electric engine, the energetic capacity of the battery, the acceleration and the maximum speed. These data are presented in Tables 1-3.

Table 2. *Technical characteristics of EV compact class*

EV type Compact class	Power [kW]	Autonomy [km]	Battery energetic capacity [kWh]	Acceleration [0-100 km/h] sec	Maximum speed [km/h]
Honda Clarity electric	120	143	25.5	7.6	140
Ford Focus electric	107	185	35	9.9	135
Hyundai IONIQ	88	200	28	9	165
Hyundai KONA I e	99	300	39	9	160
Hyundai KONA II e	150	415	64	7	180
Nissan LEAF	110	242	40	8	140
Nissan LEAF e-Plus	160	360	60	6.3	200
Chevrolet BOLT	149	383	60	6.5	150
Volkswagen e-Golf	98	190	35.8	9.6	149
KIA NIRO all-electric	149	384	64	7.8	167
KIA SOUL all-electric	89	178	30	11	144

Table 3. *Technical characteristics of EV small class*

EV type Small class	Power [kW]	Autonomy [km]	Battery energetic capacity [kWh]	Acceleration [0-100 km/h] sec	Maximum speed [km/h]
BMW i3	125	180	33.2	7.3	150
Mini Cooper e	125	320	42	6.7	160
Fiat 500e	83	135	24	8.4	141
Mitshubishi i-MiEV	48	160	35	13	128
Smart FORTWO e	30	161	17.6	11.5	130

The conjugate parameters for the analysis were: autonomy versus battery capacity, (engine) power vs. battery capacity, acceleration vs. maximum speed and energy efficiency of the vehicle reported over the distance (in km) possible to travel with a consumption of 1 kW, in an attempt to establish whether there is a dependency relationship between them. Parameter dependence may provide a primary picture of the initial design process of a new electric vehicle.

3. Results and discussions

The results obtained by the comparative analysis of two by two parameters characteristic of the electric vehicles considered in this study are presented in Figures 2 - 5.

THE ANNALS OF "DUNAREA DE JOS" UNIVERSITY OF GALATI
FASCICLE IX. METALLURGY AND MATERIALS SCIENCE
Nº. 1 - 2019, ISSN 2668-4748; e-ISSN 2668-4756
Article DOI: https://doi.org/10.35219/mms.2019.1.04

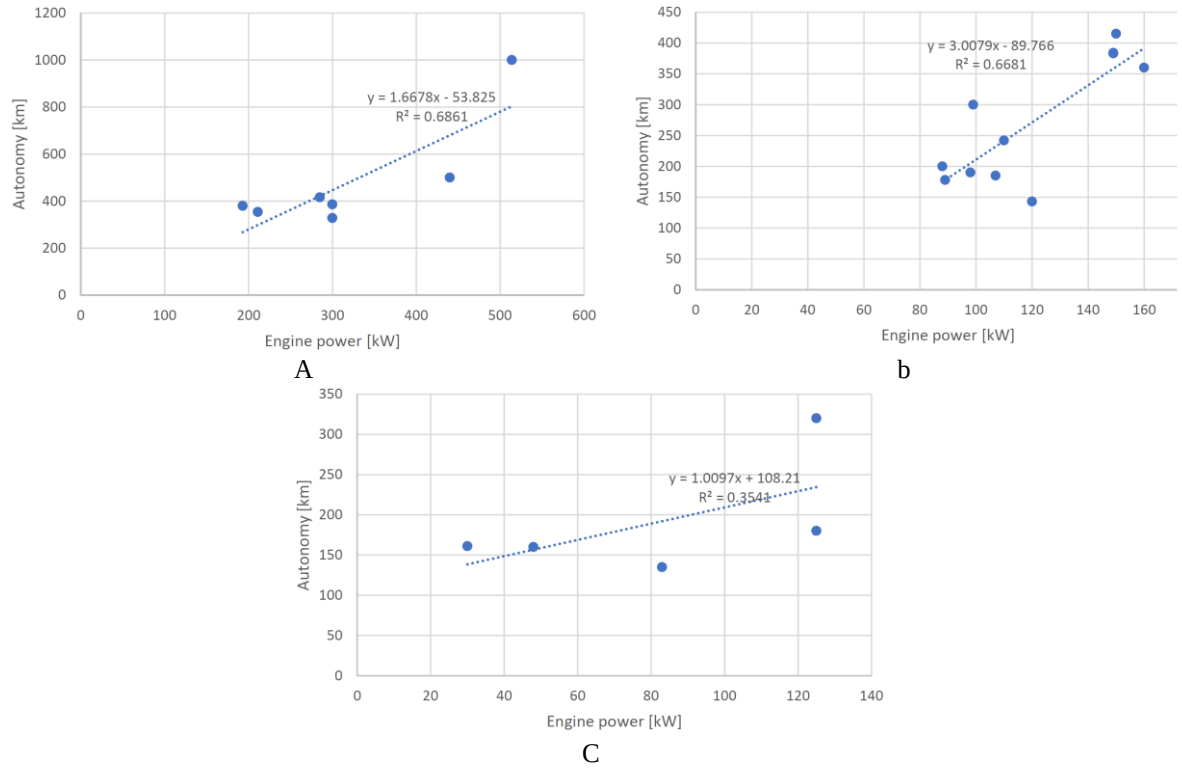

Fig. 2. *Correlation of technical characteristics and performance for autonomy vs. engine power (a-premium class; b-compact class; c-small class)*

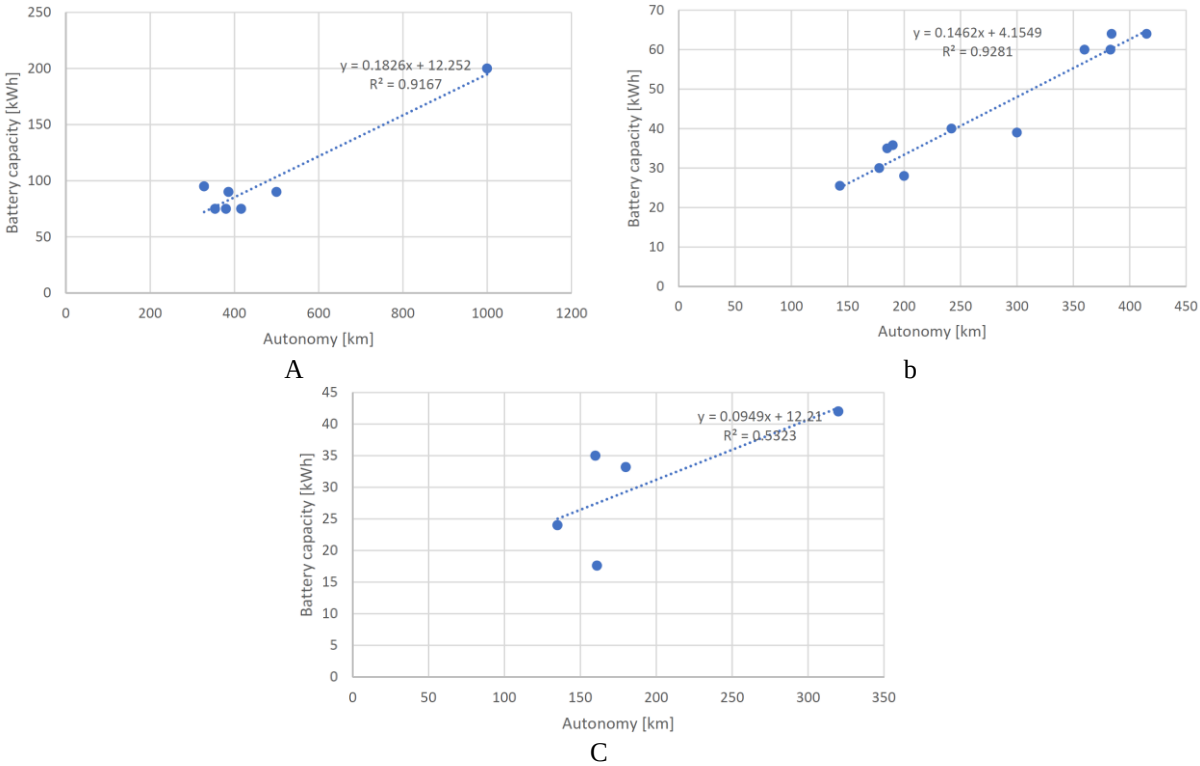

Fig. 3. *Correlation of technical characteristics and performance for battery capacity vs. autonomy (a-premium class; b-compact class; c-small class)*

THE ANNALS OF "DUNAREA DE JOS" UNIVERSITY OF GALATI
FASCICLE IX. METALLURGY AND MATERIALS SCIENCE
N°. 1 - 2019, ISSN 2668-4748; e-ISSN 2668-4756
Article DOI: https://doi.org/10.35219/mms.2019.1.04

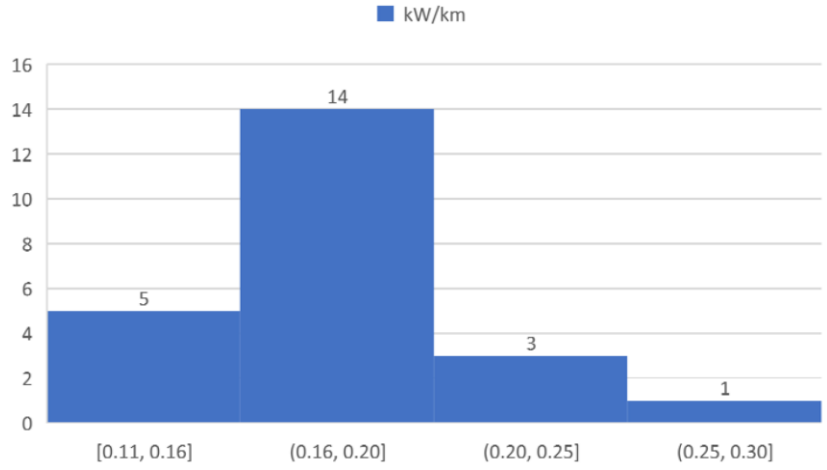

Fig. 4. *Histogram repartition of all classes EV's energetic consumption*

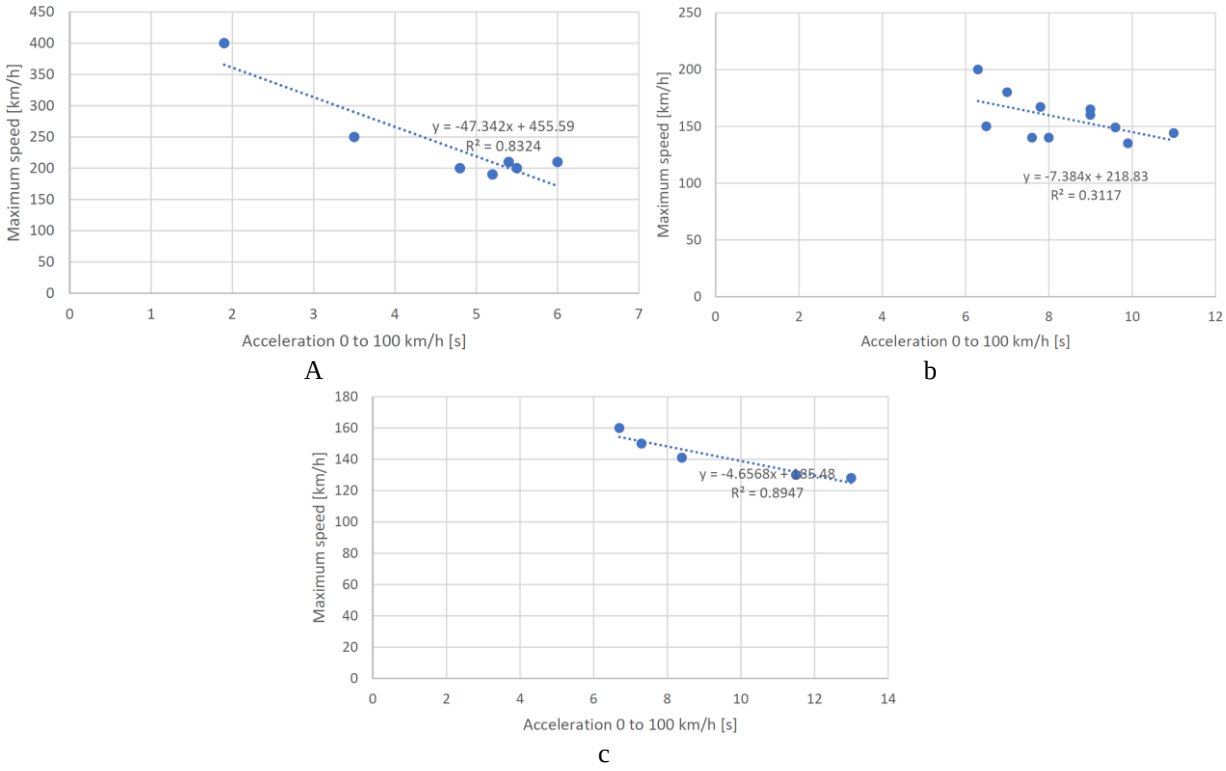

Fig. 5. *Correlation of technical characteristics and performance for maximum speed vs. acceleration 0 to 100 km/s (a-premium class; b-compact class; c-small class)*

The linear correlation was considered in the present study in order to find a straight and direct link between technical characteristics and EVs' performance.

From the point of view of the correlation between autonomy versus engine power, we notice that the best R^2 value is for premium class (0.686), and at a close value is that of the compact class (0.668) (Figure 2). The weakest correlation is encountered in the low class, the R^2 coefficient having the value of 0.354. This can be interpreted by placing greater emphasis on the design of the electric propulsion group for premium and compact classes (plus the advantage of being more powerful through the space available through body and chassis construction).

Similarly, if we see that for the premium and compact class the correlation between the battery capacity vs autonomy for the considered EVs, has

THE ANNALS OF "DUNAREA DE JOS" UNIVERSITY OF GALATI
FASCICLE IX. METALLURGY AND MATERIALS SCIENCE
N°. 1 - 2019, ISSN 2668-4748; e-ISSN 2668-4756
Article DOI: https://doi.org/10.35219/mms.2019.1.04

high values (R^2 = 0.916 for the premium class and R^2 = 0.928 for the compact class) (Figure 3).

These car market segments represent, in fact, the majority of the vehicles sold, and therefore the manufacturers did their best to produce models to meet the main requirement of the customers, which is to have autonomy closest to that of conventional vehicles equipped with an internal combustion engine using fossil fuels.

Low values of correlation factor R^2 = 0.552, in the case of the small class, can be explained by the fact that for these vehicles the main design factor is that of minimizing geometric dimensions. This results in a limitation of the size of the battery that can be placed inside the vehicle's body/chassis and directly the limitation of the battery's energy capacity.

Furthermore, in the automotive market, the small-segment vehicle segment is a low-end segment as a share of the total sales of vehicles overall class. Small-class electric vehicles have been designed and developed in order to be a "second family car" and "a green alternative" to customers for urban use.

From the point of view of comparing the dynamic performance of EVs (maximum speed vs. acceleration), the situation is different from the above. If the premium class and the small class correlations are high (R^2 = 0.832 for the premium class and R^2 = 0.894 for the small class), the weakest correlation is for the compact class (R^2 = 0.311) (Figure 5). If in the case of a small class, the high correlation factor results from the overall reduced weight of the vehicle, and for the premium class to meet customer requirements regarding dynamic performances, the compact class EV is designed to be used more for urban traffic where average speeds in large urban clusters are very low and there are numerous stops.

4. Conclusions

With the increasing demand in the current car market for different electric vehicles, manufacturers are trying to offer as many models as possible to meet the needs and expectations of customers (clients).

The autonomy of an electric vehicle is directly related to the energetic capacity of the battery, so it can be stated that autonomy is the main factor considered in primary fazes of EV's design and development. The best correlations between the technical parameters and the characteristics of the EVs considered are obtained for the premium class, all of which are required by customers in this market segment.

The compact EV class delivers the autonomy demanded by customers but is primarily designed for urban use, while the small class of electric vehicles is an environmentally-friendly alternative to the use of transport means for passengers.

From the point of view of the energy efficiency of the electric vehicles taken into consideration, the energy consumption of most electric vehicles (14 types) is between 0.16-0.20 km/kW (Figure 4).

The results of this study can also use initial data (primary) for the design and development of a new electric car model.

Acknowledgment

This research was funded by the Program "POC-A1-A1.2.3-G-2-15 Parteneriate pentru transfer de cunoștințe, nr. contract de finanțare: 11/01.09.2016, titlul proiectului: Tehnologii pentru vehicule electrice urbane inteligente URBIVEL, ID: P_40_333, MySMIS: 105565".

References

[1]. Yong J. Y., Ramachandaramurthy V. K., Tan K. M., Mithulananthan N., *A review on the state-of-the-art technologies of electric vehicle, its impacts and prospects*, Renew. Sustain. Energy Rev., 49, p. 365-385, 2015.
[2]. ***, *Worldwide EV Sales Are on The Move*, online: http://evercharge.net/blog/infographicworldwide-ev-sales-are-on-the-move/ (accessed on 12 May 2019).
[3]. ***, *China's Quota Threat Charges Up Electric Car Market*, online: http://www.thedailystar.net/business/chinas-quota-threat-charges-electric-car-market-1396066/ (accessed on 12 May 2019).
[4]. ***, *EV-Volumes-The Electric Vehicle World Sales Database*, online: http://www.ev-volumes.com/country/total-world-plug-in-vehicle-volumes/ (accessed on 8 May 2019).
[5]. ***, *EV-Volumes-The Electric Vehicle World Sales Database*, online: http://www.ev-volumes.com/country/usa/ (accessed on 8 May 2019).
[6]. ***, *European Alternative Fuels Observatory-M1 statistics*, Available online: http://www.eafo.eu/vehicle-statistics/m1 (accessed on 8 May 2019).

THE ANNALS OF "DUNAREA DE JOS" UNIVERSITY OF GALATI
FASCICLE IX. METALLURGY AND MATERIALS SCIENCE
Nº. 1 - 2019, ISSN 2668-4748; e-ISSN 2668-4756
Article DOI: https://doi.org/10.35219/mms.2019.1.05

THE IMPORTANCE OF NITROGEN IN THE HEAT TREATING OF FERROUS AND NON-FERROUS METALS AND ALLOYS

Marius VASILESCU, Mircea DOBRESCU
Politehnica University of Bucharest, Romania
e-mail: vmarius_sim_pub@yahoo.com, dobrescu.mircea@gmail.com

ABSTRACT

Nitrogen was first used as the base gas for treating and annealing semi-finished products of steel. Since then the use of industrial gases has spread to cover the full range of heat treatment processes for ferrous and non-ferrous metals and alloys. This paper is focused on titanium and titanium alloys nitriding but also on the recommended nitrogen process atmosphere for ferrous and non-ferrous metals and alloys.

KEYWORDS: nitrogen, heat treating, steels, titanium

1. Introduction

Many processes can only be performed using a mixture of industrial gases. Table 1 shows a list of some of the most important processes and atmospheres.

It is evident that a wide range of gases is employed, even for the more common treatments. For more specialist applications even more gases can be useful, including oxygen, helium, sulphur hexafluoride and carbon monoxide [1].

Table 1. *Recommended process atmospheres*

Process	Atmosphere	Comments
Low alloy steel annealing	Nitrogen/ hydrogen	Often non-flammable mixtures
	Hydrogen	For faster processing in bell furnaces
Low alloy steel hardening	Nitrogen/ natural gas	Often non-flammable mixtures
	Nitrogen/ methanol	-
Stainless steel annealing	Nitrogen/ hydrogen	Zoned for 100% hydrogen in the hot zone
Copper annealing	Nitrogen/ hydrogen	100% nitrogen for short exposure times
Aluminium annealing	Nitrogen	Low purity
Titanium annealing	Argon	-
Sintering iron-based	Nitrogen/ hydrogen/ water	Zoned
Carburising	Nitrogen/ methanol/ natural gas	Plus ammonia for carbonitriding
Ferritic nitrocarburising	Nitrogen/ ammonia/ carbon dioxide	-
Nitriding	Ammonia/ nitrogen	Nitrogen for purge

The primary function of the furnace is the treatment of any product to protect it from atmospheric oxidation. A bright product is usually required, but for some processes only protection from gross oxidation is needed. An example of the former is the annealing of copper water pipes or stainless-steel sink tops and an example of the latter is billet reheating prior to forging. The presence of only a few parts per million of oxygen will oxidise almost any metal at its annealing temperature. Even the highest purity commercially available nitrogen contains one or two parts per billion of oxygen and furnace leaks are inevitable. Therefore, to produce a bright product, this oxygen must be reacted with an active gas such as hydrogen producing H_2O, Eq. 1.

$$1/2O_2 + H_2 \rightarrow H_2O \quad (1)$$

THE ANNALS OF "DUNAREA DE JOS" UNIVERSITY OF GALATI
FASCICLE IX. METALLURGY AND MATERIALS SCIENCE
N°. 1 - 2019, ISSN 2668-4748; e-ISSN 2668-4756
Article DOI: https://doi.org/10.35219/mms.2019.1.05

Therefore, the concept of protective atmospheres is to use an inert gas with sufficient hydrogen or other reducing species to prevent adventitious oxygen, originating from air leaks, from oxidizing the work and tarnishing it.

The furnace atmosphere can also be used to modify the surface chemistry of the material. Common thermochemical treatments for steel are all based on the diffusion of carbon and/ or nitrogen into the surface layers of finished or almost finished components to produce the desired properties.

Examples of such processes are carburizing, typically applied to gears to produce a wear-resistant surface layer on a tough core and ferritic nitrocarburising, typically applied to components requiring a combination of wear and corrosion resistance on a cheap, mild steel substrate.

2. Supply technologies

Large users of nitrogen-based atmospheres have generated the required nitrogen onsite by cryogenic distillation, often as a co-product with oxygen. Such plants produce high purity nitrogen at low cost owned and operated by an industrial gas company and the gas is supplied on a contract basis. Typical users of these supply schemes would be steelworks and large aluminium plants.

New developments in cryogenic plant design over the last few years have led to the introduction of small generators, which are installed on a gas user's premises to produce relatively small volumes of nitrogen at high purity. One of the key features of these plants is the use of small amounts of liquid nitrogen to make up the heat balance in their low temperature distillation columns in the place of the expansion turbines used in larger plants. For this reason, these plants are often called „liquid assist" plants.

Non-cryogenic nitrogen generally costs substantially less to produce than nitrogen from liquid assist plants. The residual oxygen means that non-cryogenically generated nitrogen is not universally applicable. A list of some of those applications for which it is most suitable is shown in Table 2.

Table 2. *Applications for non-cryogenically generated nitrogen*

Process	Atmosphere	Comments
Steel annealing	Nitrogen/ hydrogen	Limited application. Pre-reaction usually required.
Copper annealing	Nitrogen/ hydrogen	Pre-reaction usually required.
Aluminium annealing	Nitrogen	Applicable to all grades
Carburising	Nitrogen/ methanol/ hydrocarbon	-
Austenitic nitrocarburising	Nitrogen/ methanol/ ammonia	-
Ferritic nitrocarburising	Nitrogen/ ammonia/ carbon dioxide	Reduced carbon dioxide requirement
Nitriding	Nitrogen/ ammonia	Purging only
Decarburising	Nitrogen/ hydrogen	Pre-reaction usually required.
Copper brazing	Nitrogen/ hydrogen	-

3. Nitriding of steels and stainless steels with controlled layer

It is classically assumed that only plasma nitriding is able to control all processed parameters in order to regulate the type and nature of the nitriding layer which is built. Recent scientific research has proven, on the other hand, that similar and reproductible results can be obtained with gas nitriding. It is then possible to control the type (alpha-nitride, lambda-nitride or epsilon-nitride) as well as their respective growth kinetics.

4. Titanium strengthening by impurities action

Among the interstitial elements in titanium such as C, N, O, the strongest effect is produced by nitrogen, followed by oxygen and carbon, Eq. 2.

$$HB = 196\% N + 158\% O + 45\% C + 20\% Fe + 57 \quad (2)$$

where:

HB – Brinell hardness of titanium alloy;

57 – Pure titanium hardness.

The influence of oxygen and nitrogen on the hardness of titanium is shown in Fig. 1.

When adding simultaneously oxygen and nitrogen or after plasma nitriding in a very low oxygen atmosphere, tensile characteristics are enhanced.

THE ANNALS OF "DUNAREA DE JOS" UNIVERSITY OF GALATI
FASCICLE IX. METALLURGY AND MATERIALS SCIENCE
N°. 1 - 2019, ISSN 2668-4748; e-ISSN 2668-4756
Article DOI: https://doi.org/10.35219/mms.2019.1.05

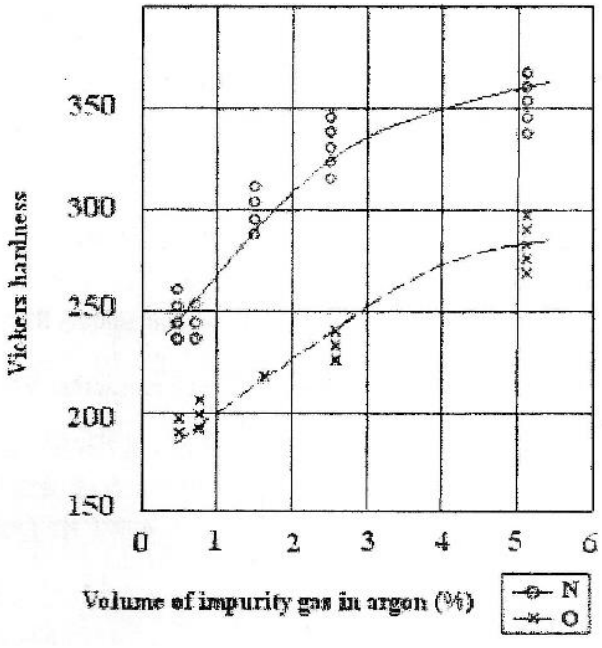

Fig. 1. *Vickers hardness of titanium vs. oxygen and nitrogen content*

5. Plasma nitriding of titanium

For plasma nitriding of titanium, microhardness is increased with temperature and duration of the treatment. The best results (1120 µHV) were obtained in the conditions 850 °C/5 h (Fig. 2) [2].

In Figure 2 is shown the hardness of titanium probe with the distance from probe surface.

By X-Ray Diffraction (Figure 3 we identified two hard compounds TiN (δ)CFC and Ti_2N $(\varepsilon)_{tetragonal}$.

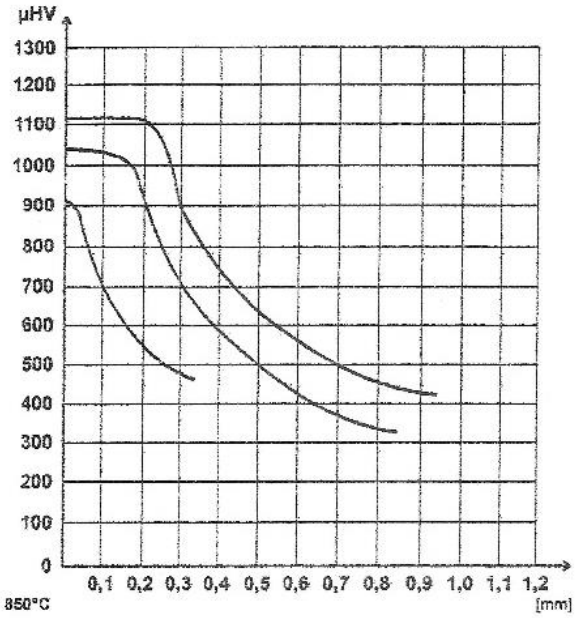

Fig. 2. *Hardness of Ti after nitriding (850 °C) vs. the distance from probe surface*

THE ANNALS OF "DUNAREA DE JOS" UNIVERSITY OF GALATI
FASCICLE IX. METALLURGY AND MATERIALS SCIENCE
Nº. 1 - 2019, ISSN 2668-4748; e-ISSN 2668-4756
Article DOI: https://doi.org/10.35219/mms.2019.1.05

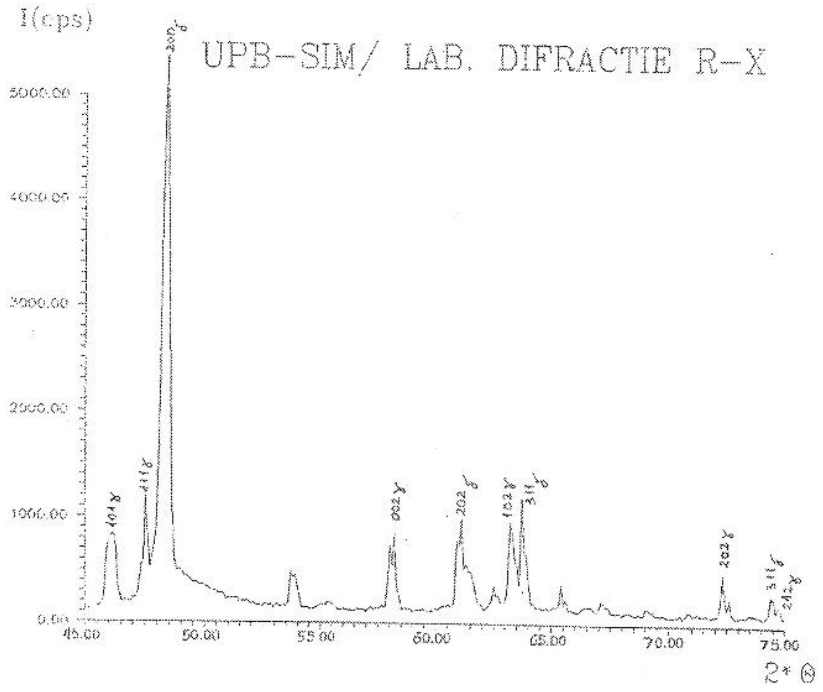

Fig. 3. *X-Ray Diffraction Pattern after Titanium Nitriding (850 °C)*

6. Oxy-nitriding of titanium

Because of the difficult control of nitriding process, some probes underwent oxidation. In spite of these facts, oxy-nitriding produces a higher microhardness (1300 μHV) in the condition 850 °C/2÷3 h. The duration of oxy-nitriding didn't influence hardness significantly [3].

By X-Ray Diffraction we identified an oxynitride TiNO with CFC cell.

To increase the strength properties of titanium, oxygen content varies in the range 0.1-0.2% [4].

A slow solution treatment temperature followed (after quenching) by an aging at low temperature (540 °C) produced a fine α – grain with the best tensile properties [5].

A simultaneous presence of small quantities of nitrogen (0.08%) and oxygen (≤ 0.34%) increase tensile strength of Ti-6Al-3.5Mo-1.7Zr-0.2Si alloy as is shown in Table 3.

Table 3. *The influence of oxygen and nitrogen on tensile strength of some titanium alloys*

Alloy	Sample No.	N (wt.%)	O (wt.%)	TS (MPa)	
				Initial (heat treated)	After plasma nitriding
Ti-1.3Mo-1.5Ni-0.7W	1	0.07	0.27	923	1000
	2	0.04	0.19	935	1100
	3	0.03	0.15	920	1050
	4	0.01	0.12	910	950
	5	0.05	0.23	930	1150
Ti-5Al-2.5Fe	6	0.04	0.18	925	1100
	7	0.06	0.22	980	1059
	8	0.09	0.32	970	1020
Ti-6Al-3.5Mo-1.7Zr-0.2Si	9	0.07	0.32	1120	1300
	10	0.03	0.30	1120	1280
	11	0.08	0.35	1150	1250
	12	0.05	0.30	1100	1290

THE ANNALS OF "DUNAREA DE JOS" UNIVERSITY OF GALATI
FASCICLE IX. METALLURGY AND MATERIALS SCIENCE
N°. 1 - 2019, ISSN 2668-4748; e-ISSN 2668-4756
Article DOI: https://doi.org/10.35219/mms.2019.1.05

7. Nitrogen for ni-ti coupling fabrication

The main application of TiNi shape memory alloys is couplings that join Ti-3Al-2.5V hydraulic tubing in jet aircraft [6]; the principle is illustrated in Fig. 4.

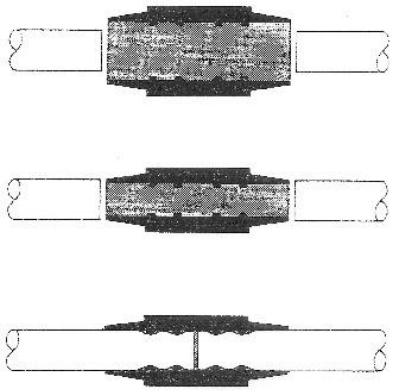

Fig. 4. *The NiTi shape-memory alloy coupling, with sealing bands on the inner surface, is machined in the austenitic condition with an inner diameter (ID) smaller than the outer diameter (OD) of the tubes to be joined. The coupling is cooled below MF in liquid nitrogen, and mechanically expanded while martensitic to an ID then, slightly cooled to ambient temperature. The coupling shrinks to fit tightly, locking the coupling and tubing tightly together to form a metal-to-metal seal*

The coupling, with sealing bands on the inner surface, is machined in the austenitic condition with an inner diameter (ID) smaller than the outer mechanically expanded while martensitic, to an ID slightly larger than the OD tube [7, 8]. The expanded coupling is stored in liquid nitrogen until ready to install, [9, 10]. Then it is slipped over the tubing ends, using simple tools designed to position the coupling properly. During subsequent warming to ambient temperature, the coupling shrinks to fit tightly. The tubing constrains the coupling from shrinking to its original size, locking the coupling and tubing tightly together to form a metal-to-metal seal [11].

8. Conclusions

Regarding the gas atmosphere processes, in the paper is shown the influence of nitrogen on heat treatment of titanium and other materials like aluminium, copper and steel.

Nitrogen is important in Ti and Ti alloys strengthening also as impurity.

For increasing titanium hardness plasma nitriding and oxy nitriding technologies are suitable.

Nitrogen is used also for Ni-Ti shape memory couplings fabrication.

References

[1]. ***, *Materials world*, no. 2, p. 25-33, 2001.
[2]. ***, Metalurgia, no. 11, p. 21-22, 2001.
[3]. Dobrescu M., Dumitrescu C., Vasilescu M., *Titanul şi aliajele sale*, Ed. Printech, 2000.
[4]. Okazaki Y., J. Japan Inst. Metals, no 59, vol. 1, p. 1098-1105, 1995.
[5]. Hocheid R., Klima R., Beauvais C., *Memoires scientifique*, Rev. Metallurg., no. 9, p. 585-590, 1980.
[6]. Yoder G. R., Flores F. H., Eylon D., Metallurgical Transaction, vol. 15A, no. 1, p. 183-187, 1985.
[7]. House J. E., House K. A., *Descriptive Inorganic Chemistry*, (3rd Edition), p. 197-214, 2016.
[8]. House J. E., House K. A., *Descriptive Inorganic Chemistry*, (2nd Edition), p. 277-299, 2016.
[9]. Occelli M. L., Auroux A., Kalwei M., Wolker A., Eckert H., *Studies in Surface Science and Catalysis*, vol. 134, p. 41-58, 2001.
[10]. Aggarwal S., Lyn C. P., Karimi I. A., Computer Aided Chemical Engineering, vol. 31, p. 895-899, 2012.
[11]. Webb G. A., *Encyclopedia of Spectroscopy and Spectrometry*, (2nd Edition), p. 1790-1799, 1999.

THE ANNALS OF "DUNAREA DE JOS" UNIVERSITY OF GALATI
FASCICLE IX. METALLURGY AND MATERIALS SCIENCE
N°. 1 - 2019, ISSN 2668-4748; e-ISSN 2668-4756
Article DOI: https://doi.org/10.35219/mms.2019.1.06

NEW MEASUREMENT METHOD FOR VERY THIN SAMPLES WITH VERY HIGH ACCURACY CONTROL OF THE LEVEL OF THE EMISSIVE POWER IN MICROWAVE ABSORPTION (8.5-9.5 GHz)

Constantin HUŢANU
"1 Decembrie 1918" University of Alba Iulia, Faculty of Sciences, Romania
e-mail: hutanu_constantin@yahoo.co.uk

ABSTRACT

Dielectric materials, especially ferroelectrics, have increasingly specialized applications in the manufacture of IT industry components. At the same time, the working frequency of the microprocessors increases steadily, reaching the microwave domain. This situation requires a very thorough study on the behaviour of dielectric materials at ultra-high frequencies and with very precise determination of their electrical and magnetic properties at these frequencies. A very important aspect in such a study is the evaluation with an extremely high accuracy, the degree of absorption of these materials in the microwave domain. The creation of an experimental installation dedicated to the very precise testing of these dielectrics at microwave frequencies, is a special challenge in the area of scientific research. The content of this article describes very accurately and completely such an experimental installation, as well as how to ensure a very high accuracy of the measurement accuracy. The samples of dielectric materials used in these measurements are made of very thin films.

KEYWORDS: high accuracy, microwave diagnosis, ferroelectrics, absorption

1. Introduction

Considering the use of dielectric materials in more and more applications in the manufacture of electronic components, a detailed study is required regarding their behaviour at increasing frequencies. In the electronic circuit manufacturing industry for the IT domain, the working frequency of these electronic components has increased progressively year by year. Currently, the working frequency of the microprocessors and memories that equip the computing systems, as well as other devices used in the process of testing and controlling electronic products and production flows, has reached the microwave value field. The electromagnetic field with microwave frequencies, radiated by these components, can influence or disrupt the functioning of other electronic components in the immediate vicinity of the radiative components, by inducing parasitic electric currents with a frequency equal to that of the radiated microwave field or with frequencies corresponding to higher order harmonics. This undesirable situation can be avoided using three methods, namely:

a) using highly absorbent polymeric materials for the electromagnetic field of microwaves, in the manufacture of radiative electronic component body/capsule;

b) using, for electronic components at risk of being disturbed by the radiative microwave field, materials immune to microwave frequencies.

c) using highly absorbent materials for the electromagnetic field of microwave irradiated, in the manufacture of capsules of electronic components at risk of disturbed or abnormal operation when they would be under the influence of an electromagnetic field of microwaves.

In most cases, the second option is incompatible with the process of manufacturing electronic or extremely expensive components.

Evaluating the first and last variant, we can easily see that for the manufacture of capsules of radiative electronic components, as well as for the manufacture of capsules of electronic components at risk of functioning in the presence of an electromagnetic field of microwaves, the use of highly absorbent dielectric materials is required.

Electronic test stands, in the field of microwave frequencies, for the study of the behaviour of solid

THE ANNALS OF "DUNAREA DE JOS" UNIVERSITY OF GALATI
FASCICLE IX. METALLURGY AND MATERIALS SCIENCE
N°. 1 - 2019, ISSN 2668-4748; e-ISSN 2668-4756
Article DOI: https://doi.org/10.35219/mms.2019.1.06

dielectric materials, in most cases, they involve using Gunn diodes to generate the electromagnetic field of microwaves. The diode is based on the so-called Gunn effect. J. B. Gunn discovered in 1963 that when a constant, relatively high electrical voltage was applied to an n-type gallium arsenide crystal (GaAs semiconductor), it could cause rapid, static current fluctuations. It was demonstrated that in crystals of very short length these current fluctuations translated into continuous oscillations, the frequencies of which are determined by the crystal's length and lie in the microwave range. The Gunn effect is based on the fact that when energy is supplied to n-type semiconductors with unevenly doped regions electrons it can jump from one energy band into a higher energy band. In the higher energy bands, the electrons are less mobile, which is noticeable in that greater field strength arises at a lower current. This means that for the Gunn effect a lower voltage is needed at a higher current and a lower current at a higher voltage. The dynamic resistance is thus negative in this range (Fig. 1).

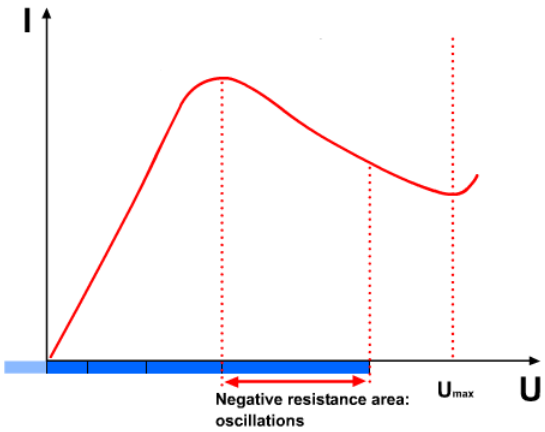

***Fig. 1.** Current-voltage characteristic of the Gunn diode*

Using an assembly Gunn diode - adjustable resonant cavity [1], we can get it a variable frequency electromagnetic field generator, in the microwave domain.

One of the disadvantages of this type of microwave generator is that the power of the microwave signal is not constant across the frequency range. Using the absorption method in the study of the absorbing properties of solid-state dielectrics [2, 3] an unknown level of microwave signal for each frequency generated can be interpreted as an absorption phenomenon. This situation can lead to false conclusions regarding the absorbing properties of the studied dielectric [4, 5].

The experimental installation that will be described in the next chapter eliminates this risk, having as its main characteristic a control of the stability of the microwave signal level, with an ultra-high accuracy.

2. Theoretical sample model

A transmission line can be represented by the circuit diagram shown below. The line is fed with the harmonic voltage $U_0e^{j\omega t}$. The source has the internal resistance Z_i. The transmission line of the length l is loaded at one end with the load resistance Z_L (Fig. 2).

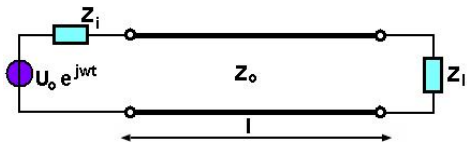

***Fig. 2.** General transmission line with source resistance Z_i and load resistance Z_l*

The basic voltage and current distribution can be computed using the wave equations:

$$\underline{U}(z) = U_0^+ e^{-\gamma z} + U_0^- e^{\gamma z}\ ;\ \underline{I}(z) = I_0^+ e^{-\gamma z} + I_0^- e^{\gamma z}$$

Where U_0^+ and U_0^- respectively I_0^+ and I_0^- are random complex constants. The abbreviation γ designates the so-called propagation constant. It has the form:

$$\gamma = \sqrt{(R' + j\omega L')(G' + j\omega C')} = \alpha + j\beta \quad (1)$$

whereby R', L', G', C' are quantities of unit length.

The real component α is called the *attenuation constant* and the imaginary component β is called the *phase constant*. There is a direct relationship existing between current and voltage on the transmission line, which depends on the characteristic impedance of the waveguide segment.

A uniform transmission line is defined as the one whose dimensions and electrical properties are identical at all planes transverse to the direction of propagation.

In a uniform transmission line, the dielectric sample may be modelled by the following circuit representation:

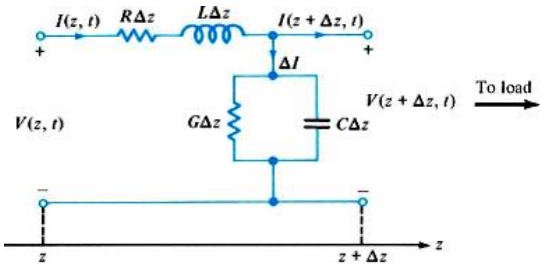

***Fig. 3.** The dielectric sample in TEM model*

THE ANNALS OF "DUNAREA DE JOS" UNIVERSITY OF GALATI
FASCICLE IX. METALLURGY AND MATERIALS SCIENCE
N°. 1 - 2019, ISSN 2668-4748; e-ISSN 2668-4756
Article DOI: https://doi.org/10.35219/mms.2019.1.06

Since the thickness of the studied dielectric material Δz can always be chosen small compared to the operating wavelength, an individual section of line may be analyzed using ordinary ac circuit theory. In the following analysis, we let $\Delta z \to 0$, so the results are valid at all frequencies (hence for any physical time variation).

It is possible that at a certain frequency of the microwave field the resonance condition [6] will be satisfied and consequently the energy absorbed from the microwave field that crosses the dielectric sample will be maximum. This situation can be highlighted by the measuring probe placed at the end of the waveguide, which will measure an electrical voltage diminished in proportion to the degree of absorption of the electromagnetic incident energy after crossing the dielectric sample [7, 8].

3. Measurement bench

The measuring stand is made up of modular microwave components, manufactured by Lucas-Nülle GmbH, and is intended for academic education and research. The measurement systems can be configured in two experimental variants:

a) according to the principle schemes made by the production company, aiming at the study of certain characteristics, phenomena and particularities specific to microwave technologies;

b) according to the user's conception, aiming at a certain experimental purpose.

Microwaves are generated by a Gunn oscillator and their propagation in conjunction with rectangular waveguides.

The recommended frequency band for experimental measurements using various configurations of these components is 8.5 to 9.6 GHz. Within the limits of this frequency band, all the components that make up the experimental installation keep approximately constant their catalogue features, the variations are less than 0.5%.

The experimental installation consists of: Gunn oscillator, isolator, variable attenuator, slotted line, coaxial measuring probe for slotted guide, N socket/SMA plug adapter, an LNC (Low Noise Converter), SMA cable, waveguide adapter, R100/N adapter and still an LNC with an SMA cable and another X-Band Measurement Interface connected by another Unitrain-I Experimenter. The experimental installation is actually an embed measurement system, because the hard part is connected to a dedicated data acquisition system/X-Band Measurement Interface that sends the signals in digital format to a software package installed on a PC. The software package takes over processes the data and interprets the results obtained after processing.

Both operations control the block and the measuring instruments are virtual.

This virtual instrument is used to adjust the power to the Gunn oscillator and simultaneously operates as a display instrument for the microwave measuring receiver.

The experimental card/X-Band Measurement Interface is connected to a hard interface (Unitrain-I Interface and Unitrain-I Experimenter) that communicates with the PC through a USB cable.

The frequency of the oscillator that generates the microwave signal can be changed by rotating the micrometric screw that actuates a piston inside the resonant cavity. The illustration below (Fig. 4) is a schematic depiction of the structure of simple, mechanically tuned Gunn oscillator used in waveguide technology. Under the carriage the tube is blocked or shorted off to create a resonant cavity. The distance to this should be selected so that the load on the Gunn diode forms a parallel resonant circuit, which occurs at a distance corresponding to about $\lambda/4$. In combination with the entry hole, and the frequency calibrating screw, the output can be transformed to match the characteristic impedance of the waveguide.

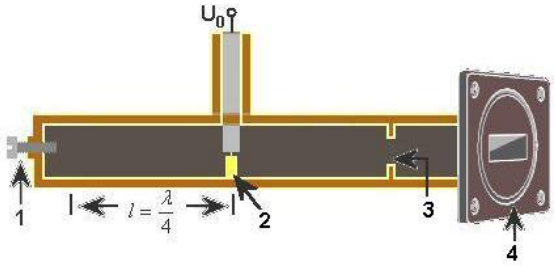

Fig. 4. *Schematic design of a mechanically tunable Gunn oscillator*

where: 1 Micrometer screw for frequency calibration, 2 Gunn diode, 3 Entry hole, 4 Flange.

The maximum power generated by the Gunn oscillator is +17 dB (50 mW) and the frequency band is between 8.5 to 9.9 GHz.

The isolator is a non-reciprocal waveguide element and is primarily used for decoupling the oscillator from waves coming back from the waveguide assembly further down the line.

An LNC (also referred to as a low-noise signal converter or input amplifier) is used to convert high frequencies into lower frequencies (IF). The X-band LNC in conjunction with an internal oscillator of 10 GHz and mixer receives the X-band signal to be measured with a frequency around 9 GHz and generates a proportional signal with an intermediate frequency (IF) in the range of 1 GHz. This IF signal is supplied by the LNC to the receiver card of the UniTrain-I Experimenter via an SMA cable and there

THE ANNALS OF "DUNAREA DE JOS" UNIVERSITY OF GALATI
FASCICLE IX. METALLURGY AND MATERIALS SCIENCE
N°. 1 - 2019, ISSN 2668-4748; e-ISSN 2668-4756
Article DOI: https://doi.org/10.35219/mms.2019.1.06

it is further processed and rectified. The LNC is also supplied with operating voltage via the SMA cable.

The attenuator can change the level of the microwave signal, taken from the output of the isolator, between the limits 0 to -20 dB. The value of the attenuation level is adjusted by rotating a micrometric screw. In order to be able to increase or decrease the microwave signal level at the output of the variable attenuator, depending on the direction of variation of the signal power at different frequencies at the output of the Gunn oscillator, the micrometric screw of the variable attenuator is positioned at division 2. This position of the micrometric screw corresponds to an attenuation of -10 dB introduced additionally by the variable attenuator. The increase or decrease of the additional attenuation level with an amount between 0 and 10 dB compared to the -10 dB attenuation set by positioning the micrometric screw at division 2, compensates for the small power variations of the signal generated by the Gunn oscillator when the generated frequency is changed.

The experimental installation of measurement can be seen in the following image (Fig. 5).

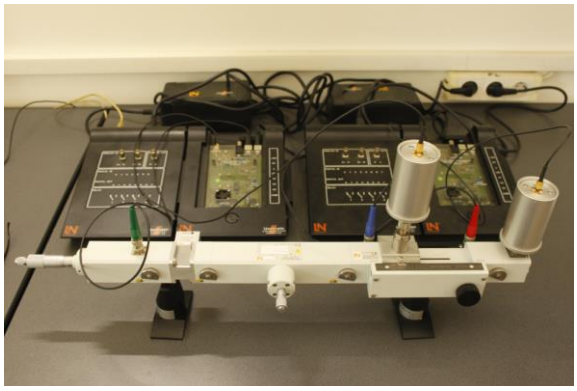

Fig. 5. *The experimental installation of measurement*

The operating mode is as follows:

a) Set the micrometer screw on the Variable Attenuator to a mark of "||" with number 0 at —symbol;

b) Set the switch to the ON position on both UniTrain-I Experiments;

c) Wait until both LEDs light up green;

d) Open the L@Bsoft application on both PCs;

e) Open the Microwave Control Center from the Instruments menu;

f) Set the voltage of the voltage for polarization of the Gunn diode to 8.22 V;

g) Rotate the micrometric screw of the Gunn oscillator until you get the value of 8.60 GHz in the FREQUENCY (GHz) window on the virtual instrument MICROWAVE CONTROL CENTER;

h) Read and note the value of the power of the microwave signal generated by the Gunn oscillator, measured at the end of the waveguide and displayed in the LEVEL window of MICROWAVE CONTROL CENTER;

i) Repeat operations from items g) and h) for frequencies of 8.70 GHz, 8.80 GHZ, ... 9.50 GHz;

The variations in the power level of the microwave signal generated by the Gunn oscillator when the working frequency is changed can be seen in Fig. 6. Bringing this level to a constant value (arbitrarily chosen from the set of previously obtained values), for any frequency in the band 8.60-9.50 GHz, is done by turning to the right or to the left (as the case may be) the micrometric screw of the Variable Attenuator (Fig. 7).

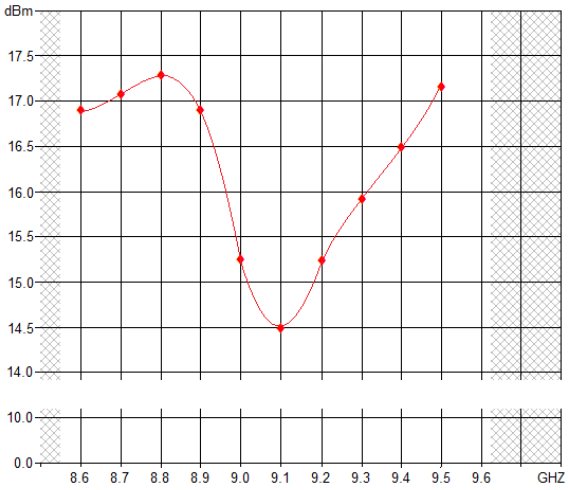

Fig. 6. *Power characteristic of the Gunn oscillator depending on the frequency*

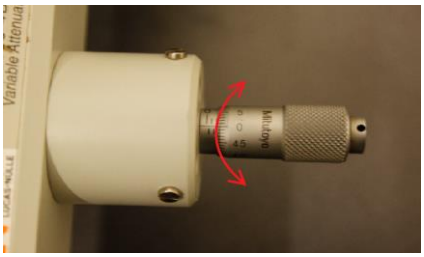

Fig. 7. *The micrometric screw of the Variable Attenuator*

Through these operations, the same power level of the microwave signal that meets the surface and passes through the sample (Fig. 8) to be analysed, placed inside the waveguide, at the exit of the Slotted guide segment can be ensured [9].

THE ANNALS OF "DUNAREA DE JOS" UNIVERSITY OF GALATI
FASCICLE IX. METALLURGY AND MATERIALS SCIENCE
Nº. 1 - 2019, ISSN 2668-4748; e-ISSN 2668-4756
Article DOI: https://doi.org/10.35219/mms.2019.1.06

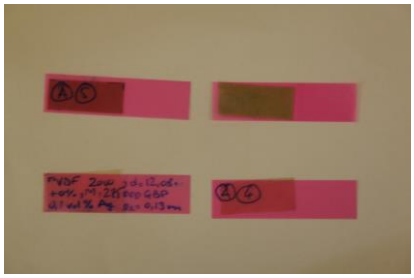

Fig. 8. *The different dielectric samples*

The microwave signal level before meeting the sample surface is taken by the probe placed at the beginning of the segment Slotted guide, and the microwave signal level after it crosses the sample thickness, is collected by the probe placed in the final segment of the experimental installation.

This experimental installation for the study of attenuation by absorption by a set of dielectric samples [10-12] can be used only for those samples that introduce attenuation by absorption smaller or at most equal to the value of the power of the microwave signal before meeting the sample surface.

The measurements were made on ultra-thin layers of dielectric or ferroelectric materials [13-15], obtained by the team of researchers and physicists from the Physics Faculty of the "Alexandru Ioan Cuza" University of Iasi [16].

A relevant result regarding the errors that could occur in absorption measurements, when there is no control of the emission power of the Gunn diode microwave generator, can be seen in the following two graphical representations (Fig. 9, 10):

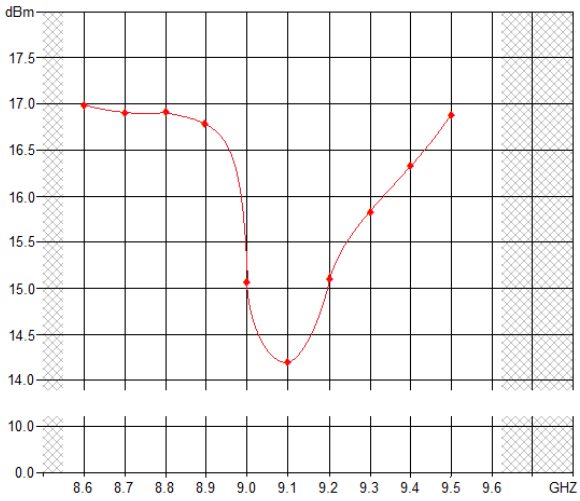

Fig. 9. *Microwave power absorption feature for PVDF sample 0% of CNT, without correction of the signal level emitted by the Gunn oscillator*

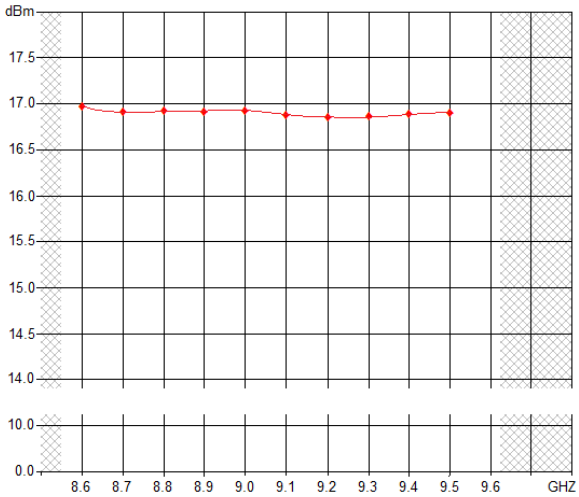

Fig. 10. *Microwave power absorption feature for PVDF sample 0% of CNT, with correction of the signal level emitted by the Gunn oscillator*

Comparing the two graphical representations, the first (Fig. 9) obtained without correcting the power variations of the microwave signal emitted by the Gunn oscillator, and the second (Fig. 10) with the corrections, major differences are observed.

The experimental results, graphically represented in the first figure (Fig. 9), could lead to the conclusion that the measured sample shows an absorption at the frequency of 9.1 GHz, but in fact this decrease of the detected signal level is due to the variation of the power emitted by the Gunn oscillator, depending on the frequency [17].

4. Conclusions

This experimental installation is designed to study ultra-thin films of dielectric material, under the aspect of attenuating a microwave radiation located in the 8.6-9.5 GHz band, with the constant value of the electromagnetic field microwave power incident on the sample surface.

The use of samples in the form of ultra-thin layers has the advantage of being able to use microwave incident radiant powers of small values, because the level of absorption by the ultra-thin layer has a low value.

It was observed that if the ultra-thin samples show non-uniformity of concentration at the surface, then phase changes of the emergent wave occur, changes that can lead to erroneous results regarding the signal level detected by the probe.

If homogeneous samples are used and microwave signal level corrections generated by the Gunn oscillator are made, then it can be ensured an accuracy of the microwave signal level estimation, which is intended to be constant regardless of the

frequency used, about 0.1 dBm relative to the measured value, which ensures better accuracy than 1.5%

References

[1]. ***, *UniTrain-I Course - High Frequency Technology 1: "Introduction to Microwave Technology"*, Course no.: SO4204-9U Version 1.1.

[2]. Sharief Sami M., Ghobrial S. I., *X-Band Measurements of the Dielectric Constant of Dust*, Proc. Ursi Commission F 1983 Symposium. Louvain. Belgium, (ESA SP-194), June 1983.

[3]. Ghobrial S. I., Sharif S. M., *Measurements of the dielectric constant of dust at 8.3 GHz*, National Radio Science Meeting, Univ. of New Mexico, Albuquerque, USA, May 1982.

[4]. Postma A. J., Terlouw J. C., *Calculations and measurements on an X-band microwave interferometer*, Journal of Nuclear Energy. Part C, Plasma Physics, Accelerators, Thermonuclear Research, vol. 5, no. 1, 1963.

[5]. Emmanuel Saint-Christophe, René Sardos, Richard Barrue, *X-band FMR measurements: establishing of relations between the complex permeability and reflection factor of ferromagnetic amorphous conductors*, Journal de Physique III, EDP Sciences, 3 (10), p. 2053-2058, 1993.

[6]. Causa M. T., Passeggi M. C. G., *X-band antiferromagnetic resonance measurements in KNiF3*, Phys. Rev. B 32, 3229, 1 September 1985, Ashwini P. Alegaonkar, Prashant S. Alegaonkar-Nanocarbons: Preparation, assessments, and applications in structural engineering, spintronics, gas sensing, EMI shielding, and cloaking in X-band, Nanocarbon and its Composites. Preparation, Properties and Applications, Woodhead Publishing Series in Composites Science and Engineering, Woodhead Publishing, p. 171-285, 2019.

[7]. Rakhi R. B., *Preparation and properties of manipulated carbon nanotube composites and applications, Nanocarbon and its Composites. Preparation, Properties and Applications*, Woodhead Publishing Series in Composites Science and Engineering, Woodhead Publishing, p. 489-520, 2019.

[8]. Raja Nor Othman, Arthur Norman Wilkinson, *Carbon Nanotube Hybrids and Their Polymer Nanocomposites*, Synthesis, Technology and Applications of Carbon Nanomaterials, Micro and Nano Technologies, Elsevier Ltd., p. 29-60, 2019.

[9]. Sharief Sami M., Ghobrial S. I., *X-Band Measurements of the Dielectric Constant of Dust*, Proc. Ursi Commission F 1983 Symposium. Louvain. Belgium, (ESA SP-194), June 1983.

[10]. Mansor M. R., Fadzullah S. H. S. M., Masripan N. A. B., Omar G., Akop M. Z., *Comparison Between Functionalized Graphene and Carbon Nanotubes: Effect of Morphology and Surface Group on Mechanical, Electrical, and Thermal Properties of Nanocomposites, Functionalized Graphene Nanocomposites and their Derivatives, Synthesis, Processing and Applications*, Micro and Nano Technologies, Elsevier Ltd., p. 177-204, 2019.

[11]. Ahmet Şenocak, Erhan Demirbaş, Mahmut Durmuş, *Phthalocyanine-nanocarbon materials and their composites: Preparation, properties, and applications, Nanocarbon and its Composites, Preparation, Properties and Applications*, Woodhead Publishing Series in Composites Science and Engineering, Woodhead Publishing, p. 677-709, 2019.

[12]. Ghobrial S. I., Sharif S. M., *Measurements of the dielectric constant of dust at 8.3 GHz*, National Radio Science Meeting, Univ. of New Mexico, Albuquerque, USA, May 1982.

[13]. Emmanuel Saint-Christophe, René Sardos, Richard Barrue, *X-band FMR measurements: establishing of relations between the complex permeability and reflection factor of ferromagnetic amorphous conductors*, Journal de Physique III, EDP Sciences, 3 (10), p. 2053-2058, 1993.

[14]. Causa M. T., Passeggi M. C. G., *X-band antiferromagnetic resonance measurements in* $KNiF_3$, Phys. Rev. B 32, 3229, 1 September 1985.

[15]. Il Sung Seo, Woo Seok Chin, D. Lee, *Characterization of electromagnetic properties of polymeric composite materials with free space method*, Composite Structures, vol. 66, issues 1-4, p. 533-542, October-December 2004.

[16]. Maria Teresa Buscaglia, Vincenzo Buscaglia, Massimo Viviani, Jan Petzelt, Maxim Savinov, Liliana Mitoseriu, Andrea Testino, Paolo Nanni, Catalin Harnagea, Zhe Zhao, Mats Nygren, *Ferroelectric properties of dense nanocrystalline* $BaTiO_3$ *ceramics*, Nanotechnology, vol. 15, no. 9, p. 1113-1117, 2004.

[17]. Pozar David M., *Microwave engineering*, 4th ed. John Wiley & Sons, Inc., ISBN 978-0-470-63155-3, 2012.

THE ANNALS OF "DUNAREA DE JOS" UNIVERSITY OF GALATI
FASCICLE IX. METALLURGY AND MATERIALS SCIENCE
Nº. 1 - 2019, ISSN 2668-4748; e-ISSN 2668-4756
Article DOI: https://doi.org/10.35219/mms.2019.1.07

REMOTE CONTROL OF RAILWAY SWITCH HEATING USING GSM MODEMS

Alexandru POPOV, Dragoș-Vasile BRATU, Sorin-Aurel MORARU
Transylvania University of Brașov, Dept. of Automatics and Technology of Information, Romania
e-mail: alexandru.popov@unitbv.ro, dragos.bratu@unitbv.ro, smoraru@unitbv.ro

ABSTRACT

This research activity examines the possibility of remote control of the heating of railway switches. The study and implementation of the remote-control system of resistive heaters using the Global Mobile Communication System (GSM) through SMS messages (Short Message Service) and AT (attention) commands is presented in this article. The research works envisaged are convergent on the functionality of a GSM protocol, which allows the user to control the heating of the remote railway switches, away from the place where the switches were installed. The notions of serial communication, electronic control and AT control have been applied to expand the system. To increase the robustness of the system, a feedback mechanism was introduced so that users will be able to get a feedback status of the system when the command was successfully sent or in the case of voltage drops and system restarts.

KEYWORDS: railway switch; resistive heaters; GSM protocol; attention command

1. Introduction

The crossing of the trains from one railway line to another is possible with the help of a special installation, called a track changer.

The railway switch is a component part of a rail changer, made up of point blades, sliding supports and two fixed rails. The actuation of the point blades is done by the handling device through the traction bar. For the switches to function adequately in extreme conditions (abundant snow, very low temperatures), each switch is equipped with a heating system composed of four resistive elements mounted on fixed and movable parts [1]. Figure 1 shows a switch equipped with a resistive heating system.

The switches are found at the entry points of stations for access from open lines, in railway stations for access to different lines, as well as at the exit of stations for changing the path. It can be stated that the size or limit of a station is given by the distance between the entry switches and the exit switches of the station. Figure 2 illustrates a railway station on double line, indicating the normal position of the switches, their numbering, as well as the distribution of the supply of the switch heaters on the power supply panels (PSP).

The command to couple or decouple the supply of the heaters is currently made by means of control keys mounted in the railway station and cables with wires that connect to the supply panels (PSP). Taking into account the high risk of control cable failure in the railway's proximity, alternative means for transmitting this command are proposed [2]. A solution proposed for solving this problem is described in the present paper and consists of the transmission of the command using GSM support [3].

2. Functional Description

The command to couple or decouple the switch heaters is sent from a mobile terminal as a written message (for example: 01 for ON and 10 for OFF), it is then received by a GSM modem mounted in the power supply box near the switches, and delivered to the remote control system (SCD) in the form of an electrical signal thus ordering the coupling or uncoupling of the power contacts which supply the PSPs. After command execution, a confirmation message is received on the phone. Figure 3 shows the control scheme of the resistive heater remote control through the GSM network [3, 4].

The components of the SCD assembly are: an 8-bit microcontroller, a global system for mobile (also

THE ANNALS OF "DUNAREA DE JOS" UNIVERSITY OF GALATI
FASCICLE IX. METALLURGY AND MATERIALS SCIENCE
Nº. 1 - 2019, ISSN 2668-4748; e-ISSN 2668-4756
Article DOI: https://doi.org/10.35219/mms.2019.1.07

known as GSM) modem, a voltage regulator, an RS232 Serial Communication module and some other electronic parts such as optocoupler, diodes, transistor, capacitors and a 12v relay, mounted on a wiring made in Express PCB and represented in Figure 4 [4, 7].

The microcontroller is of type PIC16F887 and it is a 40-pin and 8-bit architecture with nanoWatt technology. The price for it is economical and the architecture is user-friendly so it can be easy to use and to configure. The task of the microcontroller is to accomplish the communication, using the GSM Maestro 100 modem through the serial port at a speed of 300 bits per second (bps) between the sender of the SMS and the railroad switch in the end. In terms of power supply, a voltage regulator LM2575-5 of 1A is used achieving the reduction of the supply voltage from 12V continuous to 5V continuous required for PIC microcontroller and MAX232IN circuit. A 330 µH coil is used which together with the voltage regulator above mention makes a steady power supply distribution.

The MAX232IN converter is an integrated circuit which makes the transformation from logical signals (0/1 logic) to RS232 signals (+8/−8V) required for communication with the GSM modem [4, 5].

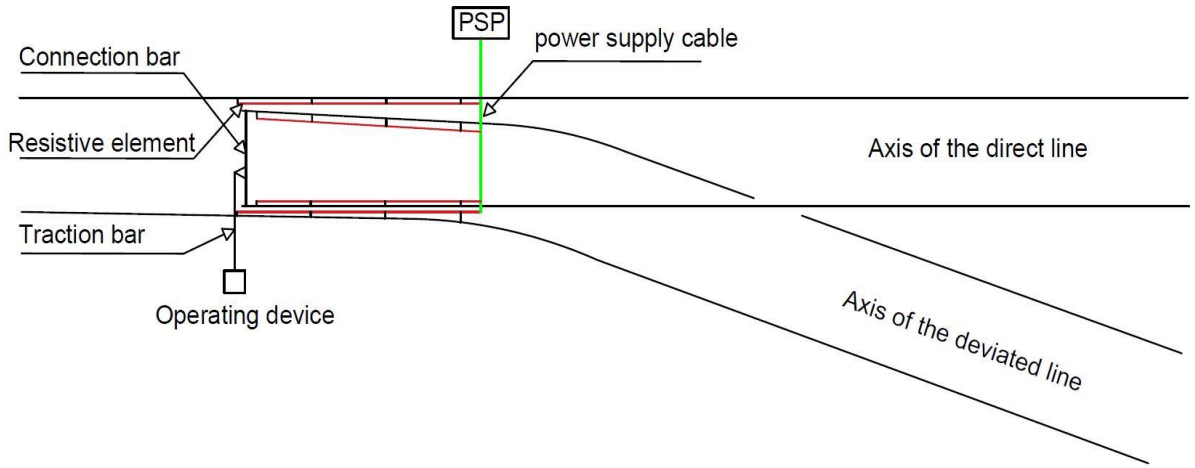

Fig. 1. *Diagram of a switch equipped with a resistive heating system*

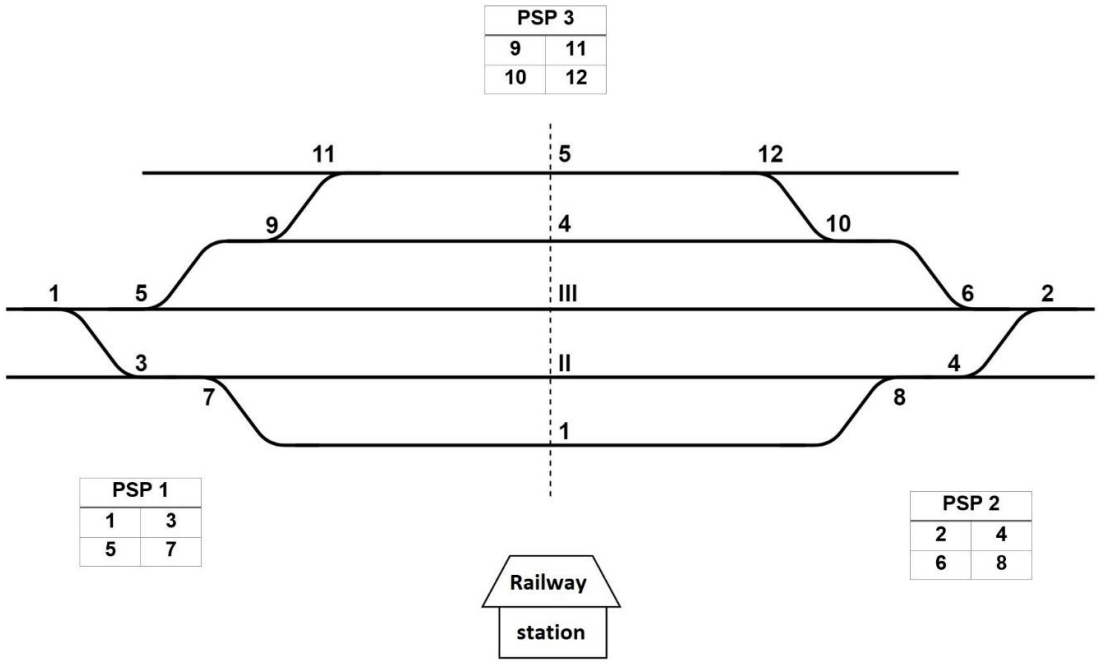

Fig. 2. *Schematic of a double-track railway station, switch position and heater power supply position on the panels*

THE ANNALS OF "DUNAREA DE JOS" UNIVERSITY OF GALATI
FASCICLE IX. METALLURGY AND MATERIALS SCIENCE
N°. 1 - 2019, ISSN 2668-4748; e-ISSN 2668-4756
Article DOI: https://doi.org/10.35219/mms.2019.1.07

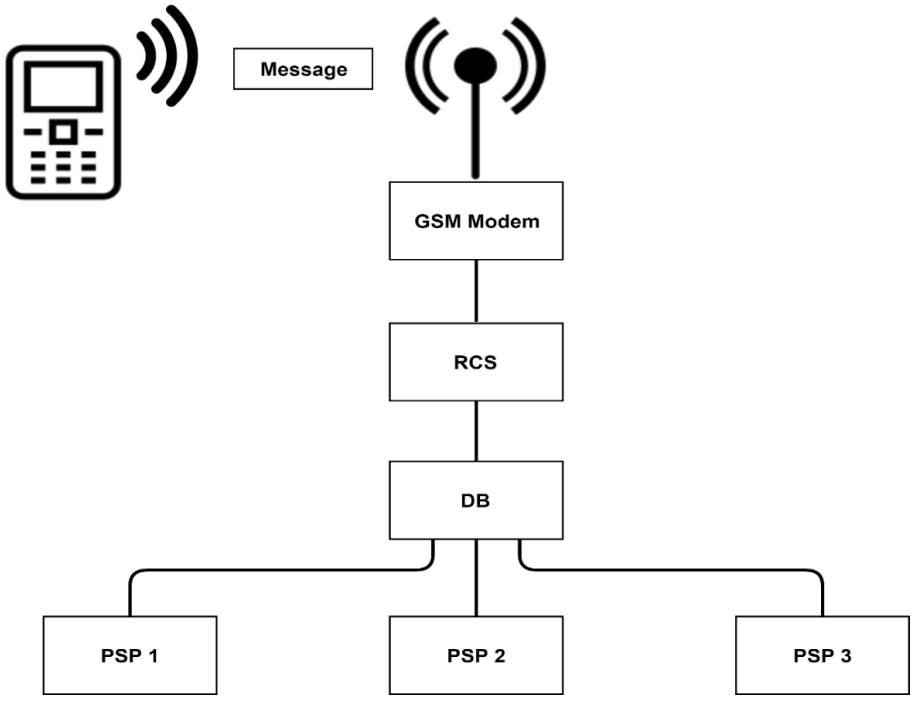

Fig. 3. *Diagram of the command system of resistive heating of railway switches using GSM networking*

Besides that, for better protection, the LTV825 optocoupler is used that performs the intermediation between the logic levels of control (0/1) from the microcontroller and the final command transistor BD139. The voltage level that passes through the transistor is a continuous voltage level of 12V and a maximum 1.5 A. This signal is used for the railroad switch relay control, and this relay will command a voltage level of 220V AC used for power contactor. The 1N4007 diode in parallel with the 12V relay coil achieves the protection of the BD139 transistor upon decoupling.

The optocoupler command is made by the microcontroller through the pin 20 (RD1 - check Figure 5) set as output. The reading of the (open / closed) state of the 12V relay is done by passing the ground connection through an auxiliary contact of the relay. The presence or absence of the ground is performed at the input pin 10 (RE2 pin) of the microcontroller set as input pin. PIC16F887 communicates via MAX232 with the two-pin modem: TX for transmission, RX for receiving characters from the modem.

AT commands are instructions used to control the modem. AT stands for ATtention. Every command line starts with "AT" and then followed by the command.

The AT commands used for this system are: AT + CMGD = 1,4 for deleting all messages received in SIM card, AT + CMGS for sending SMS, AT + CMGR for reading SMS received by modem and then read by PIC16F887 [6].

The programming of PIC16F887 was performed with the PICKit 2 programmer. The program was written in C language and the n Integrated Development Environment (IDE) used was MPLAB v8.10. The compilation of the program was done with the compiler HI-TECH PIC C Lite 9.60. The hexadecimal (.hex) file generated by the compiler was written in the program memory of PIC16F887 with the PICKit 2 programmer from MPLAB IDE v8.10 [4, 6].

3. Software Description

The software application was developed in C language. The main structure is as follows: In the beginning, some configurations are made such as the prescaler is set at a resolution of 8 bits for Timer 0, then the watchdog timer timeout is configured and the used pins are configured as output or input. In order to know the last value that was set for the relay, a reading from EEPROM (Electrically Erasable Programmable Read-Only Memory) is made and the value will be restored from the already mentioned memory. If the relay is opened then the command to open back the relay will be sent. This is advantageous in the case of a voltage drop when the board is restarted because the relay will be set with the last command that was used before (Fig. 6).

THE ANNALS OF "DUNAREA DE JOS" UNIVERSITY OF GALATI
FASCICLE IX. METALLURGY AND MATERIALS SCIENCE
Nº. 1 - 2019, ISSN 2668-4748; e-ISSN 2668-4756
Article DOI: https://doi.org/10.35219/mms.2019.1.07

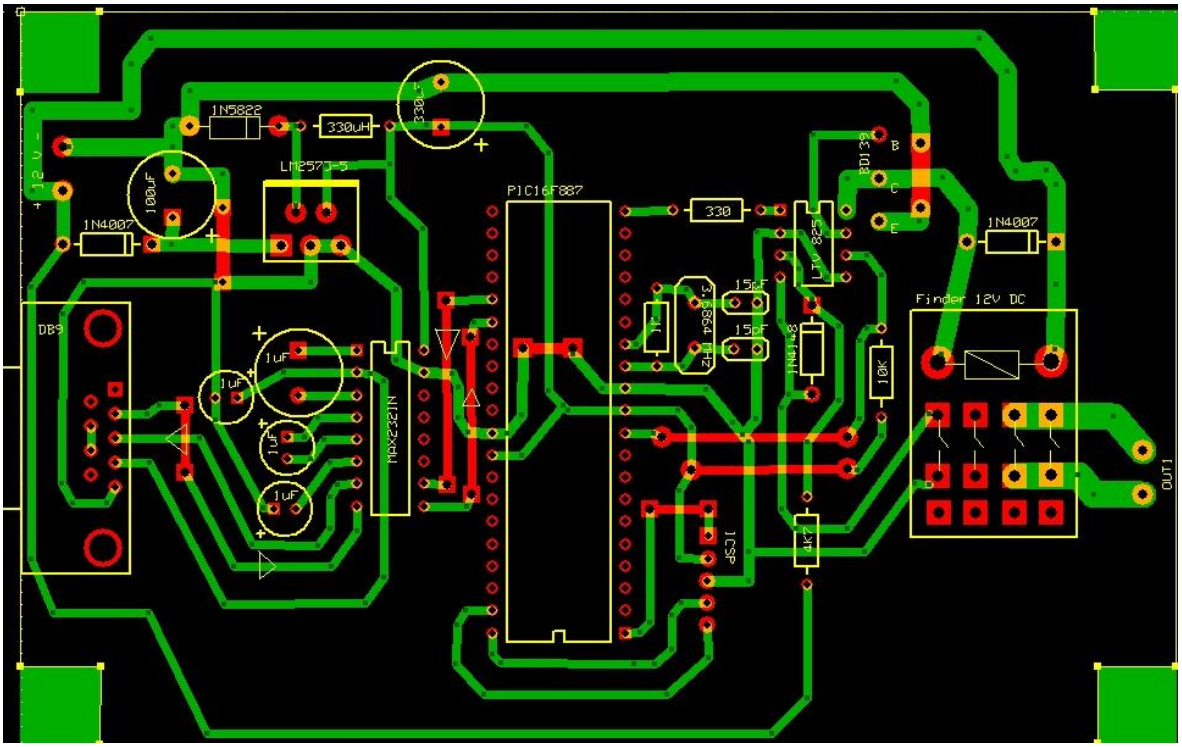

Fig. 4. *RCS components assembly schematic*

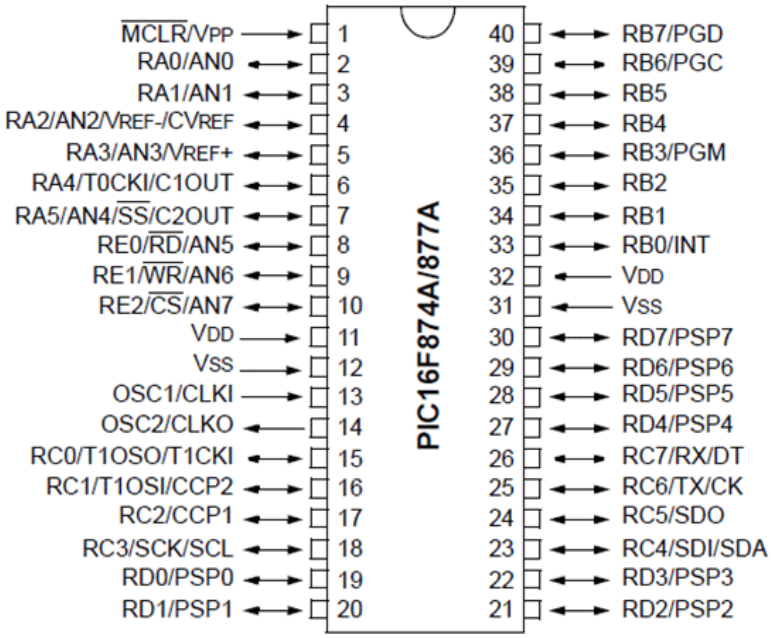

Fig. 5. *PIC16F877A pin diagram (pinout)*

THE ANNALS OF "DUNAREA DE JOS" UNIVERSITY OF GALATI
FASCICLE IX. METALLURGY AND MATERIALS SCIENCE
Nº. 1 - 2019, ISSN 2668-4748; e-ISSN 2668-4756
Article DOI: https://doi.org/10.35219/mms.2019.1.07

```
434  void main( void )
435  {
436      OPTION = 0b00000111; // configureaza prescalerul de 8 biti pentru Timer0 ( PSA = 0 ).
437      WDTCON = 0b00010111; // configurare watchdog Time-out pentru ordin de secunde ( Prescaler 16 biti configurat la 1:65536 ).
438
439      TRISA = 0b00000000;
440      TRISB = 0b00000000; // RB0, RB1, RB2, RB3, RB4, RB5 pentru relee ca pini de iesire
441      TRISC = 0b10000000; // configuration TX/RC6 as output pin.
442                          // configuration RX/RC7 as input pin.
443      TRISD = 0b00000000; // configuration port D as output port with RD1 as output pin for relay command
444      TRISE0 = 0; TRISE1 = 0; TRISE2 = 1;  // RE2 pin de intrare pentru citire stare releu
445
446
447      // disable analogue functions.
448
449      ANSELH = 0x00;
450      ANSEL = 0x00;
451
452      clrwdt();
453
454      citesteEEPROM(); // citeste din EEPROM ultima comanda efectuata asupra releului
455
456      if( stareReleu == 0x00  )
457      {
458          RD1 = 0; // deschidere releu
459      }
460      else
461      {
462          RD1 = 1; // inchidere releu
463      }
464
465      clrwdt();
466
467      configurareEUSART();
468
469      clrwdt();
470
471      //frame_error = 0; // se presupune ca nu se va receptiona nici un caracter eronat
472
473      temporizare(200); // asteapta ca modemul GSM sa se conecteze la retea la aparitia tensiunii de alimentare.
```

Fig. 6. *Main code with configurations and fail-safe features*

The next step is to configure the EUSART (Enhanced Universal Asynchronous Receiver Transceiver) module where the baud rate is configured at 300 bps along with other configurations (frequencies, asynchronous mode, enabling the interrupts for reception).

If the power is down, the modem needs some time (almost 70 seconds) to get into connection with the nearest mobile cell tower. For that a waiting time delay of 70 seconds was introduced.

Because this fail-safe mechanism is very important, firstly a message, which specifies that a problem has been detected and a voltage drop-out has happened, is being sent alongside with the state of the relay (if it is ON or NOT) so that the user will know for sure if the data from the EEPROM is successfully restored and if it is the correct one [7].

Secondly, the code will enter a continuous loop also known as while loop that will check regularly if a SMS is received from the user. If it receives a message and it is not an accepted command it will react immediately with invalid command.

If the request is valid, firstly it will send the command to the relay via RD1 and then if the PIN is set, it will save it into the EEPROM. A feedback message will be sent confirming the command and the relay is set in the desired position.

Available commands are made up on 4 bytes buffers and they are as follows: "01ON" to turn on the relay "1OFF" to turn off the relay and for the current status of the relay the command is "STAT".

Fig. 7. *Switch heating remote control device, mounted on a metal panel*

THE ANNALS OF "DUNAREA DE JOS" UNIVERSITY OF GALATI
FASCICLE IX. METALLURGY AND MATERIALS SCIENCE
N°. 1 - 2019, ISSN 2668-4748; e-ISSN 2668-4756
Article DOI: https://doi.org/10.35219/mms.2019.1.07

The mobile phone number where the messages can be sent, is configurable from the source code. The new code can be flashed on PIC microcontroller with the updated number.

This C-module has in total 12 functions including main function and it uses a 68 bytes buffer used for storing the message from the GSM modem alongside with some safety checks (in case the message is longer than 68 bytes the buffer will be overwritten!) [8].

4. Conclusions

Controlling railway switch heating elements through GSM modems eliminates the need to use control cables, and the potential failures that result from their use, which is significant, given that cable downtime results in railway switch downtime as well, impacting train traffic.

This type of equipment was designed and tested in the PRAM-TM (relay protection, automation and electrical measurement - telemechanics) laboratory in Brașov, Romania. Figure 7 illustrates the actual equipment installed and functioning.

This solution has the following advantages:

• the possibility of placing orders from a central command point;

• high accuracy and reliability;

• in the case of power failure, the system restarts executing the last received command;

• financial savings are accomplished by removing the necessity for a control cable that could reach the length of 1-2 km;

• low cost price, resulting from technological simplicity;

• high versatility (it can be further developed by adding sensors for temperature and snow deposition);

• commands can be timed, based on the weather forecast;

• the application can be integrated into complex SCADA systems, definitively eliminating the human factor;

• the speed of command execution is increased tenfold;

• the application allows for multiple commands, by generating and sending a message to multiple areas;

• redundancy can be ensured by using multiple transfer mediums at once (such as fiber optics), thereby decreasing downtime risk in case of GSM failure.

The use of the remote-control system of the heat pumps using the GSM data transmission and reception network leads to a significant improvement in the safety of trains in extreme weather conditions during winter.

References

[1]. Golovash A. N., Esipenko V. S., Pimenov I. Y., *Switch Heating Device Bibliographic data*, Patent No. RU2232222 (C1)-2004-07-10.

[2]. Yantang G., *Electric Heating Snow Removing Device for Railway Points Bibliographic data*, Patent No. CN201433383 (Y)-2010-03-31.

[3]. Baruchov V. A., Kochubey V., *Electrical Heating Device of Track Switches Type Seit-04 Bibliographic data*, Patent No. RU2582627 (C1)-2016-04-27.

[4]. Lukman A., Olayemi M. O., Kolo J., Ajao A., *Project-Based Microcontroller System Laboratory Using Bk300 Development Board with PIC16F887 Chip*, International Journal of Embedded systems and Applications (IJESA), 5 (3), September 2015.

[5]. Pan Dai, *GSM Remote Controler Heater*, Technology and Comunication, 2014.

[6]. Parab J. S., Shelake V. G., Kamat R. K., Naik G.M., *Exploring C for Microcontrollers: A Hands on Approach*, 2007.

[7]. ***, *ARC Electronics, RS232 Tutorial on Data Interface and cables*, http://www.arcelect.com/rs232.htm/, accessed 10.10.2019.

[8]. ***, *Serial data communication connection over GSM data channel*, https://go.galegroup.com/ps/anonymous?id=GALE%7CA225316041&sid=googleScholar&v=2.1&it=r&linkaccess=abs&issn=17269679&p=AONE&sw=w.

THE ANNALS OF "DUNAREA DE JOS" UNIVERSITY OF GALATI
FASCICLE IX. METALLURGY AND MATERIALS SCIENCE
N°. 1 - 2019, ISSN 2668-4748; e-ISSN 2668-4756
Article DOI: https://doi.org/10.35219/mms.2019.1.08

PRODUCTION PROCESS AND INDICATORS OF PRODUCTION SYSTEMS

Cristina SUCIU, Marioara TULPAN
University of Petroșani, Department of Industrial Engineering, Romania
e-mail: cristina_suciu27@yahoo.com, maryat1977@yahoo.com

ABSTRACT

The concept of a production process can be defined by all the conscious actions of the employees of an enterprise, directed by different machinery, equipment or installations on raw materials, materials or other components for the purpose of their transformation into products, works or services with a certain market value. Taking into account these components, the concept of a production process can also be defined by the totality of work processes and natural processes that compete for the production of products or the execution of different works or services. The production activity is carried out through the production process, which has to be characterized both socio-economically and technically.

KEYWORDS: production process, indicators, systems, industrial, enterprise

1. Introduction

The production of raw materials as a result of the process of industrial production is the main activity of the industrial enterprises. The activity of obtaining material goods presupposes the existence of a set of raw materials and materials, also called labour objects, taken from nature or representing the result of other activities. By processing them with the help of manpower operated or supervised by man, they become economic goods destined to meet the consumption needs of the society.

The production activity includes:

- the actual manufacture of industrial goods, activity carried out through the industrial production process;
- laboratory work, research and assimilation in the manufacture of new products, activities directly linked to the actual manufacture.

It is noted that the factors that condition the process of production are:

- the conscious actions of people, namely the workforce; the objects of labour, respectively natural resources;
- means of work, namely capital;
- natural processes.

From a technical and material point of view, a process of production means all the technological processes, and processes involved in the production of products or the execution of the works and services that are the object of the enterprise's activity.

Classification of production processes. Production processes are classified according to several criteria, such as: how they participate in obtaining the finished product;

► execution mode; how to obtain the finished products from the raw material;

► the degree of periodicity of the time course; the technological nature of the operations carried out;

► the nature of the activities carried out.

In relation to how to participate in the production of the finished product, the production processes are grouped into several categories.

A. basic production processes are processes that aim at transforming different raw materials into finished products, which are the object of an enterprise's business. Basic processing processes, through which the processing of raw materials and materials is carried out in order to obtain finished products.

B. Auxiliary production processes products or works that are not the subject of the core business of the enterprise, but which ensure and condition the smooth running of the core processes.

C. Serving or serving production processes are intended to perform services that are not the object of the enterprise's core business, but which contribute to their performance in both the core work processes and the ancillary processes.

THE ANNALS OF "DUNAREA DE JOS" UNIVERSITY OF GALATI
FASCICLE IX. METALLURGY AND MATERIALS SCIENCE
N°. 1 - 2019, ISSN 2668-4748; e-ISSN 2668-4756
Article DOI: https://doi.org/10.35219/mms.2019.1.08

Table 1. *Stages of the industrial production system*

STAGE	ACTIVITY
PLANNING	- planning workforce; - material consumption planning; - cost planning; - planning of research and development activity; - production planning; - planning of dissolution.
PROCESSING	- drafting the launching order in the manufacture; - production planning; - product design; - supply; - storage of materials; - manufacture of parts; - assembling parts; - product testing; - storage of products; - the transport of products.
CONTROL STAGE	- control of direct and indirect labor costs; - control of material costs; - control of indirect costs; - control of design and development costs; - control of product quality and compliance with storage conditions.
THE FINANCIAL STAGE	- drawing up wage states; - managing orders to collect and collecting them; - managing the amounts to be paid and making the necessary payments; - collection and distribution of data on direct labor costs, indirect costs, materials costs, design costs; - the implementation of new financial regulations; - tax accounting; - stock records; - making financial estimates based on available data; - cashing operations and payments.
INFORMATIONAL STAGE	- design of parts lists; - developing specifications for how to use the parts; - providing data on the safety of the parts; - elaboration of processing programs; - providing information on working standards, quality, staffing.

2. Steps of the production process

Viewed as a whole, the production process consists of operations that can be grouped according to the activity they participate in:

- technological operations;
- control operations;
- transport and storage operations.

The production process has to be divided into operations, because only in this way can the necessary number of workers in different trades be established and their distribution can be achieved as needed in different jobs.

It is also possible to establish a precise record of the results of each worker's work, both with the aim of appropriately remunerating them, and of stimulating the increase in labour productivity.

THE ANNALS OF "DUNAREA DE JOS" UNIVERSITY OF GALATI
FASCICLE IX. METALLURGY AND MATERIALS SCIENCE
N°. 1 - 2019, ISSN 2668-4748; e-ISSN 2668-4756
Article DOI: https://doi.org/10.35219/mms.2019.1.08

Whatever their nature, being executed by a worker, operations can also be called labour operations. Indicators of production systems.

Production includes all the transformation activities of an enterprise. Because of its importance, production is one of the functions of the enterprise. There are several ways to design and lead a business. The enterprise can be compared to a living, biological organism, whose existence is ensured by the performance of certain functions. The function is an abstract theoretical concept used to order the complex and varied activities of the enterprise (as opposed to functions, activities have a specific character). The systemic approach attempts to propose a model of the enterprise, which mainly highlights the interactions taking place within it.

The functional approach uses function identification. The notion of enterprise-wide operation emerged as a result of studies on division of labour and identification of objectives.

Table 2. *Elements of the production process*

ELEMENTS OF THE PRODUCTION PROCESS	CHARACTERISTICS OF THE PRODUCTION PROCESS	EXAMPLES OF ELEMENTS OF THE PRODUCTION PROCESS
TECHNOLOGICAL OPERATIONS LABOR OPERATIONS: CONTROL OPERATIONS TRANSPORT OPERATIONS	- only one executor is responsible for the execution of the operation; - the operation is performed on a particular job within the same technology;	- machining a shaft.
STAGE	- is part of the work operation; - the same work tool is used, - the same technological regime applies; - the subject of the work undergoes only one technological transformation;	- rotary turning; - finishing turning; - drilling.
PASSING OR PASSAGE	- the subdivision of the phase is repeated identically and with the same working regime;	- removing the processing insert by making several passes in the turning stage of grinding.
EXECUTION	- a group of movements of a performer, determined by a well-defined purpose;	- clamping the workpiece in the vice; - measuring the piece.
MOVEMENT	- there is the contact or the detachment of the machine operator or his control bodies, the object of the work; - the displacement of the performer occurs.	- raising your hand to the piece; - moving the piece.

3. Conclusions

The current economic context is marked by the increasing importance of quality as a determinant of the competitiveness of organizations. More and more industrial units and service organizations are concerned to use techniques and tools applied in quality management to facilitate continuous performance improvement so as to fully meet customer requirements in terms of efficiency and effectiveness. Globally, the stock of knowledge grows much faster than in the past. Simultaneously with its amplification, there is a diminishing of the dependence on the classical resources, gradually emerging the primacy of knowledge as the main capital of the organization. For example, in the US there was a 20% decrease in tangible assets to produce one-dollar sales over the existing one quarter a century ago. As highlighted at the 35th Annual Conference of the European Quality Organization, held in Prague in 1991, Dr. Joseph M. Juran, the global symbol of total quality management, for the countries of Eastern Europe, the only chance to succeed in the current situation and to quickly regain lost time is quality.

THE ANNALS OF "DUNAREA DE JOS" UNIVERSITY OF GALATI
FASCICLE IX. METALLURGY AND MATERIALS SCIENCE
N°. 1 - 2019, ISSN 2668-4748; e-ISSN 2668-4756
Article DOI: https://doi.org/10.35219/mms.2019.1.08

A brief analysis of the world economic picture of the years in which we are able to highlight unquestionable defining features: the rapid diversification and renewal of commodity supply under the impact of rapid science and technology development, the globalization of markets, facilitated by advances in telecommunications, customers and society. In these circumstances, the quality of products and services has been imposed as a determinant of the competitiveness of the organizations. On the other hand, there is growing interest in quality assurance issues at national, regional and international level.

References

[1]. Abrudan I., *Premises and landmarks of Romanian managerial culture*, Dacia Publishing House, Cluj-Napoca, 1999.
[2]. Abrudan I., *et al.*, *Competitive Engineering Materials and Technologies in the Competition Market*, Brussels, 2001.
[3]. Abrudan I., *et al.*, *Economic Engineering Manual. Production Systems Engineering*, Dacia Publishing House, Cluj-Napoca, 2002.
[4]. Abrudan I., *et al.*, *SMEs and their specific management*, Dacia Publishing House, Cluj-Napoca, 2003.
[5]. Abrudan I., *At the gates of Europe. A vision on the European integration of Romania*, Management and Economic Engineering Magazine, vol. 5, no. 4 (20), p. 5, Cluj-Napoca, 2006.
[6]. Abrudan I., *Time Factor Management*, Management and Economic Engineering Magazine, vol. 5, no. 3, Cluj-Napoca, 2006.
[7]. Abrudan I., *Leibnitz's triumph of Leibnitz's "sufficient reasoning principle" or 10 years since the founding of the Consortium of Economic Engineering in Romania*, in Management and Economic Engineering Magazine, vol. 5, no. 2 (18), p. 5, Cluj-Napoca, 2006.
[8]. Baron T., Statistical methods for analysis and quality control of production, Didactic and Educational Publishing House, Bucharest, 1979.
[9]. Baron T., *et al.*, *Quality and Reliability*, Technical Publishing House, Bucharest, 1988.
[10]. Baron T., *Theoretical and Economic Statistics*, Didactic and Educational Publishing House, Bucharest, 1996.
[11]. Bălan G., Ţîţu M., Bucur V., *The Management of Change and the Competition Advantage*, 10th International Research / Expert Conference "Trends in the Development of Machinery and Associated Technology", TMT 2006, p. 497-500, Barcelo-Lioret de Mar, Spain, 11-15 September, 2006.
[12]. Cănănău N., Dima O., Gură Gh., Barajas Gonzales Ana, *Quality Assurance Systems*, Junimea Publishing House, Iaşi, 1998.
[13]. Cicală E., *Methods of Statistical Processing of Experimental Data*, Polytechnic Publishing House, Timişoara, 1999.
[14]. Ciobanu I., *Strategic Management*, Polirom Publishing House, Iaşi, 1998.
[15]. Ciobanu E., *Certification of Quality Systems*, Q media, p. 36-40, no. 2/1999.
[16]. Ciurea S., Drăgunălescu N., *Total Quality Management*, Economic Publishing House, Bucharest, 1995.
[17]. Drucker P., *Management: Tasks, Responsibilities, Practices*, Harper & Row, 1974.
[18]. Mitonneau H., *A new orientation in quality management: seven new instruments*, Technical Publishing House, Bucharest, 126 Montgomery, D.C., Design and Analysis of Experiments, John Wiley & Sons, New York, 1991.
[19]. Nicolescu O., *The Information System of the Organization*, Economic Publishing House, Bucharest, 2000.

THE ANNALS OF "DUNAREA DE JOS" UNIVERSITY OF GALATI
FASCICLE IX. METALLURGY AND MATERIALS SCIENCE
N°. 1 - 2019, ISSN 2668-4748; e-ISSN 2668-4756
Article DOI: https://doi.org/10.35219/mms.2019.1.09

PHYSICO-CHEMICAL PROCESSES FROM THE X70 STEEL MAKING AND CONTINUOUS CASTING THAT INFLUENCE ITS PROPERTIES

Gigi STRAT[a]*, Maria VLAD[a], Gelu MOVILEANU[b], Florentina POTECAȘU[a]
[a]"Dunarea de Jos" University of Galati, Faculty of Engineering, Romania
[b]Valahia University of Targoviste, Romania
e-mail: gigistrat1967@gmail.com

ABSTRACT

The paper presents the processes of elaboration and casting that favourably influence the properties of microalloyed steel.

High strength microalloyed steel used to manufacture main oil and gas pipelines must meet, in addition to special technical conditions, economic conditions, which contribute to the protection of the environment. Secondary treatment in LF and RH installations as well as automatically controlled continuous casting can also help improving the physical, mechanical and corrosion properties of the products obtained from these steels. The making of X70 steels at OLD1-(Liberty Steel Group), according to existing technology, is the peak of performance at the current stage.

Blowing oxygen and argon into the converter is done according to a Blowing Pattern that takes into account the gas flow and the distance from the head of the blowing lance to the surface of the metal bath. Deoxidation and microalloying of the X70 steel take place in the casting ladle and during the secondary treatment in LF and RH.

For deoxidation and microalloying, some ferro-alloys which have strictly limited content of harmful elements (P, S) are used. LF microalloying materials such as: Mn-99%, Al-99%, FeTi-70%, FeV-80%, FeNb-65%, Ca-99% or SiCa-60/30% are introduced into the steel as tubular ferro-alloys and not chunks. In this way, a superior assimilation and homogeneous diffusion of the elements into the metal bath are achieved.

Secondary treatment of the X70 steel for chemical and thermal homogenization of the metal bath is achieved by advanced metal bath desulfurization using synthetic slag, lime and bauxite. Vacuum degassing with RH procedure is done to reduce hydrogen from 8-9 ppm to less than 2 ppm. At the continuous casting of these steel types, the bubbling is not used because it is intended that the floating of inclusions be easier on the surface of the metal bath.

KEYWORDS: properties, deoxidation, microalloying, steel, LD converter

1. Introduction

The launching point in the research and development of high-strength micro-alloy steels was represented by the brands used in the construction of major oil and natural gas pipelines, the steels developed and processed for use in extreme conditions, from the Arctic to the desert areas, from depths greater than 2000 m, to the altitudes necessary to cross mountain ranges, buses that extend thousands of kilometres and which must satisfy, in addition to the special technical conditions that ensure their safety in use, economic conditions and protection of the environment.

By performing the tasks elaborated on the basis of the mathematical models and by optimizing the parameters of the main processes in the elaboration and casting of the high strength mechanical steels, their properties can be improved. The steel industry has responded to current requirements by developing new steel brands that can be used in different

THE ANNALS OF "DUNAREA DE JOS" UNIVERSITY OF GALATI
FASCICLE IX. METALLURGY AND MATERIALS SCIENCE
N°. 1 - 2019, ISSN 2668-4748; e-ISSN 2668-4756
Article DOI: https://doi.org/10.35219/mms.2019.1.09

industrial sectors and which have a common set of characteristics

These steels are called HSLA - high strength microalloyed steels [1]. All these features are found in high strength microalloyed steels, which are produced and developed under different brands by the major steel producers around the world [2]. This category also includes X70 steel according to API-5L-91.

X70 steel, by its characteristics, is suitable for the manufacture of main pipes in the current state of their technologies. Medium alloy steel would have required a higher consumption of alloying elements and thus higher production prices.

2. The experimental part

The main reference properties for X70 steels:
- high mechanical strength;
- high weldability;
- high resistance even at low temperatures;
- good plasticity characteristics;
- good resistance to atmospheric and marine corrosion;
- high economic efficiency in terms of production costs.

Tables 1-4 present the main mechanical properties and chemical compositions of X70 steel type.

Table 1. *Variation of mechanical strength of X70 microalloyed steels according to API-5L / 95*

Yield Strength [MPa]	Tensile strength [MPa]	$Rp_{0.2}$/Ts
485-615	570-700	0.93

Table 2. *X70 microalloyed steels, according to API-5L / 95*

Chemical analysis	Acceptance limits	Over tolerant limits	Target	Chemical analysis	Acceptance limits	Over tolerant limits	Target
Element	**Max (%)**	**Max (%)**	**Target (%)**	**Element**	**Max (%)**	**Max (%)**	**Target (%)**
C		0.09	0.07	Mo		0.13	0.12
Mn		1.65	1.55	Ni		0.20	
P	0.02	0.018	0.02	Cu		0.10	
S	0.01	0.05	0.03	B		0.0005	0.0003
Si		0.40	0.30	Ca		0.0015	0.001
Al		0.05	0.04	N		0.007	0.006
Nb	0.07	0.06	0.05	V+Nb+Ti	0.15	0.15	
V	0.10	0.008		V+Nb	0.14	0.14	
Ti		0.025	0.02	Ce	0.39	0.39	
Cr		0.20					

Table 3. *X70-M21 microalloyed steels, according to the Arcelor Mittal Galati-Metallurgical Handbook*

	C	Mn	Si	P	S	Al	N_2	H_2	Cu	Cr	Ni	Mo	Nb	Ti	V	Ca
Min (%)	0.06	1.45	0.25			0.02						0.12	0.045	0.015		0.0005
Max (%)	0.075	1.6	0.4	0.01	0.002	0.05	0.007	2 ppm	0.1	0.2	0.2	0.13	0.055	0.025	0.008	0.0015

THE ANNALS OF "DUNAREA DE JOS" UNIVERSITY OF GALATI
FASCICLE IX. METALLURGY AND MATERIALS SCIENCE
N°. 1 - 2019, ISSN 2668-4748; e-ISSN 2668-4756
Article DOI: https://doi.org/10.35219/mms.2019.1.09

Table 4. *X70-T15 microalloyed steels, according to the Arcelor Mittal Galati-Metallurgical Handbook*

Chemical analysis		C	Mn	Si	Al	P	S	N_2	Mo	Cr	Nb	Ti	Ca	H_2 [ppm]
T15	min (%)	0.060	1.600	0.200	0.020				0.110	0.25	0.055	0.015	0.0005	max.2
	max (%)	0.075	1.750	0.350	0.060	0.015	0.005	0.007	0.120	0.35	0.065	0.025	0.0015	
	Target (%)	0.068	1.680	0.280	0.040	0.012	0.003	0.006	0.115	0.30	0.060	0.020	0.0010	

2.1. Steelmaking and continuous casting of X70

The following materials, installations and some specific operations are used in the X70 steelmaking process [3-5]:

• Technologically selected scrap iron;

• Desulphurized cast iron at% S = 20 ppm and advanced slag removed;

• Converter with functional bubbling and slag retention, calibrated;

• Clean casting pot with functional bubbling;

• Recycled steel is not inserted in the metal load;

• Bubbling only with argon for the entire duration of the breath;

• Intermediate stop for advanced slag evacuation and resumption of blowing with additional quantity of 1-ton lime [8];

• Minimum 3 minutes post bubble (oxygen activity ≤ 700 ppm and phosphorus ≤ 0.006%);

• The calculation of the necessary alloys is made on the lower limit of each element;

• Electrolytic manganese will be used during the evacuation and the ferroalloys will be administered with 1-minute breaks between them;

• Steel bubbling after evacuation will be done through a porous plug without the discovery of the metal bath;

• LF treatment (advanced steel bubbling, heating and desulphurization);

• Advanced desulfurization with lime, bauxite and synthetic slag;

• Correction of chemical analysis and microalloys with tub ferroalloys of Nb, V, Ti and SiCa;

• HR treatment for 15 minutes minimum vacuum degassing;

• The batches do not bubble for about 15-20 minutes before casting begins to float inclusions in the slag [5].

Table 5. *Chemical compositions corresponding to X70 steel making batch (%), according to the OLD1- Arcelor Mittal Galati spectral laboratory analysis*

Cod ACH / Element	Desulphurized cast iron	End of blowing	Steel after evacuation	Steel in LF, first sample	Steel in LF, second sample	Steel in LF, the third sample	Steel in LF, fourth sample	Steel in LF, last sample	Final sample from distributor
C	4.7196	0.0555	0.0524	0.0602	0.0677	0.0761	0.0723	0.0742	0.0728
Mn	0.5105	0.0824	1.2704	1.3102	1.3115	1.5012	1.4937	1.4843	1.4696
Si	0.6787	0.0010	0.2086	0.1661	0.2510	0.2813	0.2631	0.2646	0.2729
P	0.0767	0.0048	0.0052	0.0059	0.0064	0.0069	0.0066	0.0068	0.0070
S	0.0036	0.0090	0.0069	0.0044	0.0030	0.0014	0.0013	0.0013	0.0012
Al	0.0031	0.1753	0.0151	0.0232	0.0308	0.0316	0.0342	0.0393	0.0444
Ni	0.0016	0.0081	0.0086	0.0085	0.0084	0.0086	0.0085	0.0085	0.0085
Cu	0.0063	0.0112	0.0136	0.0136	0.0138	0.0146	0.0146	0.0144	0.0145
Cr	0.0186	0.0063	0.0088	0.0093	0.0097	0.0110	0.0108	0.0112	0.0157
Ti	0.0318	0.0001	0.0006	0.0007	0.0015	0.0209	0.0224	0.0206	0.0166
Mo	0.0010	0.0009	0.1172	0.1184	0.1182	0.1246	0.1251	0.1251	0.1245
Nb	0.0010	0.0003	0.0014	0.0013	0.0016	0.0420	0.0422	0.0451	0.0466
V	0.0072	0.0004	0.0014	0.0015	0.0017	0.0020	0.0019	0.0017	0.0018
Ca	0.0000	0.0166	0.0001	0.0001	0.0033	0.0103	0.0047	0.0039	0.0006
Sn	0.0042	0.0008	0.0010	0.0011	0.0013	0.0014	0.0014	0.0012	0.0015
B	0.0006	0.0000	0.0001	0.0001	0.0002	0.0002	0.0002	0.0002	0.0003
N	0.0000	0.0057	0.0024	0.0010	0.0011	0.0069	0.0033	0.0006	0.0047
Pb	0.0010	0.0005	0.0020	0.0022	0.0022	0.0024	0.0028	0.0027	0.0026
Zr	0.0010	0.0003	0.0019	0.0020	0.0020	0.0025	0.0024	0.0024	0.0024
Zn	0.0017	0.0042	0.0060	0.0065	0.0043	0.0028	0.0089	0.0059	0.0020
Co	0.0010	0.0021	0.0024	0.0024	0.0023	0.0026	0.0025	0.0025	0.0025
Fe	93.9087	99.6261	98.2768	98.2643	98.1609	97.8518	97.8813	97.8875	97.8962

THE ANNALS OF "DUNAREA DE JOS" UNIVERSITY OF GALATI
FASCICLE IX. METALLURGY AND MATERIALS SCIENCE
Nº. 1 - 2019, ISSN 2668-4748; e-ISSN 2668-4756
Article DOI: https://doi.org/10.35219/mms.2019.1.09

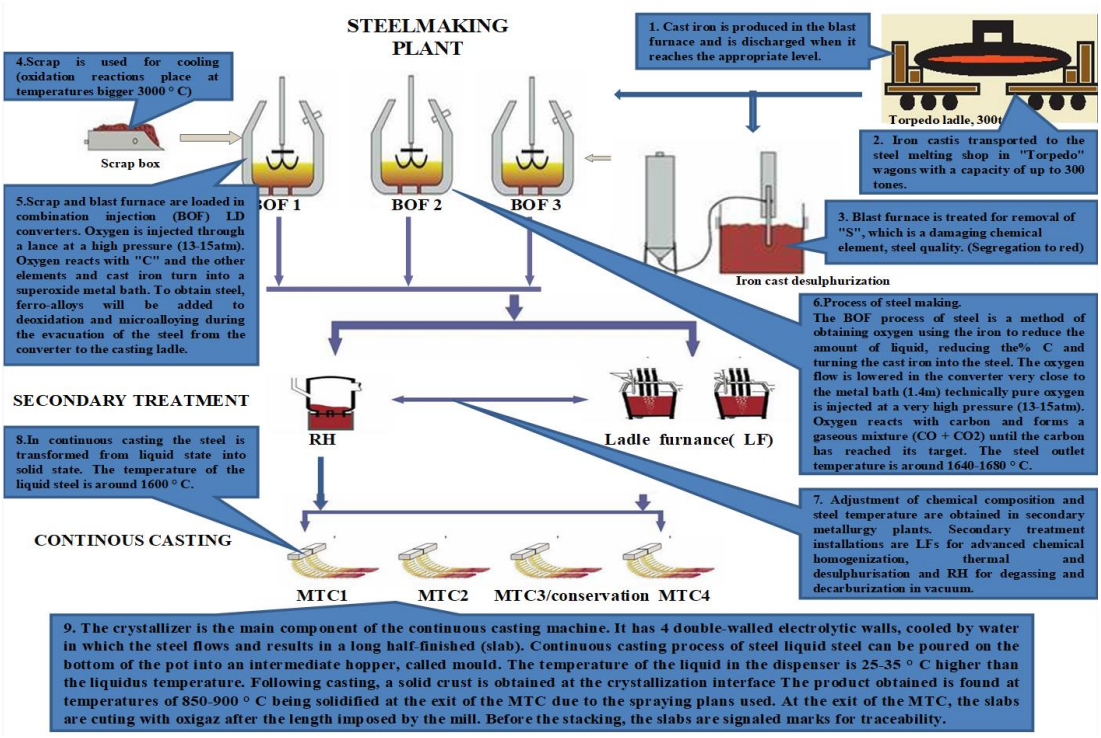

Fig. 1. *General presentation of the technological flows of making and casting steel* [1, 4]

2.2. Physico-chemical processes in steelmaking and casting of X70

In a LD converter with combined oxygen and argon blowing, Fig. 2, the basic reactions that take place are oxidation, and the movement of the metal bath is mainly generated by the energy transmitted by the oxygen jet hitting the metal bath and by the blowing energy, due to carbon monoxide (CO) formation and release [6].

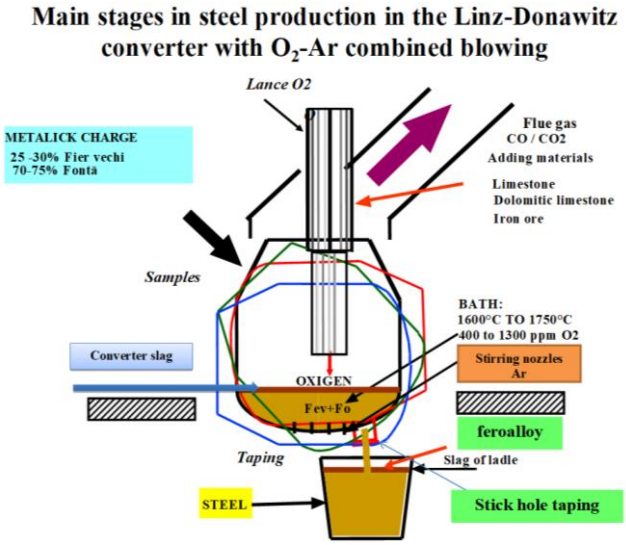

Fig. 2. *Linz-Donawitz converter with combined blowing of the O_2 - Ar* [1, 8]

In the initial phase of the process when the silica oxidation takes place, the formation of CO remains less intense. In the main decarburization phase, the formation of CO in the reaction areas of the oxygen jets and in the immediate vicinity is extremely pronounced. In the marginal areas of the converter, however, there are dead zones where variations of concentrations occur due to the differences in

THE ANNALS OF "DUNAREA DE JOS" UNIVERSITY OF GALATI
FASCICLE IX. METALLURGY AND MATERIALS SCIENCE
N°. 1 - 2019, ISSN 2668-4748; e-ISSN 2668-4756
Article DOI: https://doi.org/10.35219/mms.2019.1.09

intensity of the oxidation reactions [7]. In the final phase of the decarburization, the combustion zones are less carbon-fuelled, due to an increased slag of iron and manganese.

In the bubbling process, the inert gas (nitrogen or argon) is injected into the batch through the bottom of the converter. The amount of gas varies depending on the phase of the elaboration process. During de-silica and the main decarburization phase, the gas flow is sufficient to ensure the chemical composition and homogeneous temperature of the metal bath. In the final phase of decarburization and especially in advanced decarburization, the CO formation is too weak to generate the movement of the metal bath.

In this period the flow rate of the bubbling gas is increased to ensure the transport of carbon in the reaction areas of the oxygen jets and at the same time to prevent the slag from further oxidation of other elements. In the whole process, the reactions are close to equilibrium, balances that are reached in the post-bubbling phase and the variation of the main elements concentration and of their oxides are shown in Fig. 3.

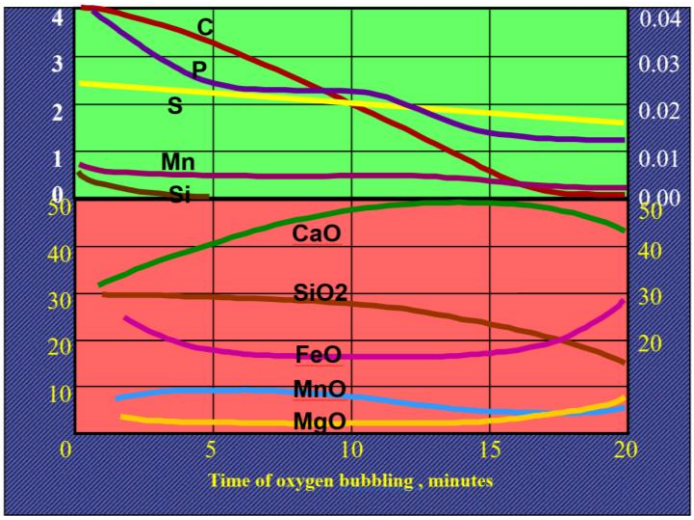

Fig. 3. *Variation of different element and the resulting oxides concentration in the converter* [4]

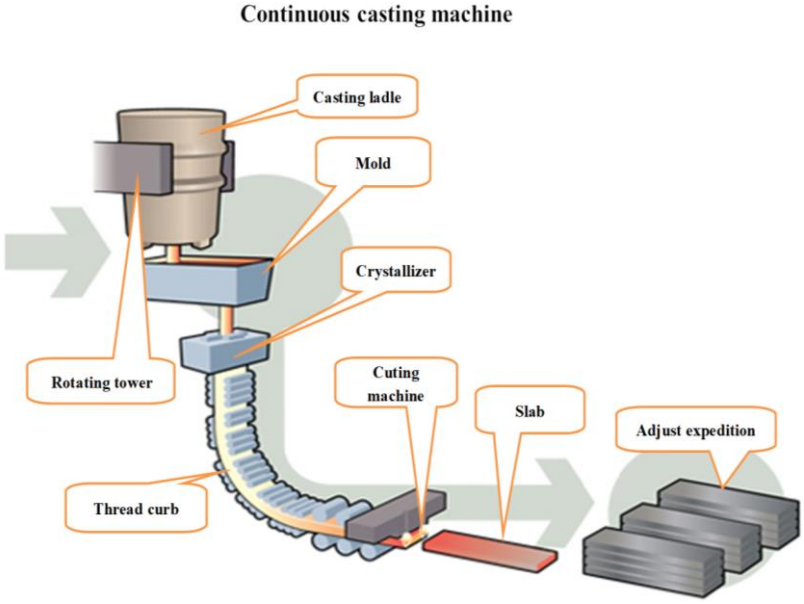

Fig. 4. *Continuous casting machine, the main scheme* [4, 5]

The bubbling process through the bottom of the converter helps the oxidation and slurry reactions of the formed oxides (oxides of silica, manganese, iron etc.) near the equilibrium state, during the main phase of the decarburization [8]. The equilibrium states between the chemical elements in the metal bath and

THE ANNALS OF "DUNAREA DE JOS" UNIVERSITY OF GALATI
FASCICLE IX. METALLURGY AND MATERIALS SCIENCE
Nº. 1 - 2019, ISSN 2668-4748; e-ISSN 2668-4756
Article DOI: https://doi.org/10.35219/mms.2019.1.09

the oxygen content are not perfectly achieved during oxygen bubbling. The lime dissolution is accelerated by injecting the inert gas into the metal bath. The addition of fluorine (CaF_2) for the fluidization of the slag is no longer necessary, which leads to increased durability of the refractory lining of the converter.

Examples of the defects types in slabs are presented in Table 7 and Fig. 7, 8.

Table 6. *Baumann analysis bulletin according to the Baumann-OLD1 Laboratory Analysis*

No. heat	No. slab	Quality	Sleb dimensions	Attack type	Casting machine	Level of segregation
911435	3	M21	250/1900	$CuCl_2$+ NH_4Cl	1/1	Class 2
911435	6	M21	250/1900	$CuCl_2$+ NH4Cl	1/2	Class 1

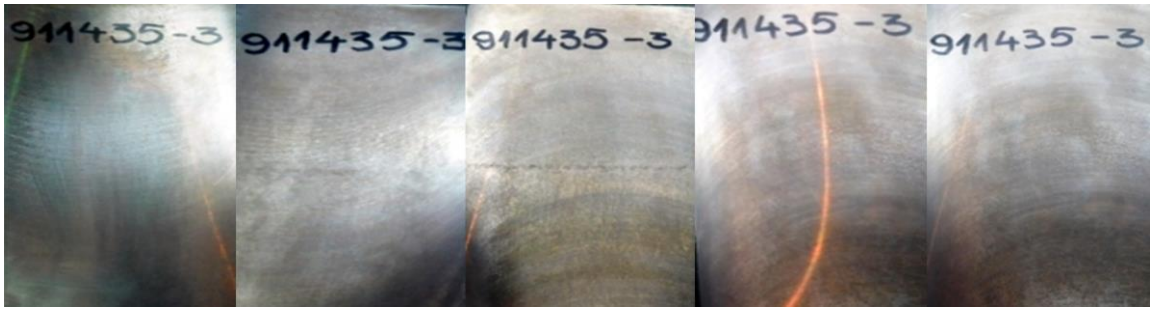

Fig. 5. *Central segregation and defective core class 2, wire 1*

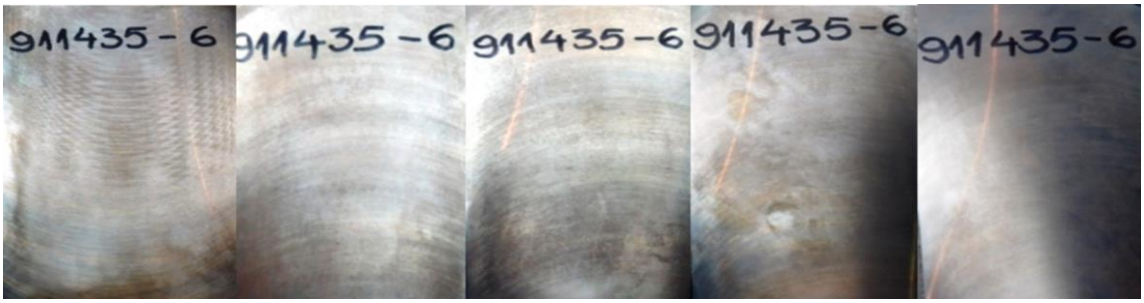

Fig. 6. *Central segregation and defective core class 1, wire 2*

Table 7. *Faults in frames according to API-5L / 95* [4, 5]

Surface defects	**Type**	**Causes**
Cracks	longitudinal	longitudinal uneven cooling in the crystallizer
	transversal	transversal adhesion of the steel to the walls of the crystallizer
	lateral	lateral abrasions of the crystallizer walls
	marginal	marginal sealing improper at the beginning
		temperature and high casting speed
		defective alignment of the supporting rolls
Microcavities and non-metallic inclusions		low temperature of steel
		oxidation of steel in crystallizer
		inadequate dry distributor

THE ANNALS OF "DUNAREA DE JOS" UNIVERSITY OF GALATI
FASCICLE IX. METALLURGY AND MATERIALS SCIENCE
N°. 1 - 2019, ISSN 2668-4748; e-ISSN 2668-4756
Article DOI: https://doi.org/10.35219/mms.2019.1.09

		inclusions of pouring powder
		impure steel with non-metallic inclusions
		driving crusts of solidified steel in crystallizer
		inadequate deoxidation of steel when making it
Internal defects		
Segregation at the center and defective cores		Improper casting temperature
Non-metallic inclusions	inclusions of pouring powder	
	local inclusions	excessive turbulent local of the steel in the crystallizer
	slag inclusions	refractory exfoliated material
	inclusions in the form of clouds	slag drive from distributor to crystallizer
	inclusions below the surface	

Fig. 7. *Surface cracks*

Fig. 8. *Deep longitudinal cracks*

Following some structural analysis presented in Fig. 9, it resulted that the microstructure noted with 1 shows that the analysed steel purity is very good, max. 1 in conformity with the existing standards. The steel is clean and globular inclusions rarely occur (sulphides modified as a result of their interaction with Al_2O_3 and CaO).

THE ANNALS OF "DUNAREA DE JOS" UNIVERSITY OF GALATI
FASCICLE IX. METALLURGY AND MATERIALS SCIENCE
N°. 1 - 2019, ISSN 2668-4748; e-ISSN 2668-4756
Article DOI: https://doi.org/10.35219/mms.2019.1.09

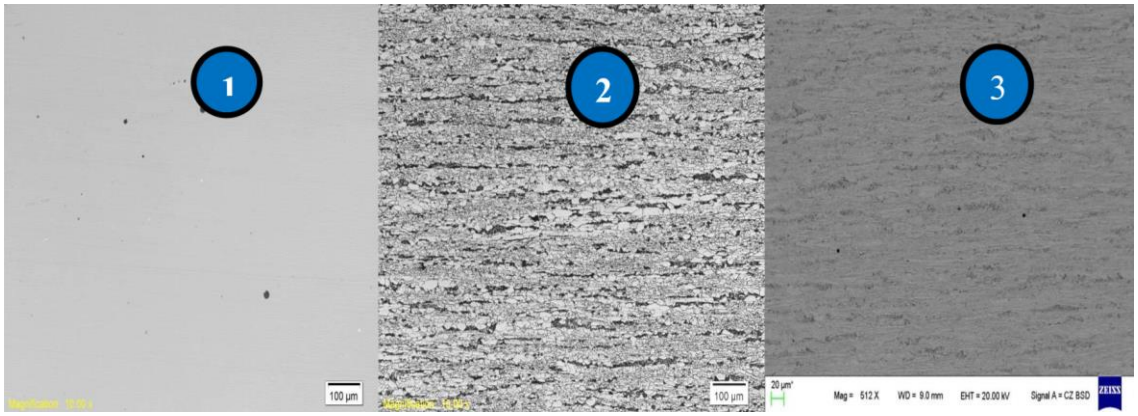

Fig. 9. *SEM images of X70 steel samples (500x), according the, Central Laboratory analysis of Liberty Steel Group Galati*

The microstructures noted with 2 and 3 are fine, with some granulation zones 8-9 and a ferrito-perlitic structure. These structures ensure good deformability [8].

3. Conclusions

For deoxidation and microalloying, iron alloys are used but they have strictly limited content of harmful elements (P, S). LF microalloying materials such as: Mn-99%, Al-99%, FeTi-70%, FeV-80%, FeNb-65%, Ca-99% or SiCa-60/30% are introduced into the steel as tubular iron -alloys and not chunks.

In this way, the superior assimilation and homogeneous diffusion of the elements into the metal bath are achieved.

Secondary treatment of the X70 steel for chemical and thermal homogenization of the metal bath is achieved by advanced metal bath desulfurization using synthetic slag, lime and bauxite. Vacuum degassing with RH procedure is done to reduce hydrogen from 8-9 ppm to less than 2 ppm. At the continuous casting of these steel types, the bubbling is not used because it is intended that the floating of inclusions be easier on the surface of the metal bath.

References

[1]. Toshihiko E. M. I., *Steelmaking technology for the last 100 years: Toward highly efficient mass production systems for high quality steels*, ISIJ International, vol. 55, no. 1, p. 36-66, 2015.
[2]. Siciliano F., Stalheim D. G., Gray M. J., *Modern high strength steels for oil and gas transmission pipelines*, Proceedings of the 7th International Pipeline Conference, TMS, 2008.
[3]. Alexandru Rau, Iosif Tripsa, *Steel metallurgy*, Didactic and Pedagogical Publishing House Bucharest, 1973.
[4]. ***, *Working procedures and instructions from OLD1-TC of Arcelor Mittal Galați*, 2014.
[5]. Peng Fei, Yi Min, Cheng-jun Liu *et al.*, *Effect of continuous casting speed on mold surface flow and the related near-surface distribution of non-metallic inclusions*, International 3. Journal of minerals metallurgy and materials, vol. 26, no. 2, p.186, 2019.
[6]. Tripșa I., Kraft N., *Steelmaking in oxygen converters*, Technical Publishing House, Bucharest, 1970.
[7]. Tripșa I., Pumnea C., *Steel deoxidation*, Technical Publishing House, Bucharest, 1981.
[8]. ***, *Technological instructions specific to X60, X65, X70 steelmaking*, ArcelorMittal Galati, OLD1, Steel Department, 2016.

THE ANNALS OF "DUNAREA DE JOS" UNIVERSITY OF GALATI
FASCICLE IX. METALLURGY AND MATERIALS SCIENCE
Nº. 1 - 2019, ISSN 2668-4748; e-ISSN 2668-4756
Article DOI: https://doi.org/10.35219/mms.2019.1.10

LOSS OF HEIGHT PRESSURE IN A LAYER OF GRANULAR MATERIALS

Adrian VASILIU
"Dunarea de Jos" University of Galati, Romania
e-mail: avasiliu@ugal.ro

ABSTRACT

During the air blown in the furnace, from the vents to the loading mouth, the gases lost from the initial pressure depend on several factors, such as the care and the granulation mixed with ores and coke from the layers of care. For the knowledge of a gas circulation through granular layers, pressure losses were studied in layers formed from pieces of materials of different shapes and sizes, using a specially constructed laboratory installation.

KEYWORDS: blast furnace, gas circulation, pressure loss, ore, coke

1. Introduction

The technology of producing iron ore from blast furnaces consisted of the passage of ore and solid fuel through an upward flow of hot gases with reducing properties. The load consisting of successive portions of ore and coke is introduced at the upper part of the furnace. Getting to the lower parts, the load takes up the heat of the ascending gases, until the temperature of the material reaches softening-melting temperatures. Also, in this range of increase in temperature of solids by heat exchange, some of the reducing gases participate in the indirect reduction of metal oxides, removing oxygen from oxides resulting in weight loss of the solid phase. It is important that the heat-reducing gases travel through the layers of material towards the upper areas of the load, yielding heat from the materials in the column and at the same time ensuring the reduction of the metal oxides [2, 3].

Gas flows at the mouth of the furnace and within the radius, in the respective section, the temperature and the analysis of the gas may have different values, the character of the operation being peripheral, central, combined or non-uniform.

The reducing gases obtained in the area of the windmills have a temperature between 1800-2000 °C, mainly in the component CO, H_2 and N_2, the reducing components represent about 36-54% of the total quantity, the percentage depending on the percentage of O_2 of the blown air and the amount of additional fuel introduced into the mouths of the wind. Ideally, the gas flow through the furnace should be evenly distributed, ensuring the same heat transfer per unit area, as well as participating in reductions, it would mean that the lowering of the materials in such a situation would be very uniform. Basically, the load of the furnace has many discontinuities both in terms of the uniformity of the granulation and of the relative distribution on the loading surface [2].

2. Objectives

For a more in-depth knowledge of gas flow through the furnace, the pressure loss in layers formed from pieces of material of unequal shapes and sizes, on specially constructed installations was studied.

The practical phase of the work consists in the execution of a laboratory installation to determine the permeability through granular layers.

The obtained results can lead to the completion of the database, so the technical and economic indicators obtained are elements of the automatic program management process in the blast furnace.

3. Theoretical considerations

During wind gusts - the loading mouth, the reducing gases lose their initial pressure, the degree of loss depending on the granulation of the mixture of ores and coke from the layers they pass through [6].

Losses due to friction, between the walls of the enclosure and the fluid stream, find their physical explanation through the process of dissipation of hydraulic energy, process conditioned by the viscosity of the fluid and the character of the flow. The calculation relation is as follows [4]:

THE ANNALS OF "DUNAREA DE JOS" UNIVERSITY OF GALATI
FASCICLE IX. METALLURGY AND MATERIALS SCIENCE
No. 1 - 2019, ISSN 2668-4748; e-ISSN 2668-4756
Article DOI: https://doi.org/10.35219/mms.2019.1.10

$$p_f = \mu \cdot \frac{L}{d_m} \cdot \frac{w_0^2}{2} \cdot \rho_{0g}(1 + \alpha \cdot t_g) \ [N/m^2] \quad (1)$$

where:

p_f - is the pressure lost by the friction between the gases and the granular materials in the load, [N/m^2];

μ - coefficient of friction material and gas, (air));

L - the length of the gas route [m];

d_m - inner diameter inside [m];

ρ_{0g} - gas/air density, normal conditions [kg/m^3];

w_0^2 - air velocity, normal conditions [m/s];

t_g - hot air temperature [^{o}C];

α - the temperature coefficient (α = 1/273).

Losses due to local resistances occur due to section changes, bends, seals that lead to the corresponding change in fluid velocity. The resistances that cause these changes are called local resistances and are calculated with relations [4]:

$$p_{rl} = \xi \cdot \frac{w_0^2}{2} \cdot \rho_{0g}(1 + \alpha \cdot t_g) \ [N/m^2] \quad (2)$$

where:

ξ – is the coefficient of local resistance.

Geometric pressure losses are calculated with the relation [4]:

$$p_g = \pm H \cdot g \left(\frac{\rho_{0a}}{1 + \alpha \cdot t_a} - \frac{\rho_{0g}}{1 + \alpha \cdot t_g} \right) [N/m^2] \quad (3)$$

where:

H - is the height of the column (layer) of material [m];

g - gravitational acceleration (g = 9,81) [m/s^2].

Dynamic pressure losses, due to the change in speed value, occur due to section changes on the gas path. In this case, the Borg relation is used for calculation [4]:

$$p_d = \frac{w_{0e}^2 - w_{0i}^2}{2} \cdot \rho_{0g}(1 + \alpha \cdot t_g) \ [N/m^2] \quad (4)$$

where:

w_{0e}^2 ,w_{0i}^2 -the speed of gas at the inlet and outlet [m/s].

Pressure losses through layers, consisting of spherical granules when passing gases, can be determined by the relation [5, 7]:

$$\Delta p = \frac{1{,}53}{\varphi \cdot 4{,}2} \left(\frac{30}{Re} + \frac{3}{Re^{0{,}7}} + 0{,}3 \right) \frac{H}{d_m} \cdot \frac{\rho \cdot w^2}{2} \ [N/m^2]$$

$$d_m = \frac{100}{x_1/d_1 + x_2/d_2 + \cdots + x_n/d_n} \ [m] \quad (5)$$

where:

R_e is Reynolds' criterion ($R_e = w \cdot d_e/v$);

d_m - the average diameter of material in the layer;

$x_{1...n}$ - the content of the fraction d in the layer;

$d_{1...n}$ - the average diameter of the granules in a fraction.

4. Laboratory measurements

The assessment of the influence of gas pressure on the pressure losses in the layer can be determined. Between the loss of pressure in a layer of materials and the coefficient of resistance (local) of the layer, there is a significant dependence. Based on these relationships and experiments, the variation curves were established for the pressure losses in the layers. Table 1.

The installation for the determination of distributed hydraulic losses is composed of a constant level reservoir that supplies a pipe with the diameter d = 300 mm, which has at the ends of a straight portion of measurement, with the length L = 1000 mm, sockets for measuring the pressures with instruments with liquid, as in Figure 1 - A.

The installation consists of a steel tube with pressure sockets at 100 mm between them, which are connected to U-shaped pressure gauges with water for measuring pressure and a float flow meter, which measures the air flow at the inlet, in the installation (Figure 1-B). The measurements are repeated 5 times, followed by an arithmetic mean of the results.

The results obtained for various materials are shown in Table 1, and the representation is in Graph 1.

THE ANNALS OF "DUNAREA DE JOS" UNIVERSITY OF GALATI
FASCICLE IX. METALLURGY AND MATERIALS SCIENCE
Nº. 1 - 2019, ISSN 2668-4748; e-ISSN 2668-4756
Article DOI: https://doi.org/10.35219/mms.2019.1.10

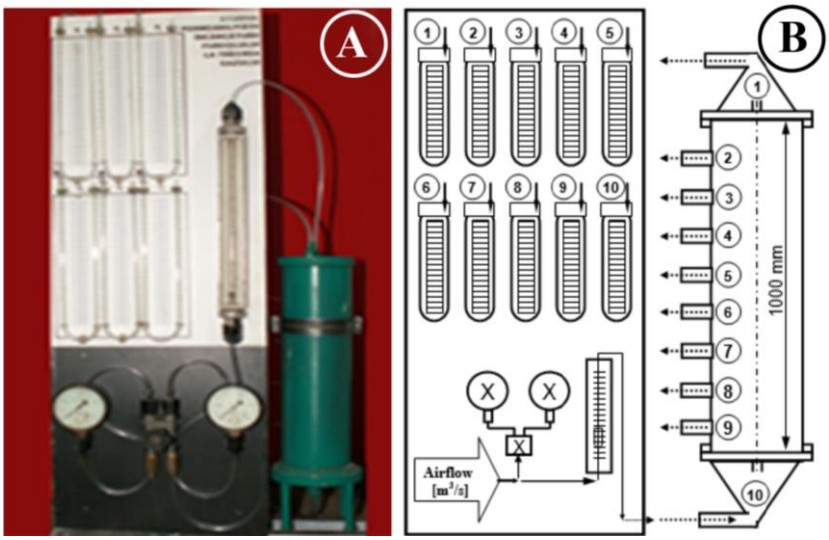

Fig. 1. *Installation to determine pressure loss in granular layers*

Table 1. *Pressure loss in granular layers*

Losses of pressure (L = 1000 mm)		Airflow [m³/s]							
		Ore			Pellets	Coke			
[mm CA]	[Pa]	P 1	P 2	P 3	P 4	P 5	P 6	P 7	P 8
50	490	0.28	0.31	0.41	0.58	0.72	1.03	1.32	1.37
100	980	0.40	0.47	0.58	0.82	1.07	1.38	-	-
150	1470	0.51	0.59	0.72	1.06	1.37	-	-	-
200	1960	0.62	0.70	0.87	1.34	-	-	-	-
250	2450	0.72	0.81	1.02	-	-	-	-	-
300	2940	0.80	0.89	1.17	-	-	-	-	-
350	3430	0.86	0.97	1.22	-		-	-	-
400	3920	0.92	1.03	-	-		-	-	-
450	4410	1.01	1.12	-	-		-	-	-
500	4900	1.03	1.18	-	-		-	-	-
550	5390	1.11	-	-	-		-	-	-
600	5880	1.17	-	-	-		-	-	-

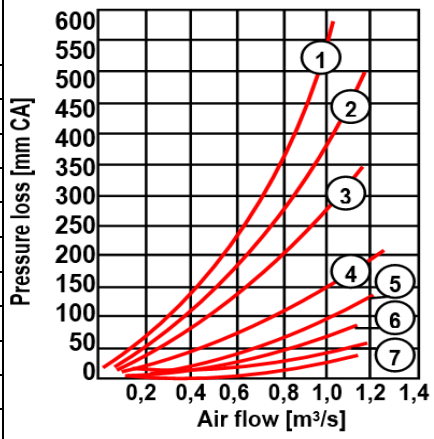

Graph 1. Loss of pressure in the layer

Legend: P1. Ore crushed and sorted; P 2. Agglomerated ore; P 3. Pieces of ore; P 4. Ore pellets (8-16 mm); P 5. Coke breeze (10-20 mm); P 6. Coke (20-30 mm); P 7. Coke (30-40 mm); P 8. Coke (40-45 mm).

5. Conclusions

In order to know the circulation of gases through the furnace, the loss of pressure in layers formed from materials of unequal shapes and sizes, on specially constructed installations was studied.

Variation curves were established for pressure losses in layers of different materials and granulation.

The volume of the voids in the raw material layer depends on the shape and the particle size range of the parts from which the respective layer is formed.

The volume of the gaps between the pieces of materials, as well as the dimensions of this layer derive from the layer and the hydraulic resistance of the gas flow step.

Calculating the pressure loss through the layer, as can be seen from the relations (1), (2), (3), one of the most important factors is the equivalent diameter of the granules from which the layer is formed.

References

[1]. ***, *ArcelorMittal Galați Documentation*.
[2]. Buzea O., *Furnace, Part II*, Sidex - Galați.
[3]. Adrian Vasiliu, *Elaboration of the Source in Furnace*, electronic format course, UGAL Galați, 2012.
[4]. Adrian Vasiliu, *Aggregates and thermal installations*, electronic format course, UGAL Galați, 2012.

THE ANNALS OF "DUNAREA DE JOS" UNIVERSITY OF GALATI
FASCICLE IX. METALLURGY AND MATERIALS SCIENCE
Nº. 1 - 2019, ISSN 2668-4748; e-ISSN 2668-4756
Article DOI: https://doi.org/10.35219/mms.2019.1.10

[5]. Teoreanu I., Becherescu D., *Thermo-technological installations*, Technical Publishing House, Bucharest, 1999.
[6]. Murguleț N., Nicolae A., *Aggregates and industrial thermal installations*, Bucharest Lithography IPB, 1998.
[7]. Nicolae A., Predescu C., *Theoretical bases of the thermo-technological aggregates in the metal materials industry*, Ed. Printech, București, 2001.

MANUSCRISELE, CĂRŢILE ŞI REVISTELE PENTRU SCHIMB, PRECUM ŞI ORICE CORESPONDENŢE SE VOR TRIMITE PE ADRESA:

MANUSCRIPTS, REVIEWS AND BOOKS FOR EXCHANGE COOPERATION, AS WELL AS ANY CORRESPONDANCE WILL BE MAILED TO:

LES MANUSCRIPTS, LES REVUES ET LES LIVRES POUR L'ECHANGE, TOUT AUSSI QUE LA CORRESPONDANCE SERONT ENVOYES A L'ADRESSE:

MANUSCKRIPTEN, ZIETSCHRITFTEN UND BUCHER FUR AUSTAUCH SOWIE DIE KORRESPONDENZ SID AN FOLGENDE ANSCHRIFT ZU SEDEN:

After the latest evaluation of the journals by the National Center for Science Policy and Scientometrics (**CENAPOSS**), in recognition of its quality and impact at national level, the journal will be included in the B^+ category, 215 code (http://cncsis.gov.ro/userfiles/file/CENAPOSS/Bplus_2011.pdf).

The journal is already indexed in:

SCIPIO-RO: http://www.scipio.ro/web/182206

EBSCO: http://www.ebscohost.com/titleLists/a9h-journals.pdf

Google Academic: https://scholar.google.ro

Index Copernicus: https://journals.indexcopernicus.com

The papers published in this journal can be viewed on the website of "Dunarea de Jos" University of Galati, the Faculty of Engineering, pages: http://www.sim.ugal.ro, http://www.imsi.ugal.ro/Annals.html.

Name and Address of Publisher:
Contact person: Elena MEREUȚĂ
Galati University Press - GUP
47 Domneasca St., 800008 - Galati, Romania
Phone: +40 336 130139
Fax: +40 236 461353
Email: gup@ugal.ro

Name and Address of Editor:
Prof. Dr. Eng. Marian BORDEI
"Dunarea de Jos" University of Galati, Faculty of Engineering
111 Domneasca St., 800201 - Galati, Romania
Phone: +40 336 130208
Phone/Fax: +40 336 130283
Email: mbordei@ugal.ro

AFFILIATED WITH:

- THE ROMANIAN SOCIETY FOR METALLURGY
- THE ROMANIAN SOCIETY FOR CHEMISTRY
- THE ROMANIAN SOCIETY FOR BIOMATERIALS
- THE ROMANIAN TECHNICAL FOUNDRY SOCIETY
- THE MATERIALS INFORMATION SOCIETY (ASM INTERNATIONAL)

Edited under the care of the FACULTY OF ENGINEERING

Annual subscription (4 issues per year)

Fascicle DOI: https://doi.org/10.35219/mms

Volume DOI: https://doi.org/10.35219/mms.2019.1

Editing date: 15.03.2019
Number of issues: 200
Printed by Galati University Press (accredited by CNCSIS)
47 Domneasca Street, 800008, Galati, Romania